Generation, function and therapeutic application of chemotactic cytokines in cardiovascular diseases

Von der Fakultät für Mathematik, Informatik und Naturwissenschaften der RWTH Aachen University zur Erlangung des akademischen Grades eines Doktors der Naturwissenschaften genehmigte Dissertation

vorgelegt von

Master of Science
Delia Projahn, Geburtsname Gliga
aus Hermannstadt, Rumänien

Berichter:

Universitätsprofessor Dr. med. Christian Weber
Universitätsprofessor Dr. rer. nat. Jürgen Bernhagen

Tag der mündlichen Prüfung: 11.11.2013

Diese Dissertation ist auf den Internetseiten der Hochschulbibliothek online verfügbar.

To my family

The results of this work will be partially published in:

Postea O, Vasina EM, Cauwenberghs S, **Projahn D**, Liehn EA, Lievens D, Theelen W, Kramp BK, Butoi ED, Soehnlein O, Heemskerk JW, Ludwig A, Weber C, Koenen RR. Contribution of platelet cx(3)cr1 to platelet-monocyte complex formation and vascular recruitment during hyperlipidemia. *Arteriosclerosis, thrombosis, and vascular biology.* 2012; 32: 1186-1193.

Projahn D, Simsekyilmaz S, Singh S, Kanzler I, Kramp BK., Langer M, Burlacu A, Bernhagen J, Klee D, Zernecke A, Hackeng TM, Groll J, Weber C, Liehn EA, Koenen RR. Controlled release of engineered chemokines from biodegradable hydrogels prevents injury extension after myocardial infarction. *Journal of Cellular and Molecular Medicine.* 2013, (in revision).

Table of contents

Abbreviations

α-SMA	Alpha-smooth muscle actin
ACE	Angiotensin-converting enzyme
AMI	Acute myocardial infarction
ApoE	Apolipoprotein E
APS	Ammonium persulfate
ASC	Acute coronary syndrome
ATP	Adenosin-5' triphosphate
BM	Bone marrow
BMC	Bone marrow cells
BMP	Heart rate
BrdU	Bromodeoxyuridine
BSA	Bovine serum albumin
°C	degree Celsius
$CaCl_2$	Calciumchloride
CAD	Coronary artery disease
CD11a/CD18	Lymphocyte function-associated antigen-1
CH_2Cl_2	Dichloromethane
cm^2	Square centimetre
CO	Cardiac output
CS/DS	Chondroitin/dermatan sulfate
C-terminus	Carboxyl-terminus
CX_3CL1	Fractalkine
CVD	Cardiovascular disease
DAG	Diacylglycerol
DCC	N,N'-dicyclohexyl-carbodiimide
DMAP	4-(Dimethylamino)-pyridin
DMSO	Dimethyl sulfoxide
DNA	Deoxyribonucleic acid
dNTP	Nucleoside triphosphate master mix
DPPIV/CD26	Dipeptidyl Peptidase IV
DTNB	5,5'-dithio-bis-(2-nitrobenzoic acid)
DTPA	3,3'-dithiopropionic acid
DTT	Dithiothreitol
EC	Endothelial cell
E. coli	*Escherichia coli*
EDTA	Ethylenediaminetetraacetic acid

EF	Ejection fraction
ELISA	Enzyme-linked immunosorbent assay
EMC	Extracellular matrix
EOC	Early-outgrowth cells
EOC medium	Endothelial cell growth medium
EPC	Endothelial progenitor cell
F1-CX$_3$CL1	Fractalkine antagonist
FACS	Fluorescence-activated cell sorting
FCS	Fetal calf serum
FDH	Fast degradable hydrogel
FPLC	Fast protein liquid chromatography
GAG	Glycosaminoglycan
GP	Glycoprotein
GPCR	G-protein-coupled receptor
HA	Hyaluronic acid
HAoSMCs	Human Aortic Smooth Muscle Cells
HBSS	Hank's balanced salt solution
HCl	Hydrochloride
HDL	High-density lipoprotein
HEPES	2-(4-(2-hydroxyethyl)-1-piperazinyl)-ethansulfonsäure
HIF-1α	Hypoxia inducible factor-1α
His	Histidine
H$_2$O	Water
H$_2$O$_2$	Hydrogen peroxide
HPLC	High performance liquid chromatography
HS/HP	Heparin sulfate/heparin
HSA	Human serum albumin
HC	Hematopoietic cell
H$_2$SO$_4$	Sulfuric acid
HUVEC	Human Umbilical Vein Endothelial Cells
IEP	Isoelectric point
IFN	Interferon
IL	Interleukin
IP$_3$	Inositol-1,4,5-triphosphate
IPTG	Isopropyl β-D-1-thiogalactopyranoside
I/R	Ischemia/reperfusion
kb	Kilo base

KCl	Potassium chloride
kDa	Kilodalton
KH_2PO_4	Potassium hydrogen phosphate
KS	Keratin sulfate
LB medium	Luria-Bertani medium
LDL	Low density lipoprotein
$LiAlH_4$	Lithium aluminium hydride
LV	Left ventricular
µm	Micrometer
M	Molar mass
mAb	Monoclonal antibody
MDC	Macrophage-derived chemokine
MCP	Monocyte chemotactic protein
MES	2-(N-morpholino)ethanesulfonic acid
Met	Methionine
mg	Milligram
$MgCl_2$	Magnesium chloride
MI	Myocardial infarction
MIF	Macrophage inhibitory factor
min	Minute
ml	Milliliter
mm^2	Square millimetere
MMP	Matrix metalloproteinase
M_n	Number Average molecular weight
MNC	Mononuclear cell
mS	Millisievert
MS	Mass spectrometry
MSC	Mesenchymal stem cell
mRNA	Messenger RNA
M_w	Weight average molecular weight
M_w/M_n	Polydispersity index
MWCO	Molecular weight cut off
Na-EDTA	Sodium-EDTA
NaOH	Sodium hydroxide
NF-κB	Nuclear factor kappa B
NK	Natural killer
nm	Nanometer

N-terminus	Amino-terminus
OxLDL	Oxidized LDL
PBS	Phosphate-buffered saline
PBSF	Pre-B-cell growth-stimulated factor
PCR	Polymerase chain reaction
PEG	Polyethylene glycol
PEG-DA	Poly(ethyleneglycol) diacrylate
PEO	Polyethylene oxide
PG	Poly(glycidol)
PKC	Protein kinase C
PMC	Platelet-monocyte-complexes
PMN/PML	Polymorphonuclear leukocytes
RANTES/CCL5	Regulated on activation, normal T-cell expressed and secreted
RFU	Relative signals
RNA	Ribonucleic acid
ROS	Reactive oxygen species
RT	Room temperature
SC	Stem cell
SDF-1/CXCL12	Stromal cell derived factor-1
SDH	Slow degradable hydrogel
SDS	Sodium dodecyl sulfate
SDS-PAGE	Sodium dodecyl sulfate polyacrylamide gel electrophoresis
SH	Thiol
siRNA	Small interfering RNA
SMC	Smooth muscle cell
SOB medium	Super optimal broth medium
SOC medium	SOB medium with 20 mM glucose
ssDNA	Single stranded DNA
(sP(EO-stat-PO)	Star-shaped poly(ethylene oxide-stat-propylene oxide)
TACE/ADAM17	TNF-α–converting enzyme
TAE	Tris-(hydroxymethyl)-aminomethane (tris)
TARC	Thymus and activation-regulated chemokine
TBS	Tris-buffered saline
TCEP	Tris (2-carboxyethyl) phosphine
TEMED	N,N,N',N'-Tetramethylethylendiamin
TFA	Trifluoroacetic acid
TGF-β	Transforming growth factor beta

THF	Tetrahydrofuran
TNF	Tumor necrosis factor
Trx	Thioredoxin
U	Unit
VCAM	Vascular cell adhesion molecule

1. Introduction

Cardiovascular disease (CVD) accounts for almost half of the morbidity and mortality world-wide and develops mostly from atherosclerosis and subsequent obstruction or thrombosis of large arteries[1]. The World Health Organisation[2] estimates 17.3 million people died from CVD in 2008, representing 30% of all global death. Of this death, an estimated 7.3 million were due to coronary heart disease and 6.2 million were due to stroke. By 2030, almost 25 million people will die from CVD, mainly from heart disease and stroke. These are projected to remain the single leading cause of death[2]. In this context, CVD can be considered to be a civilization disease, because the indigenous people were largely unaffected by this disease and its consequences. The risk factors of CVD mostly include tobacco use, unhealthy diet and obesity, physical inactivity, raised blood pressure, diabetes and raised lipids[2]. The pathogenesis of CVD arises from atherosclerosis and gives rise to cerebrovascular disease and coronary artery disease (CAD) through a slowly progressive lesion formation and luminal narrowing of arteries. Upon plaque rupture and thrombosis, these most common forms of CVD manifest as acute coronary syndrome (ACS), myocardial infarction (MI) and stroke[3]. The following introduction provides an overview about the development and pathogenesis of atherosclerosis which gives rise to the subsequent MI, and highlights the importance of chemokines and their receptors, to prevent the development of atherosclerosis and the therapy of the heart after MI.

1.1. Atherosclerosis

In the last decades the knowledge regarding the pathology of atherosclerosis increased enormously and research on this field is one of the timeliest topics in the area of medicine. In 1829 Jean Lobstein implemented the term "arteriosclerosis", in his unfinished Traité d'Anatomie Pathologique, a four-volume treatise on pathological anatomy, based upon his lifelong personal experience, that is defined as a form of CVD affecting the arteries and arterioles[4, 5]. In contrast the term "atherosclerosis" is a specific form of "arteriosclerosis" developed by the formation of fatty streaks which is an accumulation of lipid-loaded macrophages in the intima of the artery[6]. Virchow[7] proposed that the lesion of atherosclerosis results from injury of the arterial wall. Further he hypothesized that atherogenesis involved in combination of inflammatory and proliferative responses within the arterial wall preceding the degenerative changes that have been recognized in the advanced lesions of atherosclerosis. Duguid[8] modified this hypothesis that mural thrombi become incorporated into the lesion of atherosclerosis and provide a part of cellular response in lesion formation. This hypothesis was modified by Frech[9], Mustard and Packham[10], Wissler[11], Thomas et. al.[12] and Ross et. al.[13], and increased the emphasis to one of the principle alterations in atherosclerosis, the intimal accumulation of smooth muscle cells. The

response-to-injury hypothesis by Ross implies that the lesion of atherosclerosis results as a response to some form of injury to arterial endothelial cells (EC) that result in their desquamation[13]. This hypothesis was further developed by Steinberg who suggested that altered lipoproteins may account for the initiation of atherosclerosis formation[14-16]. But to date the knowledge in the area of atherosclerosis grew and it is known that hyperlipidemia is the main risk of atherosclerosis[6]. Studies in animal and humans have shown that hypercholesterolemia causes focal activation of endothelium in large and medium size arteries[17]. The development of an atherosclerotic lesion (atheroma) is initiated by the activation and dysfunction of ECs[6]. The platelet is the first blood cell to arrive at the scene of endothelial activation[17, 18]. The platelet glycoproteins (GP) Ib and IIb/IIIa engage surface molecules on the EC, which may contribute to endothelial activation[17]. The Leucocyte is the second cell which contributes to the scenario of the activated ECs. The activated ECs express several types of leukocyte adhesion molecules, which cause blood cells rolling along the vascular surface to adhere at the site of activation[17]. Once the blood cells have attached it comes to an increase in the permeability of blood vessels for lipid components in the plasma such as low density lipoprotein (LDL)[6, 17]. Monocytes migrate into the intima and subintima of the endothelium where they become loaded with cell-activating oxidized LDL (oxLDL) and other lipids and transform into macrophages. OxLDL and other lipids are taken up by scavenger receptors of macrophages which accumulate to the evolving lesion and transform to the foam cell to form early "fatty streaks" (plaques) in the intima[6, 17]. OxLDL also triggers the secretion of chemokines by ECs which drives the intimal immune cell infiltration[3]. The intima then becomes thicker as a result of a pathophysiological response to changes in fluid dynamics at atherosclerosis-prone areas of the arterial tree, such as artery branching points[6]. Early "fatty streaks" lesions consist of T-cells and monocyte-derived macrophage-like foam cells loaded with lipids followed by the accumulation of apoptotic cells, debris and cholesterol crystals which form the necrotic core[3]. The advanced atherosclerotic plaque consists of necrotic cores, calcified regions, accumulated modified lipids, inflamed smooth muscle cells (SMCs), ECs, leukocytes and foam cells[19]. The progression of plaques that leads to narrowing of the arterial lumen is further initiated by the release of cytokines, growth factors and the deposition of extracellular matrix components (EMCs). The secretion of matrix-degrading proteases and cytokines by plaque cells can cause a thinning of the fibrous cap, which prevents contact between the blood and the pro-thrombotic material in the plaque[6]. Activated, infiltrated immune cells of the plaque produce further numerous inflammatory molecules and proteolytic enzymes which can disintegrate the cap and activate cells in the core, transforming the stable plaque into a vulnerable unstable plaque that can rupture and induce a thrombus, which can block the artery and result in coronary syndromes, MI and stroke[6, 17] (Figure 1).
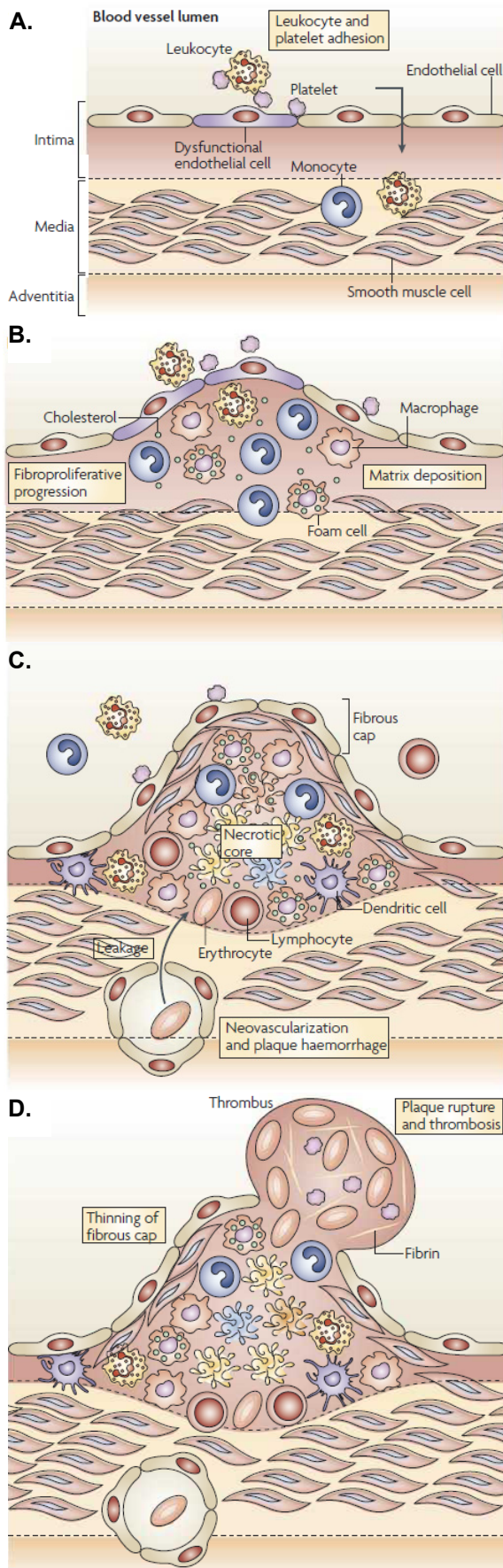
Figure 1: Development of atherosclerosis. Modified from Weber et. al.[6].

A. Endothelial-cell dysfunction and activation under pro-inflammatory conditions of hyperlipidemia leads to early platelet and leukocyte adhesion and increased permeability of the endothelium.

B. Monocytes that are recruited to the intima and subintima accumulate lipids and transform into macrophages or foam cells, which make up fatty streaks. Continued mononuclear-cell influx, deposition of matrix components and recruitment of smooth muscle cells give rise to fibroproliferative progression of the plaques.

C. Apoptosis of macrophages and other plaque cells creates a necrotic core, and a fibrous cap that consist of matrix and smooth-muscle-cell layer forms. Neovascularisation can occur within the plaque and from the adventitia, and leakage of fragile vessels can lead to plaque haemorrhage.

D. Thinning and erosion of the fibrous cap in unstable plaques, for example owing to matrix degradation by proteases, ultimately results in plaque rupture, with release of debris, activation of the coagulation system and plaque thrombus artery. This leads to arterial occlusion and MI or stroke.

1.2.   Myocardial infarction (MI)

The heart is built of long chains of striated muscle and exhibits a high content of mitochondria to sustain resistance to fatigue and maintain all vital functions of the organism[20]. MI is the leading cause of morbidity and mortality in the developed nations[3] and is associated with persistent muscle damage, scar formation and reduced cardiac performance[21]. MI generally arises as a consequence of coronary artery occlusion which results either from atherosclerotic or inflammatory processes causing lumen narrowing (stenosis) or thrombus formation, which leads to limited oxygen supply (ischemia), irreversible muscle damage and cardiomyocyte death[22]. The most common complication is the occurrence of left ventricular (LV) dysfunction and heart failure[23]. Ischemia in the heart subsequently initiates a remodeling process that involves modifications of the cellular metabolism in surviving myocytes and changes of the LV structure leading to cardiac hypertrophy, fibrosis and enlarged chambers[21]. These changes lead to a loss of the heart function, which results in the progression of cardiac recompensation and heart failure[24]. Patients with MI benefit from early myocardial reperfusion, which is the most effective strategy to improve clinical outcome[25-27]. Despite the success of reperfusion, mortality and morbidity after MI remains substantial, with 5% to 6% of patients having a subsequent cardiovascular event in the next 30 days[25-27]. After ischemia, different cellular and molecular events are involved to achieve the healing of the myocardium, such as inflammatory phase, proliferative phase and healing phase.

During the inflammatory phase, it comes to a release of reactive oxygen species (ROS) from ECs and cardiomyocytes but also to an increased expression of cytokines and adhesion molecules[23]. Other participants such as superoxide anion contributes to MI extent by including cellular changes such as mitochondrial permeability, enzyme denaturation and DNA damage, but also triggering neutrophil infiltration[23, 28, 29]. The CXCR2-binding chemokines CXCL8, CXCL2, CXCL1, CXCL6, as well as CCL3 and CCL5 are involved in the recruitment of neutrophils into the inflamed myocardium[30-32]. Within the first hours, neutrophils are recruited from the blood stream into the inflamed tissue and contribute to further cardiac damage by releasing ROS, inflammatory mediators and proteases[28, 29]. In a CCR2-dependent manner, the extravasation of inflammatory monocytes but not of resident monocytes, is sustained by neutrophils[33]. In addition and beside to cellular external help, the inflammatory response has also a fundamental role in preparing the surrounding unaffected cardiomyocytes for the stress conditions[20]. Not only infarcted tissue but also unaffected surrounded tissue synthesizes chemokines and cytokines to trigger the initiation of the defense mechanism, like activation of hypoxia inducible factor-1α (HIF-1α)[34] and place cardiomyocytes in a "pre-conditioning" state, increasing resistance to a new hypoxic event[20].

HIF-1α has the ability to mediate an increase of stromal cell-derived factor-1 (SDF-1/CXCL12) and macrophage migration inhibitory factor (MIF), which lead to targeting the CXCR4 expressing cells to the infracted area[35] (Figure 2).

During the proliferation phase the heart wall is cleaned of dead cardiomyocytes and matrix debris without having build new supporting structures yet and will ineluctably break under high blood pressure and high mechanical force[20]. After removing necrotic cells and matrix debris, an inhibition of inflammation by transforming growth factor beta (TGF-β) and interleukin 10 (IL-10) follows in order to achieve an optimal healing of the infarcted area of the myocardium. For the initiation of the healing, the inflammatory cells are replaced by resident or recruited $Gr1^{low}$ monocytes, lymphocytes and mast cells[20]. The chemokine receptor CX_3CR1[36, 37] and CCR5[37] are required for rapid tissue invasion at the site of inflammation by resident monocyte population, which initiate an early immune response and differentiate into macrophages. Resident monocytes patrol between the cardiomyocytes using CX_3CR1 receptors[33] and maintain the homeostasis of the normal tissue[20]. For an optimal blood supply and to regenerate the heart and its function angiogenesis is necessary[20]. For angiogenesis to occur, stem cells (SCs) are important to be recruited to the injured tissue. The CXCL12/CXCR4 axis plays a crucial role in controlling and modulation of the recruitment of SCs and the formation of new blood vessels[38] (Figure 2).

The healing phase is the last stage after MI, forming a mature scar which contains a dense collagen-based extracellular matrix, myofibroblasts, SCs and newly formed vessels[20]. During scar maturation, lysyl-oxidase is upregulated and induces collagen cross-linking. The formation of a stable cross-linked extracellular matrix may shield the myofibroblasts from mechanical tension promoting quiescence that promotes apoptosis of infarct myofibroblasts[39]. A prolonged presence of myofibroblasts in the infarcted myocardium may promote adverse remodeling[39]. In the past the mature infarction scar was considered as inert and disabled of biological function, but during the last years different studies[30, 40] showed that increased collagen content supports contractility and sustains heart function. The healing of the infarcted heart results in massive changes of the ventricular architecture and geometry, and is also referred as "ventricular remodeling"[32]. These molecular and cellular changes affect both the cardiomyocytes and interstitial cells and result in an increased ventricular size, altered shape of the ventricle and worsened cardiac function[32]. The remodeling of the heart after MI is associated with poor prognosis, ventricular dilation and adverse cardiac events, including the development of heart failure and ventricular arrhythmias.[31]

To develop new therapeutic strategies after MI it is essential to understand the cellular and molecular mechanisms to reduce injury and promote repair to improve LV remodeling and the function of the heart.

Normal Myocardium	Inflammatory Phase	Proliferative Phase	Healing Phase
- contraction - self regeneration	- cardiomyocyte death - chemokines/cytokines synthesis - neutrophil infiltration - Gr1 high monocyte recruitment - debris clearance - preconditioning	- inhibition of inflammation - Gr1 low monocyte infiltration - lymphocyte recruitment - angiogenesis - myofibroblast differentiation - collagen synthesis - MSCs recruitment - cardiac cell regeneration	- myofibroblast apoptosis - formation of mature scar
	0 - 4 days	0 - 3/4 weeks	2/3 - 4/6 weeks
- Cardiomyocytes - Gr-1 low Monocytes CX3CR1/Fraktalkine - Fibroblasts - Cardiac progenitor cells	- dead Cardiomyocytes CXCR4/MIF CXCR4/SDF-1α TNFα , HIF NF-kB pathway - Neutrophils CXCR2/KC CCR1/MIP-1α CXCR4/SDF-1α - Gr-1 high Monocytes CCR2/MCP-1 - Fibroblasts CCR2/MCP1 TGFß	- Gr-1 low Monocytes CX3CR1/Fraktalkine CXCR4/SDF-1α CCR5/RANTES - EPCs CXCR4/SDF-1α CXCR2/Groα/IL8 CXCR2/CXCR4/MIF CCR2/MCP1 - Lymphocytes CCR5/RANTES CCR2/MCP1 - Fibroblasts CCR2/MCP1 TGFß - Cardiac progenitor cells - MSCs CXCR4/SDF-1α MCP-3 G-CSF	- Gr-1 low Monocytes CX3CR1/Fraktalkine CXCR4/SDF-1α CCR5/RANTES - Lymphocytes CCR5/RANTES CCR2/MCP1 - Fibroblasts
ECM	Fibrin-based provisional matrix	Collagen-based matrix	Mature and dense collagen-based matrix

Figure 2: Cellular and molecular events after MI. Modified after Liehn et. al.[20].The healing after MI involves 3 overlapping phases: the inflammatory, proliferative, and healing phase. Each is characterized by specific events (red), implicating different cells, controlled by specific chemokines (orange). Extracellular matrix (ECM) evolves the mature scar (dark blue), which ensures the stability and the function of the heart. (HIF = hypoxic inducible factor; IL = interleukin; MCP = monocyte chemotactic protein; MI = myocardial infarction; MIF = macrophage inhibitory factor; MSC = mesenchymal SC; NF-κB = nuclear factor kappa B; CXCL12 = stromal cell-derived factor 1 (SDF-1); TGF = transforming growth factor; TNF = tumor necrosis factor.)

1.3.   Chemokine receptors

Chemokine receptors are large proteins binding different chemokines and chemokines themselves are able to bind several different receptors. This interaction is the most complex processes in chemokine physiology. The recognition of chemokine-encoded messengers is mediated by specific cell surface G-protein-coupled receptors (GPCRs) with seven transmembrane domains[41]. All chemokine receptors share common structural features which include: (1) an extracellular amino-terminus (N-terminus); (2) a polypeptide which loops across the plasma membrane seven times to form three intracellular and three extracellular loops; (3) a disulfide bond linking cysteine residue in the first and second extracellular loops; (4) an intracellular carboxyl-terminus (C-terminus)[42]. Compared with other members of the GPCR family, the chemokine receptors are relatively small, consisting of approximately 350 amino acid residues. There is at least approximately 20% homology between all chemokine receptors. The characteristic of the N-terminus of the receptors is rarely acidic, and the C-terminus is relatively short[42]. The GPCR family is one of the most diverse classes of cell surface receptors which perceive signals from ligands, such as hormones, biogenic, amines, pheromones, neurotransmitters, classical chemoattractants, lipid mediators, sweet, bitter, and umami tasting molecules, odorants, and light photons[41].

When a chemokine binds to its receptor, a conformational change is induced which results in a receptor activation. This activated receptor catalyzes exchange of GDP for GTP which maintains the G_i protein activation by dissociation of the α-subunit, which then induces phospholipase C activity. The active enzyme catalyzes the hydrolysis of phosphatidylinositol-4,5-biphosphate (PIP_2) to generate second messengers, i.e. diacylglycerol (DAG) and inositol-1,4,5-triphosphate (IP_3). IP_3 diffuses into the cytoplasm and binds to an IP_3 receptor on the membrane of a particulate calcium store. This binding results in the release of calcium ions, contributing to the large increase in cytoplasmic Ca^{2+} [42]. This process describes in general the G-protein-coupled signal transduction pathway.

Chemokine receptors contain three fundamental functions of the chemokine-induced "cellular reflex" which are not independent. These functions are message acquisition, message decoding, and initiation of cell responses[41]. Chemokines "are comparable with the human language" where word perception, interpretation of meaning, and induction of a response can be separated[41]. For example message acquisition means, a chemokine binds to a particular receptor and this binding is determined by receptor affinity, which varies greatly between ligands and does not necessarily translate into functional potency[41, 43, 44]. The importance of chemokines is influenced by the agonist-antagonist affinity to a particular receptor. This particular receptor can be shifted into its "productive" signaling conformation using a very good binding agonist or preventing such a shift by an antagonist[41, 45, 46]. The chemokine

relevance is dependent on the degree of potency response (efficacy) and the capability to initiate different regulatory and signal transduction pathways, which dictate the current response. The potency of a response but also its quality are dependent of the chemokine induced shift in the receptor configuration[45]. The receptor potency is variable for each receptor ligand[46].

To understand the molecular interactions responsible for matching of approximately 50 human chemokines[47] and 19 human chemokine receptors[41] will take some time, because these interactions can vary for each receptor and ligand[48]. The determination of agonist and antagonist is variable for each chemokine and its receptor, but also many signaling pathways[49] and cell responses show huge variances. Chemotaxis is the only response that is elicited by almost all chemokines in almost all receptor-bearing cells[41]. During the last years, the understanding of the mode of action of GPCRs increased, especially in the area of classical chemoattractants and its molecular events which lead from chemokine GPCRs to cell locomotion.

Chemokine receptors are primarily expressed in hematopoietic cells (HCs), including neutrophils, monocytes, lymphocytes, myeloid progenitor cell lines, eosinophils, basophils and erythrocytes[42]. Chemokines are implicated in the directional cues for the movement of leukocytes in development of homeostasis, and inflammation. Extravasation of leucocytes from the blood into the tissue is adjusted by a multistep process sequencing a series of concerted interactions between leukocytes and ECs[50]. Chemokines provide the signals for the movement that leads to extravasation of leukocytes and control their homeostatic circulation through the tissue. Lymphocytes continuously circulate through the blood, tissue and lymphatics in an organized manner and brings naive lymphocytes into the lymph nodes, where they encounter antigens and are transformed into memory lymphocytes that migrate into the tissue to ensure immunity[50]. For example, the dramatic increase of CCL5 during inflammation results in the selective recruitment of lymphocytes in the inflamed tissue[51]. Monocytes/macrophages, eosinophils, and mast cells are produced in the bone marrow (BM), adjudge primary in other tissue and also migrate *via* chemotaxis into tissue where an increased chemoattractant is present[50]. For example, monocytes/macrophages respond to CX_3CL1 chemokine *via* the CX_3CR1 receptor and require cell chemotaxis[52]. The CXCL12 chemokine was demonstrated to drive chemotaxis of HCs from BM through the CXCR4 and CXCR7 receptors, but it is also responsible for the retention of HCs in the bone marrow[53-55].

1.4. Chemokines

Chemokines belong to a superfamily of small chemotactic cytokines with a molecular weight ranging from 8 kDa to10 kDa, containing 60 to 100 amino acids and 20% to 90% sequence homology among each other at the protein level[48]. Chemokines are a small group of signaling proteins which have a central role in the migration of immune cells into the tissue and in the transmigration from the blood. Some chemokines have an activating effect on immune cells, while others are involved in the development of organs and angiogenesis. The approximately 50 different chemokines [47] are produced by immune cells and many other tissue cells. They develop their function after binding to chemokine receptors, which are widely distributed in the immune system. Chemokines operate as a communication medium with their own language that carry encrypted messages to cells that have the means to decode. Diverse stimuli of many different cell types are able to prompt the chemokine dispatches. Perceived and decoded, these messages can influence the most profound aspects of a cell's life, including not only eponymous chemotaxis and adhesion but also proliferation, maturation, differentiation, apoptosis, malignant transformation, and dissemination[41]. Without the chemokines, which can effect each cell and the whole immune system, the body could not function. Chemokines regulate various functions such as the immune survival, development, hematopoiesis, wound healing, inflammation, viral infections, or metastases[56]. Independent of the chemokine function, chemokines are defined based on their amino acid composition, specifically on the presence of a conserved tetra-cysteine motif[41]. The chemokines are classified into four major subclasses, the CXC-, CC-, C- and CX_3C-chemokines, based on the relative position of the first consensus cysteins on N-terminal part of the protein. The first two cysteins of CXC-chemokines, also called α-chemokines are separated by a non-conserved amino acid (cystein – X amino acid - cystein)[48]. This chemokine family attract neutrophils, T-lymphocytes, B- lymphocytes and natural killer (NK) cells. The α-chemokines are further subdivided into those containing the sequence glutamic acid-leucine-arginine (ELR) near the N-terminus and those that do not[50]. The first two cysteins of CC-chemokines are next to each other and are called β-chemokines[48]. This family can attract monocytes, macrophages, basophils, eosinophils and T-lymphocytes, but have little to no effect on neutrophils. Structurally, the β-chemokines can be subdivided into two families, the monocyte-chemoattractant proteins and eotaxin, which are approximately 65% identical to each other, and all other β-chemokines[50]. The C-chemokine subfamily, also known as γ-chemokines are structurally different from the other chemokine families, in that they contain only two of the four conserved cysteins. The only members of this family are the lymphotactin a and b (also called XCL1 and XCL2), which are known as chemoattractant for T-lymphocytes. These chemokines are specific ligands for the XCR1 receptor[48]. So far, only one member of CX_3C-chemokine has been identified, which is

called fractalkine (CX$_3$CL1). This chemokine subfamily is also known as δ-chemokine and has been characterized by the presence of three amino acids between the first two cysteine-residues, and includes a transmembrane and mucin-like domain[48] (Figure 3). All four chemokine families have very similar tertiary structure which is composed of a three-stranded anti-parallel β-sheet, and preceded by a disordered amino terminus and covered on one side by a C-terminal α-helix[57]. Upstream of the β-sheet is the N-terminal region, which consists of more or less disordered and extended region of 6-10 residues, followed by a long loop (N-loop) and a short helix. The overall structure is stabilized by disulfide bonds involving N-terminal and core domain cysteins[56]. It has become more and more clear that biological information required to run the chemokine system is not only stored in the sequence of the chemokines involved, but also in a structure of a class of polysaccharide called glycosaminoglycans (GAGs), which are bound to most chemokines through ionic interactions[58] (Figure 3).

GAGs are covalently attached to core proteins, present on all cell surfaces and in the intracellular matrix[58, 59]. Chemokines display a high affinity to GAGs, which led to the presumption, without such an immobilization mechanism, chemokine gradients would be disrupted by diffusion[60]. GAGs are divided into four different groups: hyaluronic acid (HA), chondroitin/dermatan sulfate (CS/DS), heparan sulfate/heparin (HS/HP), and keratin sulfate (KS). GAGs are polysaccharides consisting of a repeated disaccharide unit, composed of a hexosamine and hexose or hexuronic acid, either or both, which may be sulfated at different positions[56]. HS is the class which most chemokines bind primarily through ionic interactions[61]. HS is composed of hexosamine, which is a glucosamine, and the hexuronic acid, which is either a glucuronate or its C5 epimer, an iduronate[56]. HS molecules are not only recognized by chemokines, they are also recognized as ubiquitous protein ligands of cytokines, growth factors, morphogenetic proteins, adhesion molecules, enzymes, plasma proteins, proteins from the extracellular matrix and apolipoproteins[58]. HS influences different functions of a ligand, like the local concentration, compartmentalization, stability, structure and its activity. It plays also a role in cell proliferation, cell adhesion, matrix assembly, chemoattraction, immune response, development, lipid metabolism, angiogenesis, wound healing or pathogen attachment. GAGs influence chemokines in this manner, they enhance their immobilization and form haptotactic gradients along cell surfaces, which can affect their transport, clearance, degradation and oligomerization[56]. Chemokines are characterized to include a receptor and a GAG binding domain and both of them are crucial for an accurate function[56]. In detail, mutated chemokines which show a GAG binding deficiency are unable to induce cell migration *in vivo*[62]. The localization of the receptor binding site of a chemokine is highly conserved, whereas the GAG binding site is localized on four different areas of the chemokine surface. Depending on the positions, the GAG binding cluster, may overlap the

receptor binding domain. This depends on the concerned localization of the two binding domains, suggesting that GAGs could potentially control receptor selectivity. Distinctions between a *wild type* and a GAG deficient binding chemokine concerning their activity was observed, which could be either due to the lack of GAG binding or to changes in receptor affinity or selectivity[56]. So far, the exact role of GAG in chemokine activity is not clearly defined, for this reason it is difficult to describe the exact effect of the GAG binding site, and the chemokine function. On the other hand, the various functions of GAGs may influence chemokines, depending through which receptor the signal transduction proceeds.

In the pathogenesis of atherosclerosis and after MI a number of chemokines play very important roles. In both cases, an inflammatory reaction occurs, followed by chemokine release, which plays a crucial role in the immune response. For this study the CCL5 and CXCL12 chemokines were investigated in the context of MI and CX_3CL1 in the context of atherosclerosis.
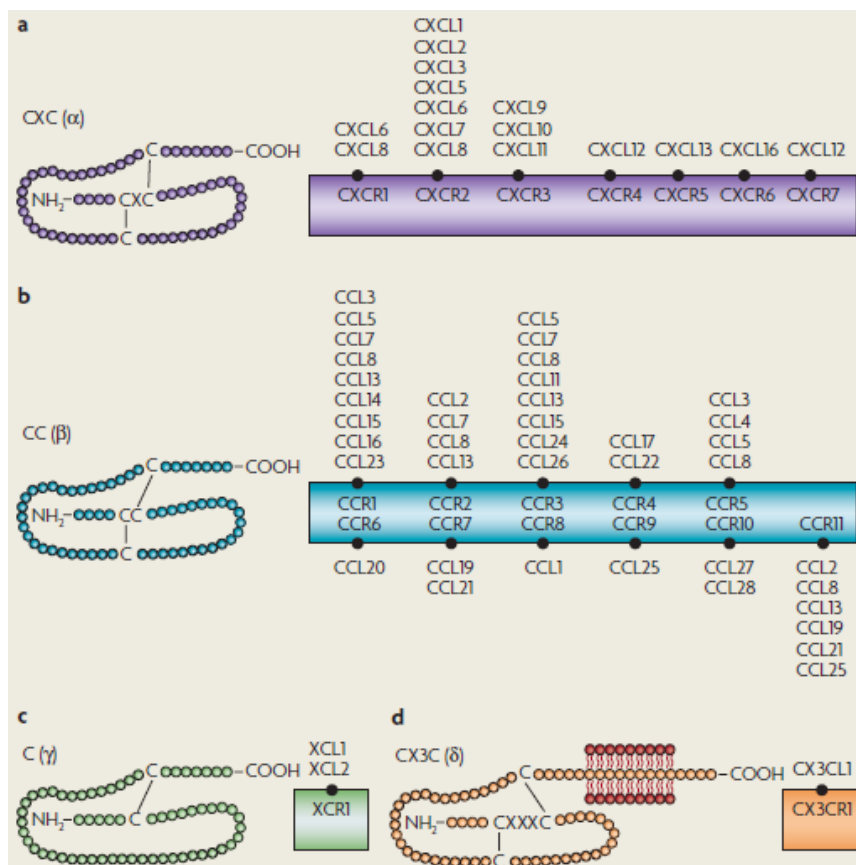
Figure 3: Overview of the secondary structure of chemokines and the corresponding chemokine receptors. Chemokines are subdivided into four families based on the relative position of the cysteine residues on the protein level. In CXC-chemokines, one amino acid separates the first two cysteine residues. In CC-chemokines, the first two cysteine residues are adjacent to each other. The C-chemokine subfamily is distinguished structurally as containing only two of the four conserved cysteine residues that are found in the other families. The CX_3C-chemokine subfamily, is characterized by the presence of three amino acids between the first two cysteine residues, as well as a transmembrane and mucin-like domain[48].

1.4.1.   CCL5 (RANTES, Regulated on Activation, Normal T-Cell Expressed and Secreted)

The CCL5 chemokine is a low molecular mass protein with 7.8 kDa, which participates in chronic inflammation by the recruitment of inflammatory cells[63, 64]. CCL5 is secreted by different cell types including ECs, SMCs, macrophages, platelets and activated T-cells[65]. CCL5 is the ligand for CCR1, CCR3 and CCR5 receptors[64, 66] and is chemotactic for T-cells, eosinophils, basophils, and leukocytes. Furthermore CCL5 plays a critical role as neutrophil and macrophage activator in inflammation, atherosclerosis and MI[67]. During inflammation CCL5 attracts immune cells *via* haptotaxis, which underlies the multistep process of immune cell extravasation from the blood vessel into tissue[68] (Figure 4).

A model of sponge-induced inflammatory angiogenesis found a dynamic expression of the chemokine CCL5 to correlate with neovascularization and inflammatory cell accumulation[69]. Interestingly, in the early stage of the process the exogenous CCL5 was observed to prevent angiogenesis. CCR5 and CCR3 are the main receptors for CCL5, consequently a deletion of CCR5 alone will still allow CCL5 to bind to CCR1[65, 66]. It has been shown that exogenous CCL5 no longer modified angiogenesis in CCR5($^{-/-}$) mice, accordingly CCL5 signals mainly through CCR5 in this model. Therefore, the activation of CCR5 by exogenous CCL5 may initiate a cascade of events leading to inhibition of sponge-induced angiogenesis[70].

The treatment with anti-CCL5 mAb significantly reduced both infarct size and post infarction heart failure in mouse model of chronic cardiac ischemia and the cardioprotective effects were associated with the reduction of leukocyte recruitment within the infarcted hearts[67]. It was already shown that functional impairment and structural remodeling after MI is reduced in the genetic absence of CCR1 due to an abrogated early inflammatory recruitment of neutrophils and improved tissue healing[30].

Braunersreuther et. al.[71] showed that the injection of chemokine CCL5 antagonist [(44)AANA(47)]-CCL5 in an *in vivo* mouse model of ischemia/reperfusion (I/R) reduce infarct size in ApoE($^{-/-}$) mice after ligature of the left coronary artery[71]. The inhibition of CCL5 exerts cardioprotective effects during early myocardial reperfusion, which is associated with reduced leukocyte infiltration into the reperfused myocardium[71]. Nevertheless, deficient mice for the CCL5 receptor CCR5 did not exhibit myocardium salvage in our model of I/R[71]. Furthermore, [(44)AANA(47)]-CCL5 did not mediate cardioprotection in these ApoE($^{-/-}$) CCR5($^{-/-}$) deficient mice, probably due to enhanced expression of compensatory chemokines[71]. The inhibition of CCL5 shows cardioprotective effects during early myocardial reperfusion, through its anti-inflammatory properties[71].

The CCL5 antagonist, Met-CCL5[72-74], which antagonizes the CCR5 receptor and its function in response to its natural ligand *in vitro*, was described. Met-CCL5 reduces the homing of early-outgrowth cells (EOCs), a step that is essential to endothelium building and the induction of neo-angiogenesis cells[65, 72]. Furthermore, Met-CCL5 is able to reduce inflammation in models of induced inflammatory and autoimmune diseases, *in vivo*. Indeed, Met-CCL5 is capable of partial agonist activity regarding receptor signaling and internalization and it does not function as a conventional receptor antagonist[74]. As receptor trafficking impacts on cell surface expression and the ability of the receptor to respond to other ligands, this information may indicate an alternative regulation of CCR5 by Met-CCL5 that allows the modified ligand to reduce inflammation[74]. These facts indicate that Met-CCL5 influences the progression of atherosclerosis and inhibits the recruitment of inflammatory cells. The blocking of chemokine receptor/ligand interactions might become a novel therapeutic strategy to reduce reperfusion injuries in patients during acute coronary syndromes.
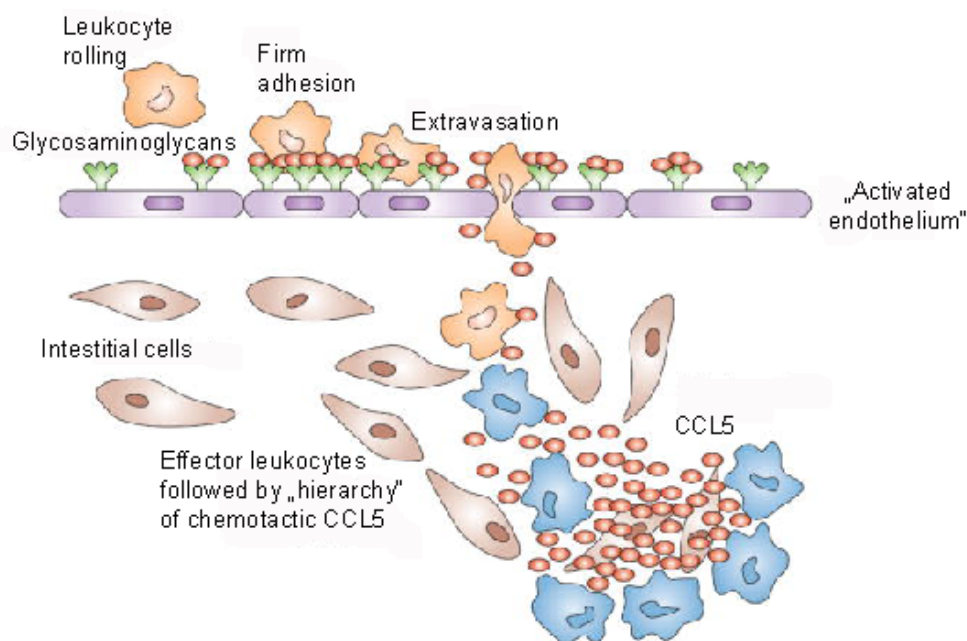
Figure 4: Role of CCL5 in inflammation. Figure modified from Krensky et. al.[68]. CCL5 (red ovals) attracts immune cells from the peripheral blood to sites of inflammation. Leukocytes 'roll' along the vascular endothelium *via* interactions with selectins. Chemokines, such as CCL5, attract immune cells *via* haptotaxis, inducing firm adhesion and diapedesis. CCL5 induces expression of integrins (e.g. CD11a/CD18 [lymphocyte function-associated antigen-1]) involved in adhesion, and metalloproteinases involved in movement through the vascular wall basement membranes and tissues. The immune cells follow the chemotactic gradient to the site of inflammation. T-cells, once activated by specific antigen, express CCL5 within 3–5 days, amplifying the immune response in time and space.[68]

1.4.2. CXCL12 (SDF-1, Stromal Cell-derived Factor 1)

The CXCL12 chemokine is also known as pre-B cell growth-stimulating factor (PBSF), which is a member of the CXC chemokine subfamily and was initially isolated from murine bone stromal cells[75]. The CXCL12 is constitutively and inducible expressed in several tissues such as BM, heart, liver, kidney, thymus, spleen, skeletal muscle and brain[76, 77]. This chemokine is highly conserved among mammalian species and is a key regulator of oriented cell migration[58]. It is able to orchestrate a huge array of functions during development but also in adult life and is importantly involved in a number of pathogenic mechanisms[58]. Indeed, knockout mice deficient in CXCL12 are not viable and die perinatally[78]. These mice show severely affected hematopoiesis with deficiencies in B-cell development, reduced myelopoiesis, and HC colonization of the BM[75, 79, 80]. In addition, CXCL12($^{-/-}$) mice show a cardiac ventricular septal defect and defective formation of the large vessels supplying the gastrointestinal tract[78]. Predominantly, the physiological effect of CXCL12 is mediated by the CXCR4 receptor, where the chemokine binds and triggers the signaling[81, 82]. This receptor was first identified in 1996 by two independent groups as the orphan receptor LESTR/Fusion, which was subsequently renamed CXCR4[81, 82]. The CXCL12 binds to the CXCR4 and induces dimerisation of the receptor and activation of inhibitory Gi proteins. Different signal transduction pathways downstream of CXCR4 were identified, including activation of tyrosine kinases, focal adhesion kinase, paxillin, extracellular-signal-regulated kinases, protein kinase C (PKC), phospholipase C-γ, and phosphoinositol 3-kinase. Furthermore, the CXCL12 binding to CXCR4 can also induce Janus kinases, the JAK/STAT transcription pathway and NF-κB[78]. The internalization of the CXCR4 receptor and its lysosomal degradation are important mechanisms causing desensitization towards CXCL12 signals, and phosphorylation of CXCR4 by PKC and G protein receptor kinases has been shown to increase its endocytosis owing to β-arrestin binding the C-terminus[83]. In addition, CXCL12 was shown to bind with high affinity to a second orphan receptor CXCR7/RDC1, which was originally cloned on the basis of its homology with conserved domains of GPCRs[84, 85]. This receptor might activate MAPK, PI3K and JAK/STAT pathways thereby regulating progenitor cell migration[86]. The CXCL12 attracts HCs from the circulating blood and induces angiogenesis through CXCR4 and CXCR7[53].

The structure of CXCL12 shows a typical chemokine fold stabilized by two disulfide bonds, which consists of a poorly structured N-terminus of 10 residues, followed by a long loop, a 3_{10} helix, a three β-sheet and a C-terminal helix[58]. Different CXCL12 isoforms, arising by alternative splicing of the same gene are known. Until now six different isoforms (α, β, γ, δ, ε, φ) of the CXCL12 were shown in rodents[87] and humans[88], respectively[58]. All the isoforms share the same three first exons corresponding to the α-isoform (residue 1-68), but differ in

their fourth exon, which give rise to a specific C-terminal domain for each of them[58]. The most prominent isoform, is the α-isoform, which encodes for a 68 amino acids peptide, while the β-isoform contains four additional amino acids at the C-terminus. Gleichmann et. al.[87] identified the splicing variant of the γ-isoform in the adult rat brain, heart and lung with the strongest expression observed in the heart, which contains 30 additional amino acids in comparison to the α-isoform at the C-terminus. However, the γ-isoform expression remains unaltered upon MI, while the predominant α-isoform, was shown to be significantly induced suggesting an important role of this isoform in the pathophysiology of MI[21, 89]. Functional studies revealed differences of this isoforms in their ability to stimulate cell migration[39]. The most studied isoforms are the α- and β-isoforms, but the γ-isoform became also more prominent over time. However, further investigations are required to understand the functional diversity of these CXCL12 variants[39].

The CXCL12 possesses the unique ability of adhesion, migration and homing of circulating CXCR4$^+$ progenitor cells to ischemic tissue[35]. In contrast to other chemokines, CXCL12 selectively immobilized HCs[90]. For this reason, the already well-characterized CXCL12 chemokine is a promising candidate for promoting tissue regeneration[53]. Under low oxygen supply during ischemia the transcription factor, HIF-1α was shown to regulate various downstream target genes such as CXCL12, which might further control the migration of progenitor and ECs towards the ischemic zone[35]. HIF-1α not only induces the expression of CXCL12 during ischemic injury, but also induces the expression of CXCR4 receptor on progenitor cells which might help to guide these cells towards CXCL12 gradients in ischemic tissue[35]. The involvement of CXCL12 in tissue repair after MI, was proven. For example, the CXCL12-mediated mobilization of BM-derived HCs to the ischemic heart was shown to result in angiogenesis and improved myocardial function (Figure 5)[21]. The interaction between CXCL12 and CXCR4 which has a significant role in regulating the homing and proliferation of SCs in the BM under homeostatic conditions has been discussed[21]. If the disruption of BM CXCL12/CXCR4 signaling under stress-induced conditions occurs, it is necessary to induce the mobilization of SCs into the circulation[91]. In parallel, the local elevation of CXCL12 levels in the inflamed or injured organ is capable of recruiting the mobilized cells to the site of injury where they can support tissue repair and regeneration (Figure 5)[21].

The effect of CXCL12 in the ischemic heart is limited by proteases that regulate the activity of many chemokines, which can increase or decrease their activity after N-terminal cleavage[92]. For example matrix metalloproteinase (MMP)-2 cleaves the CXCL12 chemokine at the N-terminus, resulting in a tetrapeptide[93], and a neurotoxic remnant[94] which decreases its activity[92]. CXCL12 is also cleaved by Dipeptidyl Peptidase IV (DPPIV/CD26), a serine exopeptidase that releases Xaa-Pro dipeptides from the N-terminus of the polypeptide[53, 95].

DPPIV is a transmembrane protein in ECs and leukocytes[53, 96]. Until now the physiological role of this cleavage is unknown, but CXCL12 inactivation by MMPs and DPPIV could cause immobilization of HCs from the BM[53]. In a previous study[53], it was shown that a protease-resistant CXCL12 (S4V) chemokine is resistant to MMP-2 and DPPVI/CD26 cleavage and retain receptor specificity of native CXCL12. Furthermore, the local delivery of the protease-resistant CXCL12 (S4V) may improve cardiac function after MI by driving chemotaxis[53], and it is a promising candidate for the therapy of MI to improve cardiac function.
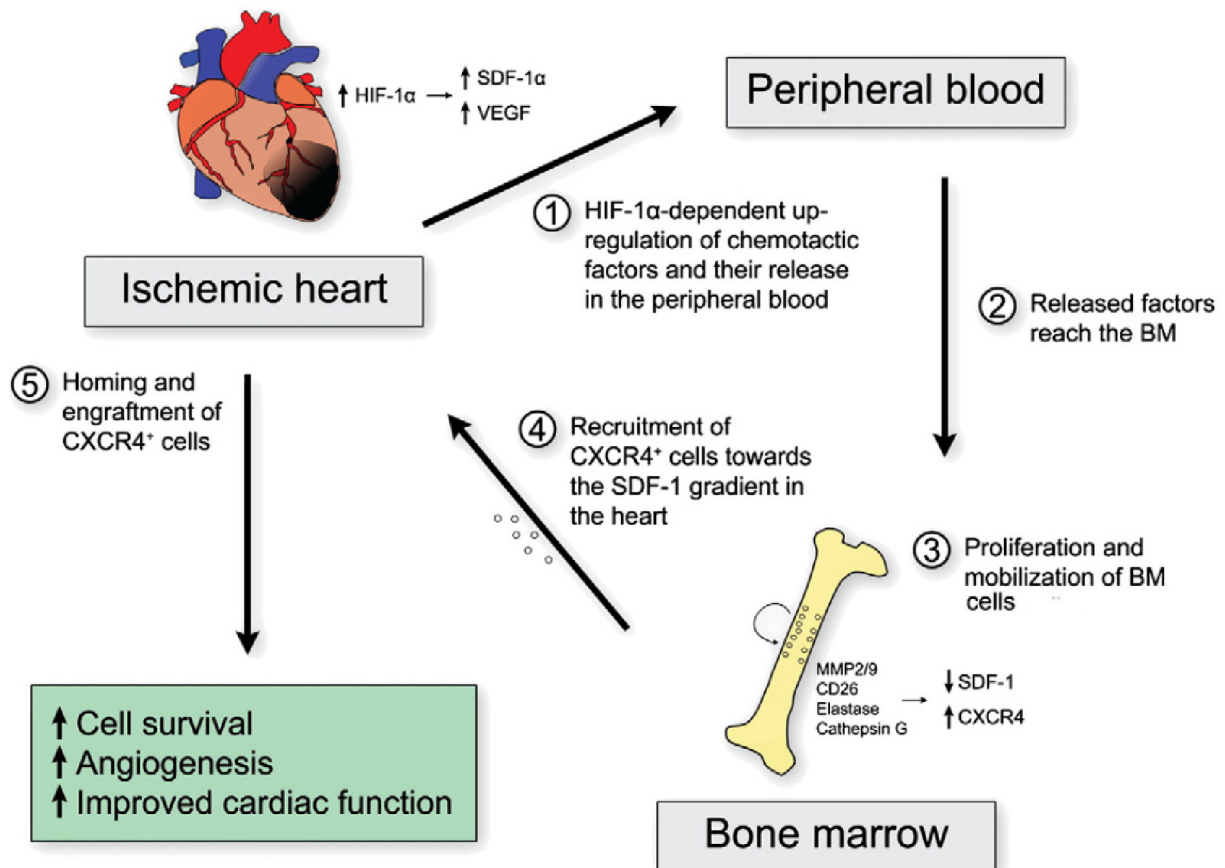
Figure 5: Potential role of CXCL12 in MI. Figure modified from Ghadge et. al.[21]. (1.) MI initiates the upregulation of the hypoxic signal HIF-1α, which then induces cell mobilization signals such as CXCL12 and VEGF and their release in the peripheral blood. (2.) These signals reach the bone marrow (BM). (3.) This leads to alterations in the BM microenvironment (e.g. MMP2/9, DPPIV, elastase, cathepsin G) resulting in proliferation and increased in CXCR4 receptor expression of progenitor cells as well as CXCL12 degradation. (4.) The changes in the BM CXCL12 gradient lead to the translocation of stem and progenitor cells into the peripheral blood and their homing towards the local CXCL12 gradient initiated in the myocardium. BM and progenitor cells selectively home to the ischemic myocardium where they are involved in myocardial repair through cardioprotective functions and induction of angiogenesis[21].

1.4.3.   CX$_3$CL1 (Fractalkine)

The CX$_3$CL1 is the only chemokine known until now, which belongs to the CX$_3$C chemokine subfamily. The CX$_3$CL1 is a large protein of 373 amino acids containing multiple domains and is structurally distinct from other chemokines[97]. Structurally, CX$_3$CL1 consists of an N-terminal chemokine domain which contains 76 amino acids with the unique 3-residue insertion between cysteins, which represents the extracellular domain. Connected to the extracellular domain, a mucin-like stalk follows, containing 241 amino acids with a predicted O-glycosylated serine and threonine. The transmembrane domain contains 19 amino acids, and is connected to an intracellular domain with a 37 amino acid residue[97]. CX$_3$CL1 exists in two different forms, i.e. a membrane-bound or soluble form after shedding from the cell surface[97]. Inflammatory cytokines such as IL-1, and interferon (IFN)-γ can induce the expression of membrane-bound CX$_3$CL1 on primary ECs[98]. The soluble CX$_3$CL1 is released by proteolysis at a membrane-proximal region by TNF-α–converting enzyme (TACE [ADAM17]) and ADAM10[99, 100]. The transmembrane protein supports integrin-independent leukocyte adhesion, whereas the soluble form of CX$_3$CL1 has a potent chemoattractant activity[90]. The soluble form exhibits its efficient chemotactic activity for monocytes/macrophages, NK cells and T-cells, whereas the membrane-bound form captures and enhances the subsequent migration of these cells in response to secondary stimulation with other chemokines.[98]. Furthermore, stimulation through membrane bound CX$_3$CL1 activates NK cells, leading to increased cytotoxicity and IFN-production. The endothelium is the first obstacle to leukocyte transmigration, the properties and functions of CX$_3$CL1 on ECs support its role as a gateway controlling leukocyte extravasation at sites of inflammation[97]. The CX$_3$CL1 chemokine domain is presented at the top of a cell-bound extended mucin-like stalk[98, 101], which functions as an adhesion molecule[102] thereby obviating the need for both the association with proteoglycans and other adhesion molecules[97]. Under static and physiological flow conditions CX$_3$CR1-expressing cells bind rapidly and with high affinity to immobilized CX$_3$CL1 or CX$_3$CL1-expressing cells[102-104]. It was shown with the help of video microscopy that CX$_3$CR1-expressing cells adhere more rapidly to immobilized CX$_3$CL1 than to vascular cell adhesion molecule (VCAM)-1 without cell tethering and dislodging under flow conditions[97, 105]. Thus, CX$_3$CL1 may facilitate the extravasation of circulating leukocytes by mediating cell adhesion through the initial tethering and the final transmigration steps[87](Figure 6).

Both leukocyte adhesion and chemoattractant activity of CX$_3$CL1 are mediated through the CX$_3$CR1 receptor, which is also involved in atherogenic monocyte recruitment[97, 106]. CX$_3$CL1 is upregulated on activated SMCs *via* NF-κB and triggers monocyte adhesion to SMCs *in vitro*[90, 107, 108]. In an endothelial denudation injury model, it was shown that the expression of

CX_3CL1 is delayed predominantly in ECs and neointimal SMCs[109]. After mechanical injury the reendothelialization is incomplete, so the CX_3CL1-expressing neointimal SMCs exposed to the blood stream may enhance chronic monocyte recruitment[110]. Indeed, CX_3CR1 deficiency protects animals from developing intimal hyperplasia as a result of decreased monocyte trafficking to the lesion. CX_3CR1 deficiency decreases VSMC proliferation and intimal accumulation either directly or indirectly as a result of defective monocyte infiltration[109]. It was already demonstrated, that TNF-α induces expression of CX_3CL1 and CX_3CR1 in rat aortic SMCs and this induction is mediated by NF-κB activation. Furthermore, CX_3CL1 induces its own expression, which is mediated by the PI 3-kinase/ PDK1/ Akt/ NIK/ IKK/ NF-κB signaling pathway. In addition, CX_3CL1 increases cell-cell adhesion and aortic SMC proliferation, indicating a role in initiation and progression of atherosclerotic and vascular disease[108]. Other studies confirm this assumption, by demonstrating high levels of CX_3CL1 mRNA expression, as well as mRNA encoding of other 16q13-chromosome–linked chemokines, CCL17 (thymus and activation-regulated chemokine [TARC]), and CCL22 (macrophage-derived chemokine [MDC]), have been observed in some, but not all, human arteries with advanced atherosclerotic lesions[111]. The distinctive staining patterns in native atherosclerosis and diabetes mellitus with atherosclerosis indicate that the expression of CX_3CL1 and CX_3CR1 may be important in the pathogenesis of these diseases[112]. Chemokines are the key regulators in monocyte migration from the blood to the vessel wall and the monocytes are the precursors of macrophages and foam cells during the progression of a atherosclerotic lesion[6]. Furthermore, it has been reported that CX_3CL1 expression is upregulated in atherosclerotic lesions of ApoE($^{-/-}$) mice and that crossing $CX_3CR1(^{-/-})$ into the ApoE($^{-/-}$) background results in decreased atherosclerotic lesion formation with reduced macrophage accumulation[113, 114]. Recently, it was observed that the reduction in atherosclerotic plaque size in hyperlipidemic mice upon aspirin administration was associated with a reduced lesional expression of CX_3CL1, a NF-κB target gene important in atherosclerosis[115, 116]. Although the macrophage accumulation in the lesions was not measured in this study, previous data suggests reduced CX_3CL1 expression to lower foam cell content in the plaques[116]. Another study shows that platelets in hyperlipidemic mice display increased CX_3CR1-expression and assemble with circulating monocytes. The formation of platelet-monocyte-complexes (PMC) and the detection of platelet-bound CX_3CL1 on inflamed SMCs suggest a significant involvement of the CX_3CR1–CX_3CL1 axis in platelet accumulation and monocyte recruitment at sites of arterial injury in atherosclerosis[117]. For influencing the CX_3CR1–CX_3CL1 axis, a CX_3CR1 antagonist called F1-CX_3CR1 with a modified N-terminus showing anti-inflammatory activity, was described[27]. The CX_3CR1 antagonist F1-CX_3CL1 strongly decreases the migration of the CX_3CR1-positive monocytic population, this study suggests that antagonists such as F1-CX_3CL1 might be useful in a

thorough analysis of inflammation pathways and in a therapeutic setting, in the ultimate prevention of the side effects of broad-spectrum inhibitors[27]. Another study showed that platelet-CX_3CR1 appears to play a notable role in PMC assembly, as preincubation of platelets with the CX_3CR1-antagonist F1-CX_3CL1 significantly decreased PMC formation. Similar observations could be made in mouse blood, since PMC formation during hyperlipidemia was dependent on CX_3CR1[117]. The F1-CX_3CL1 molecule could be used as a lead compound for the development of a novel class of anti-inflammatory substances that act by inhibiting CX_3CR1[27].
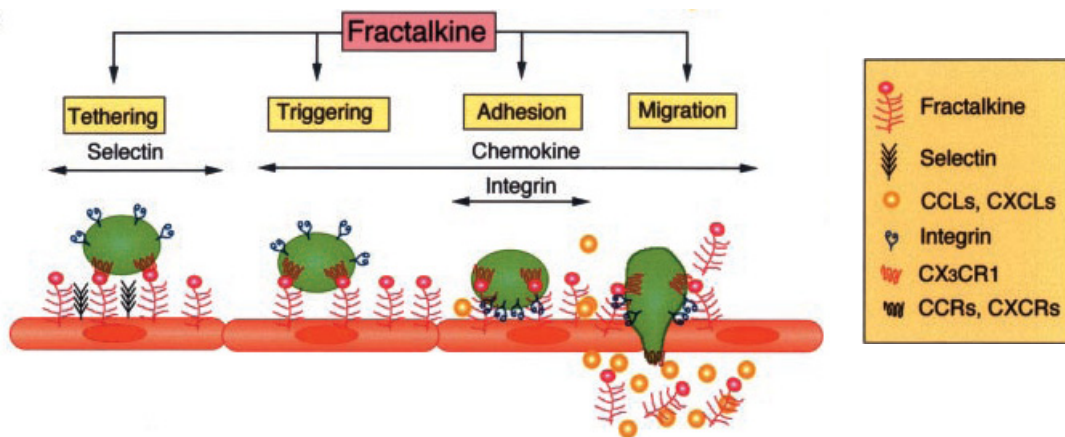
Figure 6: Schematic model of a CX_3CL1-mediated pathway in the adhesion cascade. Figure modified from Umehara et. al.[97]. CX_3CL1-mediated pathway. CX_3CL1 is expressed on ECs as the membrane-bound form and captures leukocytes in a selectin- and integrinindependent manner. Interaction between CX_3CL1 and CX_3CR1 can also increase integrin avidity, resulting in firmer adhesion. Leukocytes then extravasate through the vascular wall and into the tissue towards a chemokine gradient. CX_3CL1 may facilitate extravasation of circulating leukocytes by mediating cell adhesion through the initial tethering and final transmigration steps[97].

1.5. Biocompatible and Degradable Hydrogels

In recent years, the knowledge in the field of drug delivery grew and now it offers a suitable option of site-specific and/or time-controlled delivery of small or large molecular weight drugs and other bioactive agents[118]. To date several therapeutically active agents were formulated in biocompatible forms. These systems show many advantages in the area of drug delivery over conventional approaches. In terms of safety and efficacy, these systems are advantageous with regard to improved targeted delivery of drugs, improved bioavailability, extension of drug or gene effect in target tissue, and improved stability of therapeutic agents against chemical/enzymatic degradation[119].

In 1960, Wichterle and Lim[120] introduced a novel type of hydrophilic gel for biological use. Until now, a huge sum of efforts and studies has been devoted to advancing and extending the potentials attributed to hydrogels[118]. Growing of hydrogel technology led to substantial advances in the pharmaceutical and biomedical field[118]. Hydrogel particles are hydrophilic crosslinked polymeric particles with submicrometer size[121]. The important characteristics of hydrogels are biocompatibility, high-water content as well as tunable chemical and mechanical properties with the features of these particles such as high-surface area and overall sizes in the range of cellular compartments[121]. While the water content of a hydrogel determines its unique physicochemical characteristics, these structures have some common physical properties resembling that of the living tissues, than any other class of synthetic biomaterials, which is attributed to their highwater content, their soft and rubbery consistency, and low interfacial tension with water or biological fluids[118]. Despite their high water absorbing affinity, hydrogels shows swelling behavior instead of being dissolved in the aqueous surrounding environment as a consequence of the critical crosslinks present in the hydrogel structure[118]. These networks can be classified into two main categories according to the types of cross-linking. The network cross-linked by covalent bonds is the so-called chemical gel, while the formation of physical gel takes place *via* physical association between polymeric chains and particles[122]. In some cases, chemical and physical gelling might coexist in one hydrogel[122]. These properties make them intriguing candidates for entrapment of hydrophilic bioactive molecules such as DNA or proteins to provide a hydrophilic environment and protect them from degradation[118, 121].

In general, hydrogels can be classified based on a variety of characteristics, including the nature of side groups (neutral or ionic), mechanical and structural features (affine or phantom), method of preparation (homo- or co-polymer), physical structure (amorphous, semicrystalline, hydrogen bonded, supermolecular, and hydrocollodial), and responsiveness to physiologic environment stimuli (pH, ionic strength, temperature, electromagnetic radiation, etc.)[118]. Hydrogels may absorb between 10-20% and up to thousands of times of

their dry weight in water, but they are chemically stable or they may degrade and eventually disintegrate and dissolve[123]. They are called 'reversible', or 'physical' gels when the networks are held together by molecular entanglements, and/or secondary forces including ionic, H-bonding or hydrophobic forces[123-125]. Physical hydrogels are not homogeneous, since clusters of molecular entanglements, or hydrophobically- or ionically-associated domains, can create inhomogeneities. Free chain ends or chain loops also represent transient network defects in physical gels[123]. Chemical hydrogels may be generated by crosslinking of water-soluble polymers, or by conversion of hydrophobic polymers to hydrophilic polymers plus crosslinking to form a network[123]. Hydrophilic hydrogels with high amounts of water in their structures show distinctive properties compared to hydrophobic polymeric networks[118]. Gel formation usually proceeds at ambient temperature and organic solvents are rarely required. In-situ gelation with cell and drug encapsulation capabilities further distinguishes hydrogels from the other hydrophobic polymers[126]. Hydrogels, particularly those intended for applications in drug delivery and biomedical purposes, are required to have acceptable biodegradability and biocompatibility which necessitates the development of novel synthesis and crosslinking methods to design the desired products[118]. An ideal injectable medical hydrogel should meet the following requirements: 1) In order to guarantee the injectability, the system should be, as usual, in a sol state before administration. "A sol is a colloidal suspension of solid particles (1-500 nanometres in size) in a liquid. The sol is desired to be of sufficiently low viscosity and thus allow a smaller pinhead in injection to alleviate the pain of a patient. 2) Gelation *via* either chemical crosslinking or physical association starts to happen or is completed after injection. 3) The gels should be biodegradable or gradually dissolvable, and the products should be bioresorbable. 4) The polymer itself and its degradable products as well as some necessary additives such as crosslinking agents in the case of *in situ* chemical gelling should be biocompatible. 5) Some specific requirements should be met, for instance, a sustained release profile for a drug delivery system, or cell-adhesive capability for tissue engineering[122].

For this study a biocompatible and degradable hydrogel carrier composed of thiol-functionalized polymers based on star-shaped poly(ethylene oxide-stat-propylene oxide) (sP(EO-stat-PO)) and linear poly(glycidol) (PG) has been used. Hydrogel particles are prepared by crosslinking of the polymers in inverse mini emulsion *via* oxidation of thiol groups to disulfide bonds[121]. *In vitro* and *in vivo* studies have revealed that these thermogelling copolymers are of good biocompatibility and mechanical property[122]. Hydrogels were rapidly formed once injected and no significant immune response were observed in the surrounding of the injection sites[127, 128]. These hydrogels could be also potentially used as a drug delivery system, for a controlled release of other proteins, siRNA, and DNA.

1.6.   Myocardial infarction (MI) therapies

To obtain the restoration of the normal coronary blood flow and the regeneration of the myocardium after MI, different long-term therapies are actual. Very important for prevention of the disease is the prophylaxis of patients with suspicion for potential development of MI, even before the diagnosis is confirmed. Currently, various therapeutic approaches are being applied, for example antiplatelet agents, anticoagulants, GP IIb/IIIa antagonists, thrombolysis, beta blockers, nitrates, selective aldosterone blockers, as well as analgesia for reducing pain and anxiety. Angiotensin-converting enzyme (ACE) inhibitors or statins are also often prescribed shortly after MI[129]. Antiplatelet therapy prevents thrombus formation in the vast majority of patients presenting with an MI. The most prominent drug that is used as antiplatelet therapy is aspirin. Not only the anti-coagulant, but also the anti-inflammatory properties of aspirin influence positively the patient. In some cases, aspirin is contraindicated, due to hypersensitivity or gastrointestinal complications. Then clopidogrel is a good alternative. Clopidogrel is a thienopyridine derivative that exerts an irreversible antiplatelet effect by antagonizing adenosine phosphate. The combination of aspirin and clopidogrel provides additional antiplatelet activity[129]. The usage of heparin as an anticoagulant, which is an indirect thrombin inhibitor which complexes with antithrombin III and converts this circulating cofactor from a slow to a rapid inactivator of thrombin, factor Xa, and to a lesser extent, factors XIIa, XIa, and IXa, may be used in the clinic[130]. The development of the GP IIb/IIIa antagonists, a new class of potent antiplatelet drugs, has the potential to considerably enhance the treatment of acute myocardial infarction (AMI) patients. A number of recent studies have highlighted the potential incremental benefits with adjunctive IIb/IIIa-targeted therapy[131]. To reduce the infarct size and to improve the survival of the patients, the restoration of the perfusion to the ischemic area by lysis the clot is necessary. This may be obtained by thrombolytics, such as streptokinase and tissue plasminogen activator[129]. Beta-blocker application is a further therapeutic approach to treatment MI[129]. There are different effects on the myocardium applying beta-blockers, such as initial diminishing of myocardial oxygen demand by reducing heart rate, systemic arterial pressure, and myocardial contractility and the prolongation of diastole may augment perfusion to injured myocardium. Beta-blockade is now established as a highly effective therapy that reduces morbidity and mortality in patients with heart failure associated with reduced systolic function[132]. Furthermore the intravenous application of nitrates may be useful during the acute phase in patients with hypertension or heart failure, provided that there is no hypotension, right ventricular infarction or use of phosphodiesterase type 5 inhibitors in the previous 48 h. In the acute and stable phase, nitrates remain valuable agents to control anginal symptoms[129]. The effects of ACE inhibitors are dilation of blood vessels and decrease resistant by lowering levels of angiotensin II, for an easier flow of blood

through the blood vessel. Clinical studies using the treatment of ACE inhibitors demonstrate an improvement in hemodynamics, LV remodeling, and mortality. The effect of ACE inhibitors during the acute phase of AMI was less clear, although there was evidence of protection from ischemic damage, possibly mediated by an increase in collateral coronary blood flow[133]. For the therapy of MI, statins may be also used to lower LDL cholesterol, raise high-density lipoprotein (HDL) cholesterol and lower triglyceride levels. The benefits of statins in prevention have been unequivocally demonstrated[134], and specific trials have demonstrated the benefit of early and intensive statin therapy[135, 136]. Recent meta-analysis of trials compared more- vs. less-intensive LDL-cholesterol lowering with statins. The obtained data indicate that more-intensive statin therapy produced reductions in the risks of cardiovascular death, non-fatal MI, ischemic stroke and coronary revascularization[129]. Taken together, this major cause of death can not be cured completely with the present therapeutic approaches. For this reason, new therapeutic approaches are explored.

Current strategies have been proposed the progenitor cell therapy, which was considered as a promising therapeutic approach to provide an alternative way to regenerate the heart structure after MI. Pioneering studies in animals have shown that transplantation of adult stem cells after acute MI improves neovascularization and reduces fibrosis, preserving the left ventricular heart function[137, 138]. Unfortunately, these promising results were less pronounced in clinical studies in patients[139], probably due to incorrect translation of the knowledge from the animal to the human system. New data suggest that the main mechanism of improving the heart function by cell therapy is in fact due to the inflammation and its consecutive effects[140]. These findings are of notable significance, since it is known to be able to selectively control and manipulate the inflammatory reaction through chemokines[20].

Despite extensive research, the current knowledge regarding the control of molecular and cellular events after MI is still limited. Therefore, to be able to create efficient therapies, it is important to understand how all these processes are modulated and controlled. Chemokines and chemokine receptors have the most precise functions in leukocyte trafficking, angiogenesis, collagen synthesis, and cardiac repairing[20]. Manipulating this processes, by interfering with receptor–ligand interaction, chemokine–GAG interaction, heteromerization, or signaling pathways induced upon receptor activation[141], should enable to control and modify molecular and cellular events[20].

A novel therapeutic approach showed the injection of an antagonist blocking the chemokine CCL5, which reduce myocardial leukocyte infiltration in a mouse model of induced myocarditis. The treatment with Met- CCL5 clearly diminished the infiltration of T-cells and fibronectin deposition, critical aspects of cardiomyopathy, in the heart of the mice[142].

However, additional studies are required to clarify the role of CCL5 in post-ischemic cardiac repair.

One potentially promising strategy for repairing damaged cardiac tissue following MI involves the use of CXCL12 to prevent or reverse heart failure[143]. Different scientists have shown that the cells can be mobilized and home to areas of injury, in part in response to the CXCL12/CXCR4 interaction[143, 144]. The essential role of CXCL12 in BM homing and recruitment was already demonstrated several times[145, 146]. This promising chemokine has been tested in gene therapy as a recruiter of BM-derived cells to the myocardium, in a murine infarct model[38, 147, 148]. The CXCL12 acts through CXCR4 and indeed recruit BM-derived cells to the injured tissue, supporting the notion that this chemokine might have therapeutic potential[143]. Different clinical trials in this area have been recently completed or are still ongoing. For example, a phase 1 trial that is currently tested, is examining the effects of CXCL12 on infarcted hearts, where the ligand is injected directly into the heart and then monitoring homing of bone marrow cells (BMCs) into the myocardium of patients with ischemic heart disease. Also noteworthy is an open-label dose-escalation study to evaluate the safety of a single escalating dose of CXCL12, administered by endomyocardial injection to cohorts of adults with ischemic heart failure, which is currently enrolling patients, here naked DNA that encodes CXCL12 is being injected directly into the myocardium as a single dose at multiple sites through a percutaneous, left ventricular approach, using a needle injection catheter (ClinicalTrials.gov identifier: NCT01082094). These trials will demonstrate the safety and efficacy of using chemokines e.g. CXCL12 to treat heart failure in subjects with ischemic cardiomyopathy[143].

2.   Aim of the study

Chemotactic cytokines and their receptors exert a fundamental role in the development of atherosclerosis and in the process of ischemic tissue revitalization through angiogenesis. The first part of this work was aimed to express and purify different modified chemokines and/or chemokine antagonists to study their role in cardiovascular diseases (CVDs). These chemokines and/or chemokine antagonists are Met-CCL5, protease-resistant CXCL12 (S4V), CXCL12 (S2G4V) and F1-CX$_3$CL1, which were expressed in *E. coli* as "*inclusion bodies*" in the cytoplasm and were purified by different sequential steps with chromatographic methods using FPLC and HPLC.

The major goal of this study was to design a novel therapeutic strategy with Met-CCL5 and the protease-resistant CXCL12 (S4V) variant. Met-CCL5 is a chemokine receptor antagonist which retains the initial neutrophil infiltration during inflammation after MI. The protease-resistant CXCL12 (S4V) variant is resistant to MMP-2 and exopeptidase cleavage, but retains its chemotactic bioactivity for the recruitment of circulating hematopoietic cells and promotes neovascularization after MI. For a proper time-controlled local release of the Met-CCL5 and protease-resistant CXCL12 (S4V), two different biodegradable hydrogels were implemented. A fast degradable hydrogel (FDH) for delivering Met-CCL5 over 24 h and a slow degradable hydrogel (SDH) for a gradual release of CXCL12 (S4V) over 4 weeks. Both chemokines in biodegradable hydrogels were injected locally into the mouse heart after induction of MI. The major question of the second part of this work was:

- Is the combined therapy with Met-CCL5 in FDH and protease-resistant CXCL12 in SDH a successful therapeutic strategy for the therapy after MI?

The chemokine receptor CX$_3$CR1 is an inflammatory mediator in vascular disease. On platelets, its ligation with CX$_3$CL1 induces platelet activation followed by leukocyte recruitment to activated endothelium. Here, the role of platelet-CX$_3$CR1 during the development of atherosclerosis was explored. The third goal of this work was to find the importance of the platelet-CX$_3$CR1 and CX$_3$CL1 for the formation of platelet monocyte complexes (PMC). The question of this part of the work was:

- Does platelet F1-CX$_3$CL1 antagonist play a role in PMC formation?

3. Materials

All protocols were adapted from standard protocols unless otherwise described. The solutions are prepared with double distilled water (Heraeus Destamat, Heraeus, Germany) or Millipore water (Milli-Q Plus ultrapure purification, Millipore, MA). Reagents were purchased from Fluka (Buchs, Switzerland), Sigma (Deisenhofen, Germany), or Roth (Karlsruhe, Germany) unless otherwise specified. All animal studies were approved by local authorities and complied with German animal protection law.

3.1. Instruments

Equipment	Manufacturer
Autoclave	Systec 2540EL (Systec, Wettenberg, Germany)
Balance	Analytical Plus, (Ohaus, Pine Brook, USA)
Blotting System	iBlot[®] 7-Minute Blotting System (Invitrogen, San Diego, USA)
Centrifuges	Eppendorf 5417C (Eppendorf, Hamburg, Germany), Heraeus Labofuge 400 and Heraeus Multifuge 3 S-R (Heraeus, Osterode, Germany), Beckman Avanti[®] J 30 I (Beckman Coulter, Krefeld, Germany)
Dialysis membrane (MWCO (molecular weight cut off) = 3500Dalton (Da))	Spectrum Laboratories, Inc (DG Breda, Netherlands)
Diskus Software	Carl H. Hilgers (Königswinter, Germany)
Echocardiograph	Vevo 770[®] (Visual Sonics, Toronto, Canada)
Electroporator	Gene Pulser[®] II (Bio-Rad, Hercules, USA), Nucleofector[®] Device (Amaxa[®], Cologne, Germany)
Fermenter/bioreactor	LAMBDA laboratory instruments (Baar, Switzeland)
Flow cytometers	FACS Canto II (BD Biosciences, San Jose, CA, USA)
Fluorescence	Microplate reader SpectraFluor Plus (Tecan, Crailsheim, Germany), LS 55 Fluorescence Spectrometer (PerkinElmer, USA)
FPLC system	Äkta™ FPLC (Amersham/GE Healthcare, Uppsala, Sweden)
Gel electrophoresis	Mini-sub Cell[®] GT (Bio-Rad, Hercules, USA)

Equipment	Manufacturer
Heparin sepharose™ 6 fast flow	GE Healthcare (Uppsala, Sweden)
HPLC system	Spectra System SCM (Thermo Electron Corp., Thermo Scientific®, Waltham, USA), Varion Prostar HPLC System (Varian Inc., Palo Alto,USA), Waters Delta Prep 3000 HPLC System (Waters Corp., Milford, USA)
HisTrap™ HP	GE Healthcare (Uppsala, Sweden)
Image reader	LAS 3000 (Fujifilm, Düsseldorf, Germany)
Incubator	Innova 4230 (New Brunswick Scientific, USA)
Laminar flow cabinet	Herasafe (Heraeus, Osterode, Germany)
Lyophilisator	Alpha 2-4 LD plus (Christ, Osterode, Germany)
Microscopes	Olympus IX71, IX50, IX81 (Olympus Optical, Hamburg, Germany)
Microplate reader	GENios (Tecan, Männedorf, Switzerland)
Microtome	Cut 6062 (SLEE, Mainz, Germany)
Ni-NTA^{TM} Column	GE Healthcare (Uppsala, Sweden)
PCR thermocyclers	MyCycler (Bio-Rad, Hercules,USA)
pH-meter	InoLab level 1 (WTW, Weilheim, Germany)
Resource S	GE Healthcare (Uppsala, Sweden)
Rodent respirator	Harvard Apparatus (March Hugstetten, Germany)
Sonicator	Branson S-250 D Digital Sonifier (Branson, Danbury, USA)
SP Sepharose FF™ column	GE Healthcare (Uppsala, Sweden)
Spectrophotometer	GeneQuant^{TM} 1300 (Amersham/GE Healthcare, Uppsala, Sweden), NanoDrop 1000 (PeqLab, Erlangen, Germany)
Tricon Mono S^{TM} 5/50GL	GE Healthcare (Uppsala, Sweden)
Vydac® column C8 250x10mm, 5µm	Grace (Deerfield, USA)

3.2.   Reagents and general materials

Reagents	Manufacturer
Acrylamide (30%)/bisacrylamide (0,8%)	Roth (Karlsruhe, Germany)
Adenosin-5'triphosphate (ATP)	Sigma (Taufkirchen, Germany)
Agarose, ultra pure	Roth (Karlsruhe, Germany)
Ampicillin	Sigma (Taufkirchen, Germany)
Ammonium persulfate (APS)	Roth (Karlsruhe, Germany)
Aqua ad injectabilia	Braun (Melsungen, Germany)
Bacto-agar	Roth (Karlsruhe, Germany)
Benzonase® nuclease	Novagen/Merck Bioscience (Darmstadt, Germany)
β-mercapthoethanol	Sigma (Taufkirchen, Germany)
Bicoll	Biochrom AG (Berlin Germany)
Bouin´s solution	Sigma (Taufkirchen, Germany)
Bovine serum albumin (BSA)	Sigma (Taufkirchen, Germany)
Bromphenolblue	Sigma (Taufkirchen, Germany)
BugBuster® Protein Extraction Reagent	Novagen/Merck Bioscience (Darmstadt, Germany)
Calcein	Invitrogen (San Diego, USA)
Calciumchloride ($CaCl_2$)	Sigma (Taufkirchen, Germany)
Carbenicillin	Roth (Karlsruhe, Germany)
complete Mini, EDTA-free tablets	Roche (Penzberg, Germany)
Coomassie brilliant-blue G-250	Roth (Karlsruhe, Germany)
Cysteamine (2-mercaptoethylamine)	Biochemica (Eastern, USA)
Cysteine	Fluka (Buchs, Switzerland)
Cystine	Fluka (Buchs, Switzerland)
DAPI	Vector (Burlingame, CA, USA)
Deuterium oxide 99.9%	Deutero (Kastelbraun, Germany)
Dichloromethane (HPLC grade)	Sigma (Taufkirchen, Germany)

Reagents	Manufacturer
Dimethyl sulfoxide (DMSO)	Fluka (Neu-Ulm, Deutschland)
5,5'-dithio-bis-(2-nitrobenzoic acid) (DTNB)	Novagen/Merck Bioscience (Darmstadt, Germany)
Dithiothreitol (DTT)	Roth (Karlsruhe, Germany)
3,3'-dithiodipropionic acid	Sigma (Taufkirchen, Germany)
4 DMAP (99+%)	Sigma (Taufkirchen, Germany)
100 bp DNA ladder	New England Biolabs (Ipswich, USA)
1 kb DNA ladder	Sigma (Taufkirchen, Germany)
Enterokinase	Novagen[®]/Merck Bioscience (Darmstadt, Germany)
Ethanol	Roth (Karlsruhe, Germany)
Ethidiumbromide	Sigma (Taufkirchen, Germany)
Ethylenediaminetetraacetic acid (EDTA)	Calbiochem (Schwalbach, Germany)
Ethylene oxide-stat-propylene oxide (sP(EO-stat-PO)	Dow Chemicals (Terneuzen, Netherlands)
Fetal calf serum (FCS)	PAA (Pasching, Austria)
Fibronectin	Biochrom (Berlin, Germany)
Formalin	Roth (Karlsruhe, Germany)
Glycerol	Sigma (Taufkirchen, Germany)
Glycine	Roth (Karlsruhe, Germany)
Gomori's 1-step trichrome stain	Sigma (Taufkirchen, Germany)
Guanidine-HCl	Roth (Karlsruhe, Germany)
Hirudin	Bayer Healthcare (Leverkusen, Germany)
Hydrochloride (HCl)	Roth (Karlsruhe, Germany)
hydrogen peroxide	VWR (Darmstadt, Germany)
HEPES	Roth (Karlsruhe, Germany)
iBlot[®] gel transfer stacks nitrocellulose, regular	Invitrogen (San Diego, USA)
Imidazole	Roth (Karlsruhe, Germany)

Reagents	Manufacturer
Isopropyl alcohol	Novagen/Merck Bioscience (Darmstadt, Germany)
Isopropyl β-D-1-thiogalactopyranoside (IPTG)	Roth (Karlsruhe, Germany)
Kanamycine	Roth (Karlsruhe, Germany)
Ketamin CEVA	CEVA (Düsseldorf, Germany)
L-Glutathione oxidized	Roth (Karlsruhe, Germany)
L-Glutathione reduced	Roth (Karlsruhe, Germany)
Lysozyme	Roth (Karlsruhe, Germany)
Magnesium chloride ($MgCl_2$)	Roth (Karlsruhe, Germany)
Mayer´s hemalum solution	Novagen/Merck Bioscience (Darmstadt, Germany)
Mayer's hematoxylin solution	Applichem (Darmstadt, Germany)
MES	Roth (Karlsruhe, Germany)
Methanol	Promochem (Wesel, Germany)
Monopotassium phosphate	Roth (Karlsruhe, Germany)
Naphthol AS-D Chloroacetate Kit	Sigma (Taufkirchen, Germany)
N,N'-dicyclohexyl-carbodiimide (DCC), (99%)	Acros (Geel, Belgium)
Nucleoside triphosphate master mix (dNTP)	Eurogentec (Seraing, Belgium)
PageBlue™ Protein Staining Solution	Fermentas (Ontario, Canada)
Paraformaldehyde	Sigma (Taufkirchen, Germany)
Penicillin	PAA (Pasching, Austria)
Phosphate buffered saline (PBS)	PAA (Cölbe, Germany)
3.0 µm/ 8.0 µm pore polycarbonate membrane insert	Costar (MA, USA)
Polyethylene glycol (PEG) 8000	Promega (Madison, USA)
Poly(ethyleneglycol) diacrylate (PEG-DA)	Sigma (Taufkirchen, Germany)
Polymorphprep™	AXIS-SHIELD (Oslo, Norway)
Ponceau S	Sigma (Taufkirchen, Germany)

Reagents	Manufacturer
Potassium chloride (KCl)	Sigma (Taufkirchen, Germany)
Potassium hydrogen phosphate (KH_2PO_4)	Sigma (Taufkirchen, Germany)
Rhodamine 6G	Sigma (Taufkirchen, Germany)
Roti®-Block	Roth (Karlsruhe, Germany)
Silver nitrate	Novagen/Merck Bioscience (Darmstadt, Germany)
Sodium carbonate	Roth (Karlsruhe, Germany)
Sodium chloride	Prolabo (Montreal, Canada)
Sodium deoxycholate	Sigma (Taufkirchen, Germany)
Sodium phosphate	Novagen/Merck Bioscience (Darmstadt, Germany)
Sodium dodecyl sulfate (SDS)	Roth (Karlsruhe, Germany)
Sodium hydroxide (NaOH)	Sigma (Taufkirchen, Germany)
Sodium thiosulfate	Roth (Karlsruhe, Germany)
Streptavidin	PAA (Pasching, Austria)
Sulfuric acid (H_2SO_4)	Sigma (Taufkirchen, Germany)
Taurine	Sigma (Taufkirchen, Germany)
N,N,N',N'-Tetramethylethylendiamin (TEMED)	Roth (Karlsruhe, Germany)
Trifluoroacetic acid (TFA)	Sigma (Taufkirchen, Germany)
Tris (2-carboxyethyl) phosphine (TCEP) (99%)	Sigma (Taufkirchen, Germany)
Tris-(hydroxymethyl)-aminomethane (tris) (TAE)	Roth (Karlsruhe, Germany)
Tris-HCl	Roth (Karlsruhe, Germany)
Triton™ X-100	Sigma (Taufkirchen, Germany)
Tween®-20	Roth (Karlsruhe, Germany)
Tryptone/peptone from casein	Roth (Karlsruhe, Germany)
Urea	Roth (Karlsruhe, Germany)
Vitro Clud®	R. Langenbrinck Labor und Medizintechnik

Reagents	Manufacturer
	(Emmendingen, Germany)
Xylol	Honeywell (Offenbach, Germany)
Yeast extract	Roth (Karlsruhe, Germany)

3.3.   Cell culture materials

Name	Manufacturer
Accutase™	PAA (Pasching, Austria)
Collagen G	Biochrom
Gentamycin	Gibco® (Darmstadt, Germany)
HBSS	Gibco® (Darmstadt, Germany)
Human albumin	Baxter (Deerfield, IL, USA)
Human serum	PAA (Pasching, Austria)
L-Glutamine	PAA (Pasching, Austria)
Trypanblue	Sigma (Taufkirchen, Germany)
Trypsin	PAA (Pasching, Austria)

3.4.   Enzymes

Name	Manufacturer
BglII	Fermentas (St. Leon-Rot, Germany)
DNAse I	Sigma (Taufkirchen, Germany)
DpnI	Stratagene (La Jolla, USA)
GoTaq® DNA Polymerase	Promega (Madison, USA)
KpnI	Fermentas (St. Leon-Rot, Germany)
NotI	Fermentas (St. Leon-Rot, Germany)
PfuUltra High Fidelity DNA Polymerase	Stratagene (La Jolla, USA)
Reverse transcriptase	Invitrogen (San Diego, USA)
T4 DNA Ligase	Promega (Madison, USA)
XhoI	Fermentas (St. Leon-Rot, Germany)

Name	Manufacturer
XbaI	Fermentas (St. Leon-Rot, Germany)

3.5.   Cytokines and recombinant proteins

Name	Manufacturer
mCXCL12/SDF-1	PeproTech (Hamburg, Germany)
CCL5/RANTES	PeproTech (Hamburg, Germany)
CXCL8/IL-8	PeproTech (Hamburg, Germany)
CX_3CL1/Fractalkine	PeproTech (Hamburg, Germany)

3.6.   Antibodies

3.6.1.   Primary Antibodies

Name	mAb/Clone	Manufacturer
CD3	Rat anti-mouse/ KT3	Serotec (Düsseldorf, Germany)
CD31	Goat anti-mouse/M-20	Santa Cruz (Santa Cruz, USA)
Alpha-smooth muscle actin (α-SMA)	Mouse anti-human/1A4	DAKO (Hamburg, Germany)
F4/80	Rat anti-mouse/CI:A31	Serotec (Düsseldorf, Germany)
Human/mouse CXCL12/SDF-1	*E. coli* derived recombinant human CXCL12/SDF1α Lys 22Lys89 /79018	R&D Systems (Minneapolis, USA)
Human CCL5/RANTES	*E. coli* derived recombinant human CCL5/RANTES /16411	R&D Systems (Minneapolis, USA)
Anti-human CX3CL1/Fractalkine	NS0-derived rhCX3CL1/51637	R&D Systems (Minneapolis, USA)

3.6.2. Secondary Antibodies

Name	mAb	Manufacturer
Goat IgG, Cy3-conjugated	Rabbit anti-goat-IgG	Jackson Immuno Research (Hamburg, Germany)
Goat IgG, FITC-conjugated	Goat anti-rat-IgG	Jackson Immuno Research (Hamburg, Germany)
Goat IgG, FITC-conjugated	Goat anti-mouse-IgG	Jackson Immuno Research (Hamburg, Germany)
Rat IgG, Cy3-conjugated	Donkey anti-rat-IgG	Jackson Immuno Research (Hamburg, Germany)
Goat anti-rabbit IgG-HRP	Goat anti-rabbit IgG	Santa Cruz (Santa Cruz, USA)
Streptavidin-Biotinylated Horseradish Peroxidase Complex	-	Amersham/GE Healthcare, Uppsala, Sweden

3.6.3. Isotype controls

Name	mAb	Manufacturer
IgG2A	Rat	R&D Systems (Minneapolis, USA)
IgG1	Rat	Serotec (Düsseldorf, Germany)
Normal IgG	Mouse	Santa Cruz (Santa Cruz, USA)

3.7. Kits

Name	Manufacturer
BrdU Proliferation Assay	Novagen/Merck Bioscience (Darmstadt, Germany)
CellTiter-Blue® cell viability assay	Promega (Mannheim, Germany)
DC Protein Assay	BioRad (Hercules, USA)
ECL Western blotting detection reagents	Amersham/GE Healthcare (Uppsala, Sweden)
GoTaq® Flexi DNA polymerase kit	Promega (Madison, USA)
Human CCL5/RANTES DuoSet Elisa	R&D Systems (Minneapolis, USA)

Name	Manufacturer
Mouse CCL5/RANTES DuoSet Elisa	R&D Systems (Minneapolis, USA)
Mouse CXL12/SDF-1 DuoSet Elisa	R&D Systems (Minneapolis, USA)
QIAprep Spin Mini Kit	Qiagen (Hilden, Germany)
QIAquick gel extraction kit	Qiagen (Hilden, Germany)
QuikChange® II Site-Directed Mutagenesis Kit	Stratagene (La Jolla, USA)
QIAGEN Plasmid Midi Kit™	Qiagen (Hilden, Germany)
QIAGEN Plasmid Maxi Kit™	Qiagen (Hilden, Germany)

3.8.   Plasmids

Name	Description
pET-32a(+)	expression vector containing a Thioredoxin (Trx) Tag fused with the recombinant protein (Novagen/Merck, Darmstadt, Germany)
pET-32a(+)/mCXCL12 (S4V and S2G4V)	CCL5 expression vector, this study
pET-26b(+)	expression vector containing pelB signal sequence for secretion of the recombinant protein into periplasma (Novagen/Merck Bioscience, Darmstadt, Germany)
pET-26b(+)/Met-CCL5	Met-RANTES expression vector, this study
pET-26b(+)/F1-His-anta	F1-His-anta expression vector, this study

3.9.   Primers

3.9.1.   Site directed mutagenesis primers

Primer/Sequence

SDF1a_neu_s:
5´- GGC TGA CTG GTT TGG ACT TGT CGT CGT CGT CG -3`

SDF1a_neu_as:
5´- CGA CGA CGA CGA CAA GTC CAA ACC AGT CAG CC -3`

SDF1a_S4V_s:
5´- AGGGGCATCGGTAGCTCAGGACGACTGGTTTGGACTTGTC -3

SDF1a_S4V_as:

Primer/Sequence

5´- GACAAGTCCAAACCAGTCGTCCTGAGCTACCGATGCCCCT -3`

SDF1a_S2G_s:
5´- GGT AGC TCA GAA CGA CTC CTT TGC TCT TGT CGT CGT CG -3`

SDF1a_S2G_as:
5´- CGA CGA CGA CAA GAG CAA AGG AGT CGT TCT GAG CTA CC -3`

SDF1a_S2G_2_s:
5´- GGT AGC TCA GAA CGA CTC CTT TGC TCT TGT CGT CGT CAT CGG TAC CC -3`

SDF1a_S2G_2_as:
5´- GG GTA CCG ATG ACG ACG ACA AGA GCA AAG GAG TCG TTC TGA GCT ACC -3`

et32_as:
5´- TGG CAT CCG TGG TAT CCC GAC T -3`

Met-CCL5_s:
5´- ATC ATA TGT CCC CAT CCT CGG ACA CCA C -3´

Met-CCL5_as:
5´- ACG GAT CCT AGC TCA TCT CCA AAG AGT TG -3´

3.9.2. Sequencing primers

Primer/Sequence

T7:
5´- TAA TAC GAC TCA CTA TAG GG -3`

T7 term:
5´- CTA GTT ATT GCT CAG CGG T -3`

pUC57s:
5´- GTA AAA CGA CGG CCA GTA -3`

3.9.3. Reverse transcriptase primer

Primer/Sequence

Oligo dT:
5´- TTT TTT TTT TTT TTT -3´

3.10.   Bacterial strains and cell lines

Name	Manufacturer
BL21 (DE3) pLysS	Stratagene (La Jolla, USA)
DH5α™	Invitrogen (San Diego, USA)
XL1-Blue	Stratagene (La Jolla, USA)
Rosetta™ (DE3) pLysS	Novagen/Merck Bioscience (Darmstadt, Germany)
Human Umbilical Vein Endothelial Cells (HUVEC)	PromoCell (Heidelberg, Germany)
Human Aortic Smooth Muscle Cells (HAoSMCs)	PromoCell (Heidelberg, Germany)
Jurkat T-cells	Leibniz-Institute DSMZ-German Collection of Microorganisms and Cell Culture (Braunschweig, Germany)

3.11.   Bacterial and cell culture media

Name	Components
LB (Luria-Bertani) medium	0.5% (w/v) yeast extract 1% (w/v) peptone 1% (w/v) NaCl
LB agar medium	LB medium with 1.4% (w/v) agar
SOB (Super Optimal Broth) medium	0.5% (w/v) yeast extract 2% (w/v) peptone 10 mM NaCl 2.5 mM KCl 10 mM MgCl 10 mM MgSO$_4$
SOC medium	SOB with 20 mM glucose
TB medium	1.2% (w/v) peptone 2.4% (w/v) yeast extract 0.4% (v/v) glycerol
EOC Medium	Endothelial Cell Growth Medium MV2 (PromoCell, Heidelberg, Germany) Endothelial Cell Growth MV2 Supplement (PromoCell, Heidelberg, Germany)

Name	Components
HUVEC Medium	Endothelial Cell Growth Medium (PromoCell, Heidelberg, Germany)
	Endothelial Cell Growth Supplement (PromoCell, Heidelberg, Germany)
HAoSMC Medium	Smooth Muscle Cell Medium (PromoCell, Heidelberg, Germany)
	Smooth Muscle Cell Medium Supplement (PromoCell, Heidelberg, Germany)
Jurkat T-cell Medium	RPMI 1640 (PAA, Pasching, Austria) 10% FBS + 2 mM L-Glutamine

3.12. Solutions

Name	Components
Antibody buffer	0.13% EDTA 0.15% bovine serum albumin (BSA) In phosphate-buffered saline (PBS)
Blocking buffer (western blot)	5% (w/v) of nonfat dry milk in TBST
Destaining solution (Coomassie blue staining)	12.5% (v/v) isopropanol 30% (v/v) EtOH
DNA loading buffer (6x)	30% (v/v) glycerol 6 mM EDTA 0.25% (w/v) bromophenol blue 0.25% (w/v) xylenecyanol
Electrophoresis buffer (SDS-PAGE)	250 mM Tris base 1.92 M glycine 1% (w/v) SDS
Mini/Midiprep and maxiprep buffer I	50 mM glucose 25 mM Tris-HCl, pH 8.0 10 mM EDTA, pH 8.0
Mini/Midiprep and maxiprep buffer II	200 mM NaOH 1% (w/v) SDS
Mini/Midiprep and maxiprep buffer III	3 M potassium acetate, pH 5.5
TSS buffer	10% (w/v) Polyethylene glycol 5% (v/v) DMSO 20 mM $MgCl_2$ in 1x LB medium (1.3.13)

Name	Components
TAE electrophoresis buffer (1x)	40 mM Tris-acetate 1 mM EDTA
TBS (1x) (western blot)	25 mM Tris-HCl, pH 7.4 2.7 mM KCl 137 mM NaCl

3.13. Mice

Wild type C57BL/6J mice were purchased at Charles River, England.

4. Methods

4.1. Cell culture

4.1.1. Bacterial culture

Plasmid transformed *E. coli* were cultured on LB plates with ampicillin (100 µg/ml) or kanamycine (35 µg/ml) or chloramphenicol (40 µg/ml) and grown for 24 h at 37°C. To achieve a single colony growth, a single bacteria colony was picked and inoculated in a mini culture LB medium with appropriate antibiotics and shaken overnight at 37°C. To achieve a desired amount of expressing bacteria, the bacterial mini culture was inoculated in 1L of LB medium and cultured over night at 37°C with vigorous shaking. The culture was then used for preparing frozen glycerol cultures, plasmid DNA or fusion protein purification. For long-term storage of bacteria, a glycerol stock culture was prepared by growing bacteria in culture medium over night with the appropriate antibiotics. 500 µL of the bacterial culture was added to 80% glycerol and then mixed thoroughly in a small 1.5 mL tube. The stock solution was subsequently frozen in nitrogen and stored at -80°C. For repeated overnight culture, bacteria were held at room temperature (RT) until the surface was thawed. A small amount of cells was picked and LB plates were inoculated and grown over night at 37°C. The frozen stock was immediately returned to storage at -80°C.

4.1.2. Preparation of competent cells

From a single colony on a petri dish, the preculture was started in 5 mL LB media and incubated overnight at 37°C with vigorous shaking. The next day, 750 µL of the preculture was inoculated in 100 mL LB media and cultured 1 to 2 h until a OD600 of approximately 0.4 reach. Subsequently, the culture was cooled down on ice and than centrifuged for 10 min, 3000 g and 4°C. The bacterial pellet was resuspended in 10 mL ice-cold TSS buffer. The suspension was aliquoted in 500 µL, frozen in liquid nitrogen and stored at -80°C.

4.1.3. Heat-shock transformation of competent cells

The competent *E. coli* were thawed on ice. 100 µL of competent *E. coli* were mixed with 1-10 ng of plasmid DNA in a cold 1.5 mL microfuge tube and incubated for 30 min on ice. The bacteria were heat-shocked at 42°C for 90 sec, and then incubated for 2 min on ice. 500 µL antibiotic-free LB medium was added and the bacteria were incubated for 1 h at 37°C with gently shaking. Transformed bacteria were selected by plating 100 µL of the bacterial suspension on the antibiotic-containing agar plates. Only bacteria containing the desired plasmids, which contain the antibiotic resistance cassette, are able to grow on the agar antibiotic plates. One or more colonies were picked and expanded in LB medium and used for DNA preparation.

4.1.4. Maintaining of mammalian cell culture

The cell culture was performed in a laminar flow cabinet under sterile conditions. All reagents were purchased sterile or have been sterilized through a 0.2 µm filter. The cells were incubated in a CO_2 incubator at 37°C with 5% CO_2. For all adherent cells, the cell culture flask was coated with Collagen G (4 mg/mL) using a 1:1000 dilution with PBS and incubated for 30 min at 37°C. The supernatant was discarded and the flask was washed with PBS. The cells were cultured until they reached 90% confluence and were then split in reasonable quantities to obtain an adequate density. To detach the adherent cells, accutase was used and incubated for 5 min at 37°C in the CO_2 incubator. For inactivating the accutase additional medium was used. The cells were than centrifuged for 5 min at 200 g. Human umbilical vein endothelial cells (HUVECs) were cultured in endothelial cell growth medium and human aortic smooth muscle cells (HAoSMCs) were cultured in smooth muscle cell medium with the corresponding supplement and containing 50 µg/mL gentamicin to avoid contamination with bacteria. For growing cells in a suspension the maximum density of the culture was allowed to be 10^5-10^6 cells/mL. The cell suspension was centrifuged for 5 min at 200 g.

For freezing the cells, the cells were resuspended at a concentration of 10^6-10^7 cells/mL in fresh media containing 13% (v/v) DMSO and aliquoted in cryovials. The aliquots were stored into a styropore box and left to freeze gradually in the -80°C freezer overnight and transferred to liquid nitrogen for long-term storage. To thaw the cells for further cultivation, cryovials were immediately put in a 37°C water bath for 2-3 min. Directly, after the cell suspension is thawed, cells were slowly added to 4 mL warm fresh media. The cells were centrifuged and resuspended in the corresponding fresh media.

4.2. DNA techniques

4.2.1. Electrophoresis of DNA on agarose gel

The separation of double stranded DNA fragments with lengths between 0.1 kb and 10 kb was done according to their lengths on agarose gels. Agarose was dissolved in 1x TAE buffer to obtain a final concentration between of 0.75-2% (w/v) of the agarose gel. After complete solubilisation of the agarose in the microwave and cooled down to 50°C, 0.5 mg/L ethidium bromide was added and poured into the gel apparatus. The DNA was diluted with loading buffer and separated on the gel at 110 V performed in 1x TAE buffer containing 0.1 µg/mL ethidium bromide. The DNA fragments were visualized on a UV light transilluminator and photographed for documentation.

4.2.2. Isolation of plasmid DNA from Agarose (QIAquick gel extraction kit)

To isolate the digested DNA fragments with a specifically defined size from the agarose gel, the QIAquick gel extraction kit was used. The excised gel slice with the selective target fragment was initially depolymerized by heating at 50°C. The DNA contained in the depolymerized excised gel slice (>100 bp) binds at pH <7.5 and with a high salt concentration selectively to the membrane of the silicate ion exchanger column. The dissolved agarose and other contaminants are not bound to the column and removed by washing step. The purified DNA was then eluted from the membrane under basic pH and low salt concentrations.

4.2.3. Purification of plasmid DNA (QIAprep spin mini kit)

For the isolation of plasmid DNA, the QIAprep Spin Mini Kit was used. For the preparation and purification of plasmid DNA from *E. coli,* the appropriate protocols and systems from Qiagen were used. The method is based on the alkaline lysis of bacteria with extraction of DNA and the binding to a silica membrane under conditions of high salt concentrations and low pH (<7.5). Under basic pH and low salt concentrations, the bound and washed DNA can be eluted. The method is based on the principle of anion exchange chromatography.

4.2.4. Ligation of DNA fragments

For ligation of DNA fragments, the insert and linearized plasmid vector were added in a ratio of about 1:5 to a reaction tube in the presence of T4 DNA ligase and the corresponding 10x ligation buffer, filled with water up to a volume of 10 or 20 µL and incubated overnight at 4°C.

4.2.5. Oligonucleotide primers

All oligonucleotide primers for this study were synthesized from Eurofins MWG Operon (Ebersberg, Germany) and delivered in lyophilised form. The oligonucleotides were dissolved in sterile water to obtain a 100 µM stock solution. Primer solutions with desired concentration for the PCR reaction were prepared from these stocks. The sequencing primers usually have a length of 18-20 bases and a melting point of 55-65°C. The primers for mutagenesis PCR and/or the primers for conventional PCR have a length of up to 47 bases, having a melting point of about 72°C or higher. The GC content was chosen to be 40-60%, if possible.

4.2.6. Polymerase chain reaction (PCR)

The PCR was described by Saiki et. al.[149]. The PCR was used for *in vitro* amplification of DNA fragments. The GoTaq Flexi DNA polymerase kit and two primers were used, which flanked the amplified DNA. As a template the plasmid DNA was used which contain the

coding region of CXCL12 or CCL5. For denaturation of the DNA a temperature of 95°C was used. The annealing temperature for the primers was calculated with the following formula:

$$T \text{ Annealing} = 2°C \text{ (for AT-pair)} + 4°C \text{ (for GC-pair)} - 4°C^{150}$$

The polymerization of the DNA was performed at 72°C, wherein the elongation time depends on the length of the amplified DNA fragment. The Taq polymerase is able to amplify 1000 bases per minute, so the polymerization time was calculated by multiplying the length of the expected fragment (in kb). Unless otherwise specified, 30 cycles were performed. The PCR was prepared on ice; following components were used for one reaction:

Amount	Reagents
10 µL	5x Green GoTaq Flexi buffer
1 µL	template (1 µg)
8 µL	25 mM MgCl$_2$
1 µL	10 mM PCR nukleotide
1 µL	10 µM forward primer
1 µL	10 µM reverse primer
27.75 µL	ddH$_2$O
0.25 µL	GoTaq DNA Polymerase (5 U/µL)

After the PCR reaction 10 µL of the PCR reaction was used to analyze the amplified template on agarose gel electrophoresis.

4.2.7. DNA Site directed mutagenesis

The QuikChange II Site-Directed Mutagenesis Kit allows site-specific mutation in virtually any double-stranded plasmid, thus eliminating the need for subcloning and for ssDNA rescue. The mutagenesis is carried out by the DNA synthesis starting with two mutagenesis primer (forward and reverse). Here, the reaction is catalyzed by a thermostable DNA polymerase (Pfu polymerase). The Pfu polymerase has a 3'‑5' exonuclease activity that detects improperly installed deoxynucleotides during synthesis and removes it (proofreading). The amplification of this enzyme has a 10x time lower error rate than Taq polymerase. The Pfu polymerase does not contain the adenosine at the 3'-end of the DNA strand and the resulting

products feature smooth ends, in contrast to other polymerases. The following components were used for one reaction:

Amount	Reagents
5 µL	10x reaction buffer
2 µL	10 ng dsDNA template
1.25 µL	125 ng forward primer
1.25 µL	125 ng reverse primer
1 µL	dNTP mix
38.5 µL	ddH$_2$O
1 µL	PfuUltra HF DNA Polymerase (2.5 U/µL)

Parameters for the thermocycler:

cycle	temperature	time
1	95°C	30 sec
	95°C	30 sec
18	55°C	1 min
	68°C	1 min/kb of plasmid length

After PCR reaction, the PCR product was digested with 1 µL DpnI for 1 h at 37°C. Only methylated DNA is recognized and digested by the restriction enzyme DpnI. The plasmid used for the PCR reaction was isolated from a *dam+ E. coli* strain, therefore the sequence of the plasmid 5' – Gm – ATC - 3' is methylated from bacteria. The amplified DNA sequence containing the mutation is not methylated and can not be digested by restriction enzyme. 1 µL of the digestion was transformed into XL-1 Blue super competent cells, Stratagene and plated on agar plates containing the appropriate antibiotic.

4.2.8.   Mini-preparation of plasmid DNA

E. coli overnight culture was grown in LB media at 37°C with the corresponding antibiotics. The bacteria cells were centrifuged at 14.000 rpm for 1 min, the supernatant was removed and the pellet was resuspended in 100 µL buffer I. 200 µL of buffer II (lysis buffer) was

added, gently mixed and incubated for 5 min at RT. The suspension was neutralized by adding of 200 µL ice-cold buffer III, mixing by inverting the tubes for 4-6 times and incubated on ice for 5 min. The suspension was centrifuged by 15.000 rpm for 3 min, the supernatant was transferred to a fresh microcentrifuge tube and 900 µL of pre-cooled 100% ethanol was added for precipitation at -70°C for 10 min. The suspension was centrifuged at 15.000 rpm for 10 min, the supernatant was removed and the pellet was washed with 200 µL 70% ethanol and air-dried for a few minutes, then resuspended in 30-50 µL 10 mM Tris-HCl, pH 7.8.

4.2.9. Maxi-preparation of plasmid DNA

The large-scale purification of plasmid DNA from *E. coli* was performed using the Qiagen Plasmid Midi or Maxi Kit according to the manufacturer's instructions.

4.2.10. Restriction digest

For analytical approaches 1 µg of DNA, restriction endonucleases and the respective manufacturer's recommended reaction buffer in test tubes filled to 10 µL with distilled water was used. After an incubation period of 1-2 h at 37°C, the resulting DNA fragments were separated by gel electrophoresis and analyzed. The desired pattern of bands were excised from the gel and used for subsequent gel elution.

4.2.11. Measurement of DNA concentration

The concentration of DNA was determined by using the NanoDrop ND-1000 UV-photometer. The absorbance was measured at a wavelength of 260 nm. Absorption of 1.0 at 260 nm corresponds to a concentration of 50 µg/mL double stranded DNA. The purity of the DNA was determined by 260/280 ratio and should be over 1.8.

4.2.12. DNA Sequencing

The sequencing reaction of the plasmid DNA was performed by Eurofins MWG Operon. The sequencing results were monitored by using the program Gene Runner version 3.05 (http://www.generunner.com). In addition, database comparisons were done to search for DNA and protein sequences with similarity to the edited sequences for this work using the programs BLASTX, BLASTN and BLASTP[151], the National Center for Biotechnology Information (NCBI, Washington, USA) and related databases (http://www.ncbi.nlm.nih.gov).

4.3.   Protein analyses

4.3.1.   Protein concentration assay

The DC Bio-Rad protein assay is a colorimetric assay for the determination of the protein concentration. This reaction method is modified after the well known Lowry method[152] and is based on the reaction of proteins with an alkaline copper tartrate solution and Folin´s reagent The measurement was done according to manufacturer's instruction. 5 µL of the standard (BSA) or sample was used, adding 25 µL copper tartrate solution, followed by the addition of 200 µL of folin reagent. The Bio-Rad DC protein assay was measured at 750 nm with a microplate reader.

4.3.2.   Sodium dodecyl sulfate polyacrylamide gel electrophoresis (SDS-PAGE)

The isolated proteins from each FPLC purification step were analyzed by SDS PAGE. 20 µL of the sample was mixed with 5 µL of 5x SDS loading buffer containing SDS and ß-mercaptoethanol to denature precleared proteins at 90°C for 10 min. SDS is an anionic detergent that disrupts nearly all noncovalent interactions in native proteins and ß-mercaptoethanol reduce disulphide bonds. The proteins were electrophoresed on a polyacrylamide gel. The gel consists of two layers: a stacking gel (pH 6.8) which consists of a lower percentage of 5% where the proteins are concentrated and ensures the simultaneous entry into the separating gel at the same height; and a separating gel (pH 8.8) with a higher percentage between 12-15% that separates the proteins according to their size.

The stacking and the separating gels consisted of the following components:

	Stacking gel	Separating gel
Acrylamide/Bis	5% (w/v)	12-15% (w/v)
Tris-HCl (pH 8.8)	125 mM	375 mM
SDS	0.1% (w/v)	0.1% (w/v)
APS	0.1% (w/v)	0.1% (w/v)
TEMED	0.1% (v/v)	0.1% (v/v)

For the electrophoresis the Mini-sub cell GT, Bio-Rad was used. The electrophoresis was carried out at 120 V until the negatively charged SDS-proteins complexes migrate in the

direction of the anode at the bottom of the gel. The gel was used for Coomassie blue staining and western blotting.

4.3.3. Coomassie blue staining

For non-specific detection of proteins in SDS gels the Coomassie staining was performed with PageBlue Protein Staining Solution and an incubation time of 3-4 h or overnight. The gels were destained with destaining solution. To analyze and distinguish the mass of the proteins the image reader LAS 3000 was used.

4.3.4. Western blot

Proteins separated by SDS-PAGE were transferred to a nitrocellulose membrane using the iBlot Blotting System and the procedure was done according to the manufacturer's instructions. First the iBlot anode stack was placed to the bottom of the iBlot gel transfer device, the prerun gel was placed on the transfer membrane of the anode stack and a filter paper soaked with deionized water was placed on the prerun gel. The iBlot cathode stack was placed on the top of the presoaked filter paper with the copper electrode facing up and aligned to the right of the bottom stack followed by iBlot Disposable Sponge on the inner side of the lid, so the metal contact is to the top. The lid was closed and the blotting was performed for 7 min. At the end of the transfer, the nitrocellulose was removed and cut for an optimal size. To prevent nonspecific binding the already blotted nitrocellulose membrane was blocked with 1x Roti-Block for 1 h at RT. The excess of Roti-Block was removed by washing 3x with 1x TBS/0.05% (v/v) Tween, the primary antibody was diluted with 1x Roti-Block and incubated for 1 h at RT or over night at 4°C. The primary antibody was removed by washing 3x with 1x TBS/0.05% (v/v) Tween, subsequently the HRP-conjugated secondary antibody was diluted in 1x Roti-Block and incubated for 1 h at RT. Excess antibody was removed by washing 3x with 1x TBS/0.05% (v/v) Tween. To detect the specific proteins, ECL solution was used as substrate for this reaction, following the manufacturer's protocol. For analyzing the proteins the image reader LAS 3000 was used.

4.4. Recombinant protein expression and purification

4.4.1. Expression and isolation of F1-CX$_3$CL1 (CX$_3$CL1 receptor antagonist)

The expressed, isolated and purified CX$_3$CL1 antagonist was previously published by Dorgham et. al.[27], which is here also called F1-CX$_3$CL1. Glycerol stock containing the pET-26b(+)/F1_anta_His sequence in BL21 (DE3) pLysS *E. coli* was streaked on LB agar plates containing kanamycine/chloramphenicol double antibiotics and incubated overnight at 37°C. 100 mL of preparatory culture medium (2.5 g yeast extract, 5 g peptone, 4 g NaCl, 500 mL deionized water) containing kanamycine/chloramphenicol was inoculated with the bacteria

from the agar plate and grown over night at 37°C, centrifuged at 10.000 rpm for 10 min and the supernatant was disposed. Expression medium containing kanamycine/chloramphenicol was inoculated with all bacterial cells from the preparatory culture medium and was grown at 37°C until the optical density at 600 nM (OD_{600}) was approximately 1. After adding 500 µM IPTG, growth was continued at 37°C over night followed by harvesting the bacterial cells at 10.000 rpm for 10 min. The bacterial cells were dissolved in 100 mL 10 mM KH_2PO_4 pH 7 and sonicated 2x for 1 min. 1 mM $MgCl_2$ and 10 µL benzonase nuclease were added and sonicated 2x for 1 min. 5 mM EDTA, 1 tablet of protease inhibitor (complete Mini, EDTA-free tablet) was added and sonicated 2x for 1 min. 100 mL 10 mM of KH_2PO_4 pH 7 was added and centrifuged at 15.000 rpm for 10 min. The pellet was resuspended in 50 mL 25 mM KH_2PO_4 pH 7, 0.25% sodium deoxycholate, centrifuged at 15.000 rpm for 10 min. This step was repeated 2x. The pellet was again resuspended in 50 mL 25 mM KH_2PO_4 pH 7, centrifuged at 15.000 rpm for 10 min. This step was repeated 2x. The pellet was dissolved in 2.5 mL 6 M guanidine-HCl, 50 mM Tris pH 8, 1 mM DTT and the pellet was dissolved under stirring conditions at 60°C for 1-2 h. The solution was cooled down and centrifuged at 15.000 rpm for 30 min. The precipitate was centrifuged and the inclusion bodies were lyophilized over night. The CX_3CL1 receptor antagonist was purified in a 2-step procedure.

4.4.1.1. First purification step of F1-CX$_3$CL1 using HisTrap HP

The lyophilized pellet was resuspended in 4 mL 6 M guanidine-HCl and 20 mM sodium phosphate. First the column was washed with buffer A (6 M guanidine-HCl, 20 mM Tris pH 7.5), the protein was filtered over a 0.22 µm filter, loaded with buffer A on the column and washed with 5 column volumes. The bound protein was eluted with buffer B (6 M guanidine-HCl, 20 mM Tris pH 7.5, 250 mM imidazol) applying a gradient elution (0 min: A:B 100:0; 10 min: A:B 0:100). The concentration of the fractions under the peak were proofed and analyzed on a SDS-PAGE. The fractions of interest were pooled, subsequently diluted with 100x redox buffer (100 mM Tris pH 8.5, 5 mM EDTA, 0.2 mM oxidized glutathione, 1 mM reduced glutathione). The protein was refolded over night at 4°C. The protein was dialyzed with 10 mM potassium phosphate, 5 mM EDTA for 2 h, followed by a second dialyzation with 0.1% TFA in deionized water over night at 4°C. The F1-CX_3CL1 protein was cleaved from the His Tag by means of enterokinase digestion using 0.35 U enterokinase per mg protein and used for further purification.

4.4.1.2. Second purification step of F1-CX$_3$CL1 using Resource S

The lyophilized pellet was resuspended in 20 mM Tris pH 7 and digested with enterokinase (0.5 U/mg protein) over night. The column was washed with buffer A (20 mM MES pH 6), the protein was filtrated wit a 0.22 µm filter, loaded with buffer A on the column and washed with 5 column volumes. The bound protein was eluted with buffer B (20 mM MES pH 6, 1 M NaCl)

applying a gradient elution (0 min: A:B 100:0; 10 min: A:B 0:100). The concentrations of the fractions under the peak were analyzed on a SDS-PAGE. The desired fractions were pooled and dialyzed with 0.1% TFA in deionized water over night at 4°C. The pure protein was lyophilized over night and stored at -20°C.

4.4.2. Met-CCL5 expression and purification

The CCL5 antagonist was expressed, isolated and purified as previously published by Proudfoot et. al.[153]. and is called here also Met-CCL5. Glycerol stock containing the pET-26b(+)/Met-CCL5 sequence in Rosetta (DE3) pLysS *E. coli* was streaked on LB agar plates containing kanamycine/chloramphenicol double antibiotic and incubated overnight at 37°C. Expression medium containing kanamycine/ chloramphenicol was inoculated with the colonies of the agar plates and grown to an OD600 of 0.7 at 37°C. After adding 100 µM IPTG, growth was continued at 37°C for 3-4 h followed by centrifugation at 4.500 rpm for 30 min. First the cells were wiped up in solution buffer (50 mM Tris, 1 mM Na-EDTA, 10 mM dithiothreitol, 25% sucrose, pH 8), following a sonication step. 0.4 mg lysozyme, 20 µg DNAse I and 2 µmol/mL $MgCl_2$ was added to the suspension. Following the addition of lysis buffer (50 mM Tris, 1% Triton X-100, 1% deoxycholate, 100 mM sodium chloride, 10 mM dithiothreitol, pH 8), the suspension was incubated for 1 h at RT, followed by the addition of 7 µmol/mL Na-EDTA. After the addition of 3.5 µmol/mL $MgCl_2$, the suspension is incubated until the viscosity has decreased to the viscosity of water. 7 µmol/mL Na-EDTA was added followed by centrifugation at 11.000 g for 20 min at 4°C. The pellet was washed withwashing buffer I (50 mM Tris-HCl, 100 mM $NaCl_2$, 1 mM Di-Na-EDTA, 1 mM dithiothreitol, 0.5% Triton X-100) and centrifuged at 11.000 g for 30 min. The pellet was washed with washing buffer II (50 mM Tris-HCl, 100 mM $NaCl_2$, 1 mM Na-EDTA, 1 mM dithiothreitol) and centrifuged at 11.000 rpm for 30 min. The protein was purified from inclusion bodies and the pellet was dissolved in 6 M guanidine-HCl, 50 mM Tris pH 8, 1 mM dithiothreitol at 60°C, followed by a centrifugation step at 11.000 g for 20 min and the supernatant was dialyzed to 1% acetic acid. After centrifugation at 11.000 g for 20 min, the supernatant was lyophilized. The pellet is dissolved in 6 M guanidine-HCl, 5 mM Tris pH 8 and 1 mM dithiothreitol. Refolding of the protein was performed with a 1:10 dilution in renaturation buffer (50 mM Tris pH 8, 0.01 mM oxidized glutathione and 0.01 mM reduced glutathione) while stirring over night at 4°C. The suspension was centrifuged at 10.000 g for 30 min. The pH of the supernatant was adjusted to pH 5 using acetic acid whereas the conductivity was adjusted at 20 mS with H_2O. The Met-CCL5 protein was purified by a 2-step procedure.

4.4.2.1. *First purification of Met-CCL5 using SP Sepharose FF column*

The first purification step consisted of affinity purification using a SP Sepharose FF column. First the SP Sepharose FF column was washed with buffer A (50 mM sodium acetate

pH 4.5) and the protein is loaded by a loop with 1 mL/min buffer A. The bound protein was eluted with elution buffer (50 mM sodium acetate pH 4.5 and 2 M NaCl) applying gradient elution (0 min: A:B 100:0; 20 min: A:B 0:100). Protein rich fractions were pooled together followed by two different dialyzing steps, first with 1% acetic acid and second with 0.1% TFA. The protein was lyophilized, subsequently dissolved in 0.1% TFA for the further purification by HPLC.

4.4.2.2. Second purification of Met-CCL5 using HPLC chromatography

The second purification step was performed by means of reverse phase HPLC chromatography using a Vydac® column C8 250x10 mm, 5 µm with buffer A (0.1% TFA) and buffer B (0.1% TFA and 90% acetonitrile) applying gradient elution (0 min: A:B 100:0; 25 min: A:B 0:67) with a flow of 2 mL/min. After elution, the Met-CCL5 was dialyzed to 0.01% TFA and lyophilized for long-term storage.

4.4.3. Protease-resistant CXCL12 (S4V and S2G4V) expression and purification

The protease-resistant CXCL12 was expressed, isolated and purified as previously published by Segers et. al.[53] and is named here also CXCL12 (S4V). Glycerol stock containing the modified pET-32a(+)/CXCL12 sequence in Rosetta (DE3) pLysS *E. coli* was streaked on LB agar plates containing ampicillin/kanamycin double antibiotics and incubated overnight at 37°C. Pre-warmed 4 L of expression medium in a LAMBDA MINIFOR fermenter/bioreactor was inoculated with the colonies of the agar plates and grown to OD600 of 0.4 at 37°C. Growth was continued at 30°C until OD600 of 1.0. After adding 20 µM IPTG induction was continued at 30°C over night. The cells are harvested by centrifugation at 4.000 rpm for 30 min. The supernatant was removed and the pellet resuspended in 1x PBS. Dissolved lysozyme was added to the suspension and incubated at RT for 15 min. BugBuster Protein Extraction Reagent was added to the cells and incubated for 10 min. After adding of 25 U of benzonase nuclease, the cells were incubated until the viscosity was like water and the lysate was subsequently centrifuged at 4.000 rpm for 15 min. The supernatant was removed and the remaining pellet extracted three times using extraction buffer containing Triton X-100, 100 mM taurine, 50 mM sodium phosphate pH 7.5, 5 mM EDTA. The pellet was washed two times using 50 mM sodium phosphate pH 7.5. The pellet was dissolved in 6 M guanidine-HCl solution, 50 mM sodium phosphate pH 7.5 and cysteine was added to a final concentration of 6 mM. The solution was centrifuged at 4.000 rpm for 30 min, whereas the pellet was discarded. The solution was diluted 1:6 in 50 mM sodium phosphate pH 7.5 and cystine was added to a final concentration of 8 mM. The solution was allowed to stir over night for refolding at RT. The protease-resistant CXCL12 (S4V) and CXCL12 (S2G4V) were purified by a 3-step procedure.

4.4.3.1. First purification of protease-resistant CXCL12 (S4V and S2G4V) using Ni-NTA column

The first purification step consisted of affinity purification by the Histidine Tag present in the CXCL12 (S4V) and CXCL12 (S2G4V) protein with Ni-NTA column. The Ni-NTA resin was washed with buffer A (phosphate buffered saline pH 7.5 and 1 mM cysteine), the protein was loaded by a loop with 1 mL/min buffer A and bound protein was eluted using buffer B (phosphate buffered saline pH 7.5 and 1 mM cysteine, 250 mM imidazole) applying gradient elution (0 min: A:B 100:0; 10 min: A:B 0:100).

4.4.3.2. Second purification of protease-resistant CXCL12 (S4V and S2G4V) using Heparin Sepharose 6 fast flow column

The second purification step was performed using heparin sepharose 6 fast flow column, a buffer A (50 mM Tris pH 8, 1 mM cysteine) and the protein was loaded by a loop with 1 mL/min buffer A. The protein is eluted with buffer B (50 mM Tris pH 8, 1 mM cysteine, 1 M NaCl) applying a gradient elution (0 min: A:B 100:0; 10 min: A:B 0:100). The eluted protein was dialyzed with 50 mM Tris pH 8 and 2 mM cysteine. The CXCL12 (S4V) and CXCL12 (S2G4V) protein was cleaved from the Thioredoxin (Trx) Tag by means of enterokinase digestion using 0.35 U enterokinase per mg protein.

4.4.3.3. Third purification of protease-resistant CXCL12 (S4V and S2G4V) using Tricon Mono S 5/50GL

The last purification step was performed using the Tricon Mono S 5/50GL, buffer A (50 mM MES buffer pH 6) and the protein was loaded by a loop with 1 mL/min buffer A. The protein was eluted with buffer B (50 mM MES buffer pH 6, 1 M NaCl). After elution, the CXCL12 (S4V) and CXCL12 (S2G4V) protein was dialyzed to 0.01% trifluoroacetic acid and lyophilized for long-term storage.

4.5. Synthesis of biocompatible and degradable hydrogels

Hydroxy-terminated, six arm, star shaped poly (ethylene oxide-stat-propylene oxide) (sP(EO-stat-PO)) with a backbone consisting of 80% ethylene oxide and 20% propylene oxide (Mn = 12000 g/mol, Mw/Mn = 1.12) was obtained from Dow Chemicals for the further synthesis of biodegradable hydrogels. Prior to functionalization sP(EO-stat-PO) is purified by precipitation in THF/cold diethylether as solvent/non solvent system. N,N'-dicyclohexyl-carbodiimide, 4 DMAP, 3,3'-dithiodipropionic acid, tris(2-carboxyethyl) phosphine, poly(ethyleneglycol) diacrylate (575 g/mol), hydrogen peroxide (30% w/w), dichloromethane, cysteamine and 5,5'-dithio-bis-(2-nitrobenzoic acid) were used as received. Tetrahydrofuran (THF) used was dried over $LiAlH_4$.

4.5.1.   Synthesis of Thiol Functionalized sP(EO-stat-PO)

Thiol functionalized sP(EO-stat-PO) (SH-sP(EO-stat-PO)) has been prepared in a 2-step synthesis as previously described by Groll et. al.[121]. In the first step, sP(EO-stat-PO) has been crosslinked with disulfide crosslinker followed by reduction of the disulfide bonds to thiol groups in the second step. Typically, four alcohol groups have been transferred into thiol groups, leaving two unreacted -OH groups in the hydrogels

4.5.1.1.   Step 1: Cross linking of –OH groups

For cross linking of four -OH groups of sPEG, a solution consisting of 3,3'-dithiopropionic acid (DTPA) (1.0 eq with respect to one -OH) (0.1051 g, 0.5 mmol) in dry THF (4 mL) was added drop wise to a solution consisting of the purified sPEG (Mn = 12000 g/mol, 3 g, 0.25 mmol, 4 –OH = 1.0 mmol), DCC (1.1 eq with respect to one -COOH) (0.2269 g, 1.1 mmol) and DMAP (1.1 eq with respect to one -COOH) (0.1343 g, 1.1 mmol) in CH_2Cl_2 (6 mL) in an ice bath at 0°C over 10 min. The resulting mixture was allowed to stir at RT for 12 h. The formed hydrogel is washed three times with CH_2Cl_2, twice with THF, ethanol and water followed by evaporation of remaining solvents on the rotary evaporator. Finally, the product is dried in a vacuum oven at 35°C for 12 h.

4.5.1.2.   Step 2: Reduction of disulfide bonds

Step 2: TCEP was used for the reduction of disulfide bonds. TCEP (1.5 eq with respect to the disulfide units) (0.429 g, 1.5 mmol) was reacted with the cross linked polymer in 1x PBS buffer (pH 4) at RT for 2 h under inert gas atmosphere. Subsequently, the solution was dialyzed (MWCO = 3500 Da) for two days at RT against aqueous HCl solution (pH 3.5). Finally, the polymer solution is lyophilized and stored at 4°C for further use. The free thiol content of the polymer was determined using Ellman's method. SEC (THF): Mn = 12900 g/mol, Mw/Mn = 1.1223.

4.5.1.3.   Hydrogel cross linked via Michael addition of thiols (slow degradable hydrogels [SDH])

SH-sP(EO-stat-PO) (0.0300 g, 2.5×10^{-3} mmol, 7.5×10^{-3} mmol with respect to SH groups (3 SH groups per molecule)) was dissolved in 1x PBS buffer pH 8.0 (30 µL) and mixed thoroughly. To this solution, PEG-diacrylate (0.0107 g, 1.86×10^{-3} mmol, 3.72×10^{-3} with respect to ACR groups (2 ACR groups per molecule)) and 3 µM of CXCL12 (S4V) were added. This equals a molar ratio 1:5 SH-polymer:ACR-PEG. All components were homogenized fast.

4.5.1.4.   Hydrogel cross linked via oxidation of thiols (flow degradable hydrogels [FDH])

SH-sP(EO-stat-PO) (0.0300 g, 2.5 x 10^{-3} mmol, 7.5 x 10^{-3} mmol with respect to SH groups (3 SH per molecule)) is dissolved in 1x PBS buffer pH 7.4 (30 µL) and mixed thoroughly. To this solution 20 µL of 0.1 M H_2O_2 and 0.5 µM of Met-CCL5 were added. All components were homogenized fast. The gelation of the hydrogel starts in 5 min, so if the gels have to be transferred in well plates or mold it has to be done within this time. Cross linking then continues and will be 95% finished after 2 h and fully finished after 12 h.

4.6.   Fluorescence based Assay

4.6.1.   Flow Cytometry

The laser based flow cytometry technique is a biophysical technology for analyzing cells by their size, granularity and protein expression. This technique employed cell counting, sorting, biomarker detection and protein engineering. In a buffer stream, one cell at a time passes by an argon laser, which excites fluorescently labeled cells. Measurements of the size (forward scatter) and granularity (sideward scatter) are independent from the fluorescence signal. In this study the flow cytometry technique was utilized for cell counting of transmigrated cells from the cell recruitment assay (4.7.4). In a buffer system the transmigrated cells (neutrophils and EOCs) were counted 1 min using a FACS Canto II flow cytometer and FLOW JO Software.

4.6.2.   Enzyme-linked immunosorbent assay (ELISA)

ELISA is a method for determining the concentration of antigens in biological samples. The method used here is based on the principle of a sandwich immunoassay. The amount of mouse CXCL12, mouse CCL5 and human CCL5 from human sera was determined but also supernatants from the release assay were measured with this method using DuoSet ELISA Development Kits (mouse CXCL12/SDF-1, mouse CCL5/RANTES, human CCL5/RANTES) in accordance with the manufacturer's instructions. A capture antibody specific for the antigen of interest is pre-coated onto a microtiter plate and incubated over night at RT. After aspiration and washing, the plate was blocked with 1% BSA in PBS for 1 h and aspiration/washing was repeated. The standards and samples were added for binding to the capture antibody and incubated for 2 h. After aspiration/washing, the detection antibody was added and incubated for 2 h. To remove the unbound detection antibody the aspiration/washing procedure was done followed by adding streptavidin-HRP and incubated for 20 min. The last step, was set by the substrate solution and the reaction yields blue then turns to yellow when the reaction was stopped with 2 M H_2SO_4. The optical density was determined using a microplate reader at 450 nm/570 nm. A standard curve was generated

for each set of sample assayed and the concentrations of the samples were calculated according to the standard curve. All samples were performed in duplicates or triplicates.

4.6.3. Histochemistry and Immunhistochemistry

4.6.3.1. Assessment of infarction size and collagen content

The infarcted area and collagen content was determined in serial sections (5 µm) of the infarcted myocardium (10 sections per mouse) through quantifying Gomori's 1-step trichrome stain-positive area using Diskus software and expressed as percentage of LV area and collagen are measured in six different fields from infarcted area per section and expressed as collagen content/mm².

4.6.3.2. Quantitative immunohistochemistry and immunofluorescence

The number of neutrophils, smooth muscle cells (SMCs) and vessels are determined in serial sections (3 per mouse, 200 µm apart) of the infarcted and treated myocardium. Sections are stained for neutrophils using chloracetatesterase, for SMCs using monoclonal mouse anti-human α-actin (smooth muscle) clone 1A4 and for vessels using goat anti-mouse CD31 monoclonal antibody (mAb) clone M-20. Areas with specific immunostaining are quantified using Diskus software by comparison to isotype controls and expressed as percentage of the infarcted area and cells are numbered in six different fields from infarcted area per section and expressed as cells/mm².

4.7. Functional assay

4.7.1. Isolation of angiogenic early-outgrowth cells (EOCs)

The EOCs were isolated according to the established protocols[154] from citrate/dextran anticoagulated peripheral blood buffy coats of healthy volunteers. Mononuclear cells (MNCs) were separated by density gradient centrifugation with Bicoll. The MNCs were washed 2x with PBS, resuspended in EC growth medium MV2 and plated on fibronectin-coated (10 µg/mL) 6-well plates (10^7 cells per well). At day 4, the medium was changed and at day 5-7 the adherent cells were detached with accutase for 5 min at 37°C, counted and subjected to activity assay. Experiments with human material were approved by the local ethics board and all individuals gave informed consent.

4.7.2. Isolation of neutrophil from peripheral blood

The neutrophil isolation was done according to Bøyum et. al.[155], using a isoosmotic density barrier (1.077 g/mL) containing metrizoate and a polysaccharide. This density barrier separates human peripheral blood mononuclear cells, which band at the interface from PMNs and erythrocytes and pellet the cells. The density and osmolarity of the barrier was

later increased[156] to permit the simultaneous separation of the PMNs and erythrocytes. Whole blood was drawn from patients in the presence of EDTA (1.6 mg EDTA/mL blood) in an open system using a butterfly needle. For the isolation of neutrophils, 4.5 mL of Polymorphprep was layed in a 15 mL falcon tube, covered with the same amount of EDTA-blood and centrifuged at 500 g for 30 min. After centrifugation the Polymorphprep is divided in different layers. The lowermost layer contains erythrocytes, subsequently the Polymorphprep, followed by the neutrophil layer, again a Polymorphprep layer, followed by the monocytes and the uppermost layer containing the serum. The top layers were aspirated and the neutrophils were transferred to a fresh 15 mL falcon tube. The neutrophils were washed in HBSS buffer containing 1% BSA and centrifuged at 300 g for 5 min. The supernatant was aspirated and the erythrocytes were lysed with lysis buffer for 10 min, again centrifuged and the supernatant was aspirated. The neutrophils were taken up again in HBSS buffer containing 1% BSA. Experiments with human material were approved by the local ethics board and all individuals gave informed consent.

4.7.3.   Static cell-adhesion assay

Three different independent experiments were done for parallel-plate flow chamber adhesion to analyze the CX_3CL1 receptor antagonist, Met-CCL5 and the protease-resistant CXCL12. Flow-resistant adhesion on ECs in response to recombinant chemokines was assessed in customized flow chambers as described in Postea et. al.[117].

4.7.3.1.   Whole blood adhesion assay for analyzing the F1-CX$_3$CL1

To analyze the F1-CX_3CL1, whole blood was drawn in the presence of 2.9 µM of recombinant Hirudin in an open system using a butterfly needle. The first 1-2 mL of drawn blood was discarded to prevent platelet activation. The leukocytes in the blood were labeled by the addition of rhodamine 6G (1 µM). In some experiments, a blocking anti-CX_3CL1-antibody, isotype control (5 µg/mL), the CX_3CR1-antagonist F1-CX_3CL1 or the heat-inactivated F1-CX_3CL1 (5 µg/mL) were added and incubated for 30 min at 37°C. HAoSMC were cultured in 35 mm dishes, activated with TNFα (10 ng/mL) for 4 h and assembled into flow chambers. Whole blood was perfused for 4 min at a wall shear stress of 1.5 dynes/cm^2 and subsequently perfused with Hank's buffer containing HEPES (10 mM), $CaCl_2$ and $MgCl_2$ (1 mM each) and 0.5% human albumin to wash away erythrocytes allowing video microscopic quantification of adherent fluorescent cells. Adherent leukocytes were manually counted in at least 6 fields and expressed as cells/mm^2.

4.7.3.2.   Neutrophil adhesion assay for analyzing the Met-CCL5

After density barrier separation of venous blood (4.7.1), the isolated neutrophils were labeled by the addition of calcein (1 µM). Commercially available CXCL8 (200 ng/mL) and CCL5

(200 ng/mL) both used as positive controls, and Met-CCL5 (200 ng/mL) were added to 500.000 neutrophils/reaction and incubated for 30 min at 37°C. HUVECs were cultured in 35 mm dishes and were activated with TNFα (10 ng/mL) for 4 h and assembled into flow chambers. Neutrophils were perfused for 3 min at a wall shear stress of 1.5 dynes/cm^2 and subsequently perfused with Hank's buffer containing HEPES (10 mM), CaCl$_2$ and MgCl$_2$ (1 mM each) and 0.5% human albumin subsequently followed by video microscopic quantification of adherent fluorescent cells. Adherent neutrophils are manually counted in at least 6 fields and expressed as cells/mm^2.

4.7.3.3. *Lymphocytic cell adhesion assay for analyzing the protease-resistant CXCL12 (S4V and S2G4V)*

Jurkat T lymphocytic cells were labeled by the addition of calcein (1 µM). The commercially available CXCL12 *wild type* (200 ng/mL) as a positive control, CXCL12 (S4V) (200 ng/mL) and CXCL12 (S2G4V) (200 ng/mL) are added to 500.000 Jurkat T lymphocytic cells/reaction and incubated for 30 min at 37°C. Human Umbilical Vein Endothelial Cells (HUVEC) were cultured in 35 mm dishes and were activated with TNFα (10 ng/mL) for 4 h and assembled into flow chambers. Jurkat T lymphocytic cells are perfused for 3 min at a wall shear stress of 1.5 dynes/cm^2 and subsequently perfused with Hank's buffer containing HEPES (10 mM), CaCl$_2$ and MgCl$_2$ (1 mM each) and 0.5% human albumin subsequently followed by video microscopic quantification of adherent fluorescent cells. Adherent lymphocytes are manually counted in at least 6 fields and expressed as cells/mm^2.

4.7.4. Cell recruitment assay

Activities of purified Met-CCL5 and the protease-resistant CXCL12 (S4V and S2G4V) were assayed by migration of neutrophils and EOC respectively and compared with the commercially available CXCL8 and CCL5, or CXCL12 *wild types* using Transwell chambers[157]. 500.000 cells were plated in the upper well of 6.5 mm transwell with 3.0 µm (for neutrophils) or 8.0 µm (for EOCs) pore polycarbonate membrane insert and chemokines (100 ng/mL) was added to the lower well. Cells are counted in the lower well after 1 h incubation for neutrophils and after 3 h incubation for EOCs. All experiments were performed in triplicate.

4.7.5. Release assay

4.7.5.1. *Release of Met-CCL5 from fast degradable hydrogels (FDH)*

15 µL of hydrogel cross linked *via* oxidation of thiols containing 0.5 µM Met-CCL5 was incubated with 250 µL 1x PBS, 10 mM reduced glutathion and incubated over 24 h. After 0, 2, 4, 8, 12 and 24 h 250 µL 1x PBS, 5 mM reduced glutathion was replaced and the

supernatant was analyzed using human CCL5/RANTES DuoSet ELISA kit (according to manufacturer's instructions (4.6.2).

4.7.5.2. Release of protease-resistant CXCL12 (S4V) from SDH

15 µL of hydrogel cross linked *via* Michael addition of thiols containing 3 µM protease-resistant CXCL12 (S4V) was incubated with 250 µL 1x PBS, 5 mM reduced glutathion and incubated over 4 weeks. After 0, 3, 6, 9, 12, 15, 18, 21, 24, 27 and 30 days 250 µL of 1x PBS, 5 mM reduced glutathion was replaced and the supernatant was analyzed using mouse CXCL12/SDF-1 DuoSet ELISA kit according to manufacturer's instructions (4.6.2).

4.7.6. Biocompatibility assay

The biocompatibility of the protease-resistant CXCL12 (S4V), Met-CCL5 and biodegradable hydrogels were analyzed by two different methods, one was led by a proliferation assay and the other was a cell viability test performed.

4.7.6.1. Proliferation assay

Proliferation assay with HUVEC's in the presence of protease-resistant CXCL12 (S4V), Met-CCL5 and biodegradable hydrogels were performed. The BrdU Proliferation Assay is a non-isotopic immunoassay for the quantification of bromodeoxyuridine (BrdU) incorporation into new synthesized DNA of actively proliferating HUVEC's. The procedure is carried out according to manufacturer's instructions. The samples are incubated and analyzed after 4 and 72 h according to manufacturer's instructions.

4.7.6.2. Cell viability assay

CellTiter-Blue cell viability assay with HUVEC's in the presence of protease-resistant CXCL12 (S4V), Met-CCL5 and biodegradable hydrogels were performed. The CellTiter-Blue cell viability assay provides a homogeneous, fluorometric method for estimating the number of viable HUVEC's present in multiwell plates. The CellTiter-Blue assay is based on the ability of living HUVEC's to convert a redox dye (resazurin) into a fluorescent end product (resorufin). Viable HUVEC's retain the ability to reduce resazurin into resorufin. Nonviable HUVEC's rapidly lose their metabolic capacity, thereby losing their ability to reduce the indicator dye, and thus do not generate a fluorescent signal. The procedure is done according to manufacturer's instructions and was analyzed after 0, 1, 2, 3, 4 and 24 h.

4.8.   Animal models

4.8.1.   Mouse model of myocardial infarction (MI) and injection of biodegradable hydrogels containing chemokines

Eight week old male C57BL/6 mice (n = 6-9 per group) were subjected to coronary occlusion as described earlier[30, 158]. Briefly, mice were intubated under general anesthesia (using ketamine and xylazine) and positive pressure ventilation was maintained using a rodent respirator. Hearts were exposed by left thoracotomy and MI is induced by suture occlusion of the left anterior descending artery (LAD) over a silicone tube. Biodegradable hydrogels SDH and FDH (15μL) were mixed with crosslinking agent and loaded with buffer or 0.5 μg Met-CCL5 and/or 3 μg CXCL12 (S4V) and subsequently injected separately in a standardized manner, using a 36 gauge needle into 2 directly adjacent sites of the mouse myocardium at the border of the infarct area directly after inducing MI. The muscle layer and skin incision were closed with a silk suture, after polymerization was complete. The animals were treated with a single dose of buprenorphine (0.1 mg/mL) and kept under standard conditions one day or 4 weeks after MI until further investigation. Heart function of the mice was evaluated by echocardiography 1 day before, and 4 weeks after MI. All animal experiments and study protocols were approved by local authorities, complying with Romanian animal protection laws.

4.9.   Statistical analysis

Data were represented as mean value ± standard errors. Data analysis was performed with Prism 4 software (Graph Pad) using one-way parametric ANOVA followed by Newman-Keuls post hoc testing or Kruskall-Wallis non-parametric testing with Dunns post hoc comparison, where appropriate. Differences with $P < 0.05$ were considered significant.

5.   Results

MI is a threatening consequence of atherosclerotic narrowing of coronary vessels. The most important goals are to understand the process of atherosclerosis, to identify possible therapeutic options for preventing the development of atherosclerosis and to develop possible therapeutic applications after MI. Chemokines play a very important role in the development of atherosclerosis and for the therapy after MI. This study examines different modified chemokines and/or chemokine antagonists, which play an essential role in the development of atherosclerosis and for the therapy after MI. The first part of this work describes the recombinant expression and purification of F1-CX$_3$CL1, Met-CCL5, protease-resistant CXCL12, and the synthesis of degradable hydrogels. The second part of this work describes a potential *in vivo* therapeutic approach with Met-CCL5 and the protease-resistant CXCL12 for the therapy after MI. The third part examines the role of F1-CX$_3$CL1 antagonist on platelet-monocyte complex formation during atherosclerosis.

CX$_3$CL1 participates in diverse inflammatory processes including arterial atherosclerosis and inflammation and binds with the N-terminal part of the protein to its unique receptor CX$_3$CR1. Both, platelets and monocytes express the CX$_3$CR1 receptor[117]. To investigate the contribution of CX$_3$CL1 in the PMC formation, a CX$_3$CL1 antagonist, named F1-CX$_3$CL1 was used. Six amino acids of the CX$_3$CL1 were modified on the N-terminal part of the protein to obtain the F1-CX$_3$CL1 antagonist[27] (Table 1). The described F1-CX$_3$CL1 antagonist was first published by Dorgham et. al.[27]. F1-CX$_3$CL1 bound specifically to cells expressing CX$_3$CR1, without being a signaling molecule and did not induce chemotaxis, calcium flux, or CX$_3$CR1 internalization as the naturally occurring CX$_3$CL1 *wild type*[27].

The CCL5 chemokine is a proinflammatory cytokine that plays a critical role as neutrophil and macrophage activator in inflammation, atherosclerosis and after MI[67]. After MI, neutrophils are recruited within hours into the infarcted area and promote an inflammation reaction. To avoid the recruitment of neutrophils into the infarcted area and to decrease the inflammation reaction, a CCL5 antagonist, named Met-CCL5 was chosen. Met-CCL5 contains an additional methionine residue on the N-terminal part of the protein to antagonize CCR5 and CCR1 receptors[153] (Table 1). This methionylated protein is completely inactive in CCL5 bioassays of calcium mobilization and chemotaxis of promonocytic cell lines[153].

After MI, regeneration of the heart muscle is very important. Because, the appropriate blood supply is crucial for heart survival and function, angiogenesis is considered as an optimal therapeutic target. The CXCL12-CXCR4 ligand-receptor axis is implicating in angiogenesis of the heart[35, 159, 160]. The CXCL12 chemokine promotes tissue regeneration by mediating angiogenic EOCs recruitment into the ischemic area[161], while CXCR4 stimulates proliferation,

cell survival and angiogenesis[162, 163]. The CXCL12-CXCR4 communication is essential for improving neo-myoangiogenesis and left ventricular remodelling[164]. After vascular injury, the CXCL12 expression is upregulated[165], but this effect is limited by local proteases such as MMP-2 and DPPIV which cleaves the CXCL12 and becomes inactive[53]. Thus, proteolytic activity limits the effectiveness of CXCL12 in the inflammatory environment of infarcted myocardium[53]. The receptor binding site of the CXCL12 chemokine on the CXCR4 and CXCR7 receptor are located on the N-terminal site of this protein[166]. Because the cleavage sites of MMP-2 and DDPIV are also located on the N-terminus of the CXCL12 chemokine[53], it was necessary to modify serine at position 4 to valine and to add an N-terminal serine obtaining the protease-resistant CXCL12 (S4V) (Figure 7A-B) (Table 1). The described modification was first published by Segers et. al.[53]. The receptor specificity and activity of the CXCL12 (S4V) chemokine described by Segers was retained for both CXCR4 and CXCR7, but with a lower activity towards CXCR4 receptor compared to native CXCL12[167]. The CXCL12 (S2G4V) is an antagonist (inactive control) only for the CXCR4 receptor with an additional exchange of proline to glycine at position 2 (Table 1).

chemokine or antagonist	N-terminal amino acid sequence
CX3CL1 *wild type*	-QHHGVTKC
F1-CX3CL1[27]	ILDNGVSKC
CCL5 *wild type*	-SPYSSDTT
Met-CCL5[153]	MSPYSSDTT
CXCL12 *wild type*	-KPVSLSYR
CXCL12 (S4V)[53]	SKPVVLSYR
CXCL12 (S2G4V)	SKGVVLSYR

Table 1: N-terminal amino acid sequence of the modified chemokines and/or chemokine antagonists in comparison to the N-terminal amino acid sequence of the *wild type* chemokines.
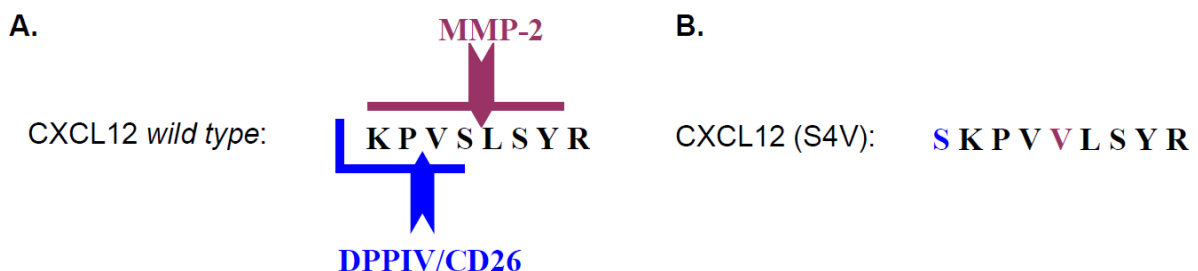

Figure 7: The first 8 amino acids of the naturally occurring CXCL12 chemokine. A. *Wild type* CXCL12 indicating the location of MMP-2 and DPPIV cleaving sites. **B.** CXCL12 (S4V) showing the modifications to provide resistance to MMP-2 and DPPIV, i.e. mutation of serine at position 4 to valine and addition of an extra N-terminal serine. Figure modified from Segers et. al.[53].

For the *in vivo* investigation of Met-CCL5 and protease-resistant CXCL12 in mice after MI, synthetic hydrolysable hydrogels were implemented. Here the local role of Met-CCL5 and protease-resistant CXCL12 under controlled release using degradable hydrogels was investigated with the intention to recruit SC into the infarcted area for promoting a faster regeneration, and to prevent the infiltration of neutrophils into the inflamed myocardium for an improved healing of the heart after MI.

In vitro the role of F1-CX$_3$CL1 antagonist to platelet-monocyte complex formation during the progression of atherosclerosis was studied. The chemokine receptor CX$_3$CR1 is an inflammatory mediator in vascular diseases. On platelets, its ligation with CX$_3$CL1 induces platelet activation followed by leukocyte recruitment to activated endothelium[117]. For this reason, to evaluate the expression and the role of platelet-CX$_3$CR1 during hyperlipidemia and during vascular injury, is important.

5.1. Cloning, expression and isolation of F1-CX$_3$CL1, Met-CCL5, protease-resistant CXCL12 (S4V) and CXCL12 (S2G4V)

The constructs for F1-CX$_3$CL1, Met-CCL5, protease-resistant CXCL12 (S4V) and CXCL12 (S2G4V) were created using the pET system and standard molecular biology techniques. The cloning of Met-CCL5 was done by Birgit Kramp in the working group of PD Dr. Rory Koenen (University Hospital of the LMU Munich, Institute for Cardiovascular Prevention (IPEK), Munich, Germany). The cloning of the protease-resistant CXCL12 (S4V) and CXCL12 (S2G4V) has been published earlier[168]. The F1-CX$_3$CL1 and Met-CCL5 were cloned in the pET-26b(+) plasmid, while the protease-resistant CXCL12 (S4V) and CXCL12 (S2G4V) were cloned in the pET-32a(+) plasmid. The cloning of F1-CX$_3$CL1 into the pET26b(+) vector was done with the restriction enzymes Not I and Nde I (Figure 8A). The pET26b(+) vector for the expression of the F1-CX$_3$CL1 protein contains the following: T7 promoter and terminator, pBR322 and f1 origin, His Tag, *lacI* coding sequence, kanamycin coding sequence and multiple cloning sites. The cloning of Met-CCL5 into the pET26b(+) vector was done with the restriction enzymes BamH I and Nde I (Figure 8B). The pET26b(+) vector for the expression of the Met-CCL5 protein contains the following: T7 promoter and terminator, pBR322 and f1 origin, *lacI* coding sequence, kanamycin coding sequence and multiple cloning sites. For cloning the protease-resistant CXCL12 (S4V) and CXCL12 (S2G4V) into the pET32a(+) vector, the cleavage enzymes Kpn I and Not I were used (Figure 8C-D). The expression vector pET32a(+) for protease-resistant CXCL12 (S4V) and CXCL12 (S2G4V) contains a T7 promoter and terminator , pBR322 and f1 origin, Trx Tag, *lacI* coding sequence, kanamycin coding sequence and multiple cloning sites. The expression of the target genes (F1-CX3CL1, Met-CCL5, protease-resistant CXCL12 (S4V) and CXCL12 (S2G4V)) was induced by the addition of IPTG, under the control of T7

transcription and translational signals and expressed in *E. coli* as "inclusion bodies". The proteins were purified using different strategies.

The recombinant F1-CX$_3$CL1 was purified in a 2-step procedure: first, the isolation of the protein was done by FPLC, HisTrap HP column, followed by the refolding of the F1-CX$_3$CL1, followed by a second isolation step using the Resource S column (Figure 9). The isolation of recombinant Met-CCL5 was also performed in a 2-step procedure: first, the refolding of the Met-CCL5 was performed, followed by cation exchange chromatography using FPLC and SP-Sepharose FF column and HPLC purification using a Vydac® reverse phase column (Figure 9) in a second step. The recombinant protease-resistant CXCL12 was purified in 3 steps: first, refolding of the protease-resistant CXCL12 (S4V) and (S2G4V) followed by affinity purification with Ni-NTA, Heparin Sepharose™ and enterokinase digestion of the Trx Tag and Tricorn Mono S™ 5/50GL by means of cation exchange chromatography (Figure 9). Two different CXCL12 chemokines, the so called CXCL12 (S4V), which is resistant to proteases MMP-2 and DPPIV and the inactive control CXCL12 (S2G4V), which functions as an antagonist for the CXCR4 receptor, were expressed and purified in the same manner.
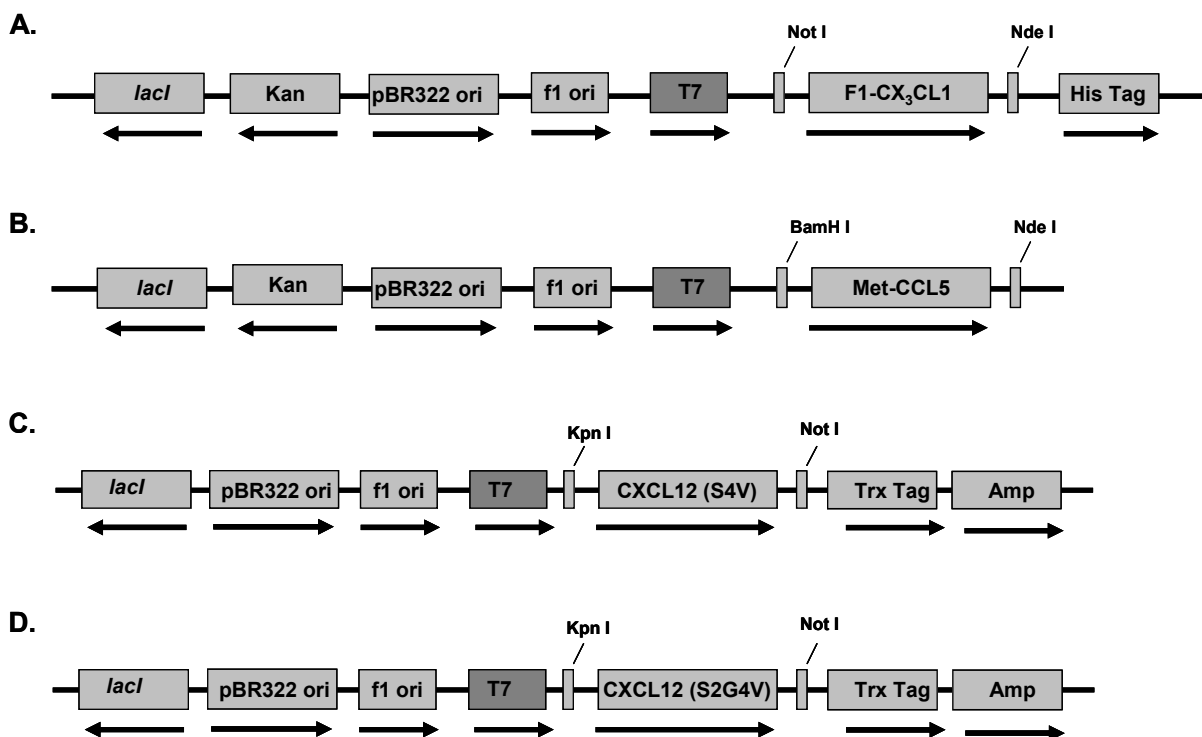

Figure 8: Constructs for F1-CX$_3$CL1, Met-CCL5, CXCL12 (S4V) and CXCL12 (S2G4V) fusion proteins and vectors. A. F1-CX$_3$CL1 were cloned in the pET26b(+) vector under the T7 promoter and containing a His Tag. **B.** Met-CCL5 were cloned in the pET26b(+) vector under the T7 promoter. **C.** CXCL12 (S4V) and **D.** CXCL12 (S2G4V) were cloned in the pET232a(+) vector under the T7 promoter and containing Trx Tag.
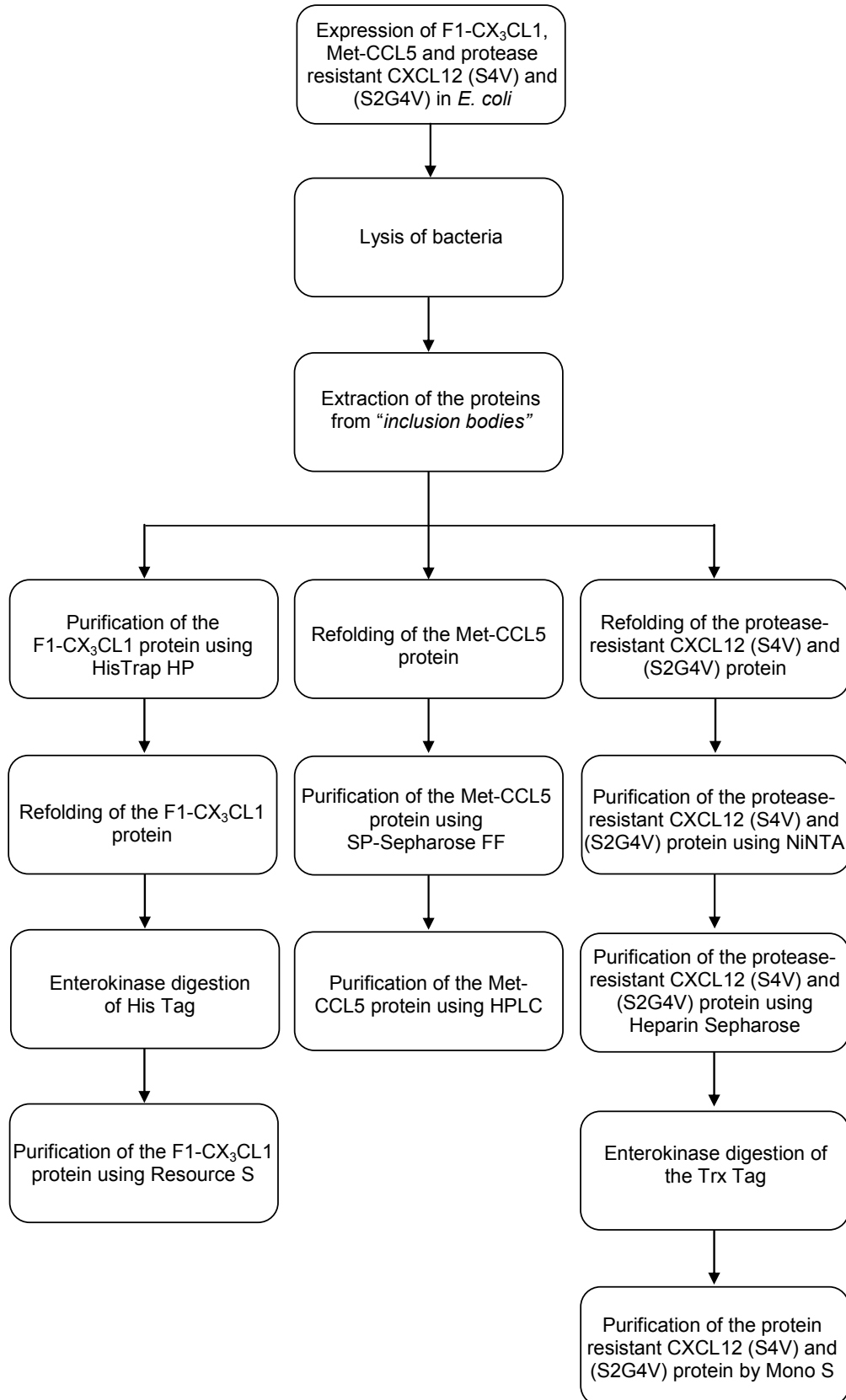
Expression of F1-CX$_3$CL1, Met-CCL5 and protease resistant CXCL12 (S4V) and (S2G4V) in *E. coli*

Lysis of bacteria

Extraction of the proteins from "*inclusion bodies*"

Purification of the F1-CX$_3$CL1 protein using HisTrap HP

Refolding of the Met-CCL5 protein

Refolding of the protease-resistant CXCL12 (S4V) and (S2G4V) protein

Refolding of the F1-CX$_3$CL1 protein

Purification of the Met-CCL5 protein using SP-Sepharose FF

Purification of the protease-resistant CXCL12 (S4V) and (S2G4V) protein using NiNTA

Enterokinase digestion of His Tag

Purification of the Met-CCL5 protein using HPLC

Purification of the protease-resistant CXCL12 (S4V) and (S2G4V) protein using Heparin Sepharose

Purification of the F1-CX$_3$CL1 protein using Resource S

Enterokinase digestion of the Trx Tag

Purification of the protein resistant CXCL12 (S4V) and (S2G4V) protein by Mono S

Figure 9: Scheme of the expression and isolation strategy of F1-CX$_3$CL1, Met-CCL5 and protease-resistant CXCL12.

5.1.1.   F1-CX$_3$CL1 expression and isolation

The F1-CX$_3$CL1 protein was expressed in *E. coli* as "*inclusion bodies*" (Figure 9). To dissolve the "*inclusion bodies*" for the purification with FPLC, 6 M guanidine-HCl was used. Guanidine-HCl is one of the strongest denaturants used in physiochemical studies of protein folding. The F1-CX$_3$CL1 protein contains a His Tag on its N-terminus (Figure 8). A His Tag is an amino acid motif in proteins that consists of at least six histidine residues. For the first isolation step of the F1-CX$_3$CL1, the FPLC and the HisTrap HP column were used. HisTrap HP columns are prepacked with nickel sepharose and designed for simple, high-resolution purification of His Tagged proteins by immobilized metal ion affinity chromatography. The run was done at a flow rate of 1 mL/min and 1 mL fractions were collected (Figure 10A). The fractions under the peak were analyzed by SDS-PAGE (Figure 10B). The calculation of protein concentration for each fraction was measured by Lowry protein assay. A representative example for the first step of the isolation of F1-CX$_3$CL1 is shown in Figure 10. The fractions of interest C5-C10 containing the F1-CX$_3$CL1 protein were pooled for refolding.

A refolding step was necessary because the F1-CX$_3$CL1 protein was previously denatured with guanidine-HCl. The refolding was done over night at 4°C using 100 mM Tris pH 8.5, 5 mM EDTA, 0.2 mM oxidized glutathione, 1 mM reduced glutathione. After refolding, the protein was dialysed in 10 mM potassium phosphate, 5 mM EDTA for 2 h. A second dialysis with 0.1% TFA in deionized water over night at 4°C was necessary. The enterokinase digestion was required to cleave off the His Tag from the F1-CX$_3$CL1. To separate the F1-CX$_3$CL1 from the His Tag, the FPLC and the Resource S column were used. The Resource S is an ion exchange chromatography method which can separate molecules or groups of molecules that have only slight differences in charge, like the F1-CX$_3$CL1 and the His Tag. Separation is based on the reversible interaction between a charged molecule and an oppositely charged chromatography medium. The run was performed at a flow rate of 1 mL/min and 1 mL fractions were collected (Figure 11A). The fractions under the respective chromatogram peak were analyzed on SDS-PAGE (Figure 11B) and the protein concentrations for each fraction were measured by Lowry protein assay. The fractions under peak 1 D15-D14 and peak 2 D13-D11 were pooled together. Peak 2 seems to be the F1-CX$_3$CL1, because the isoelectric point (IEP) changes after enterokinase digestion from 8.79 to 9.34 and Mw from 10828.35 to 8735.12. For this reason peak 2 was used for further examination.

The purity and mass of F1-CX$_3$CL1 chemokine was determined by means of MALDI-TOF (Figure 12A). The mass of the F1-CX$_3$CL1 chemokine corresponds to the expected mass of 8.73 kDa. The identity of the isolated F1-CX$_3$CL1 was confirmed by Western blot analysis in

comparison to the commercially available recombinant CX_3CL1 *wild type* using specific mAb (Figure 12B).

A.

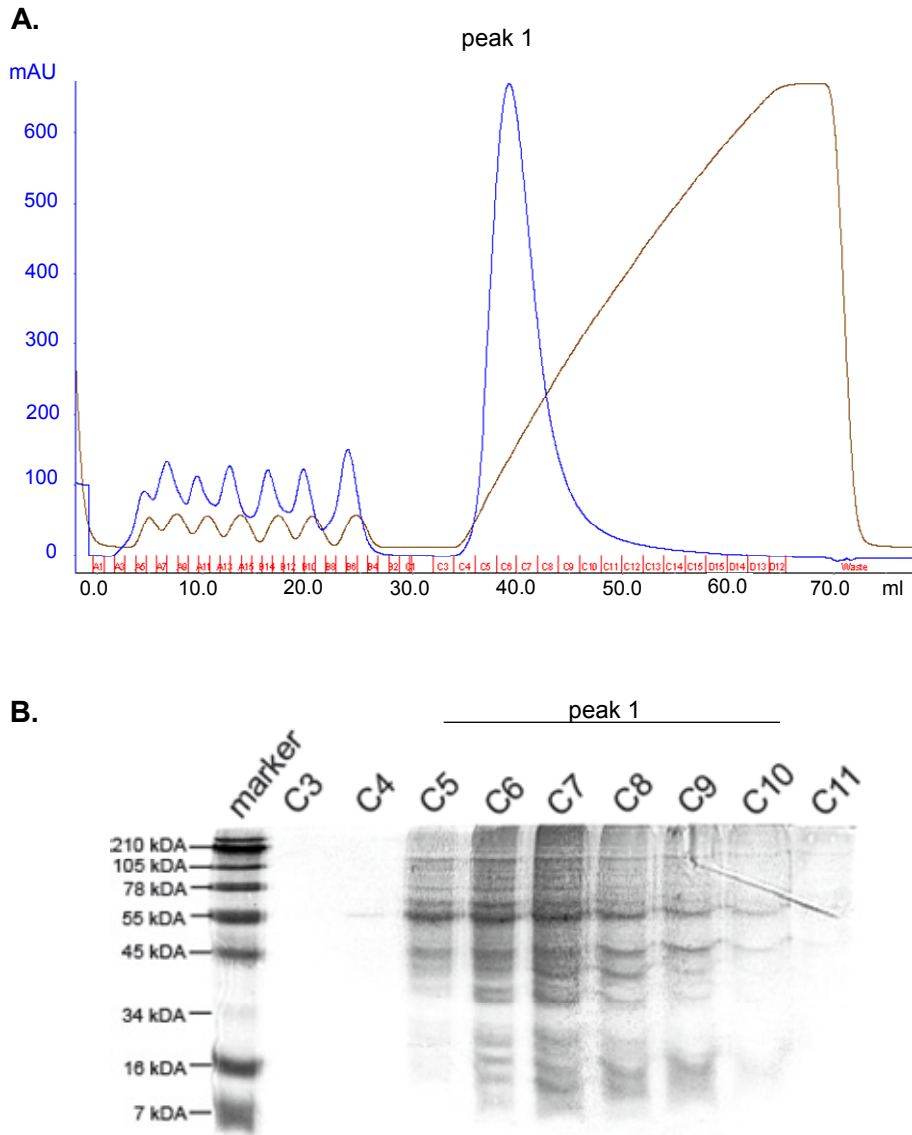

peak 1

B.

peak 1

Figure 10: First isolation step of F1-CX$_3$CL1. A. Representative FPLC trace using HisTrap HP column. The protein was eluted using buffer B (6 M guanidine-HCl, 20 mM Tris pH 7.5, 250 mM imidazol) and collected in 1 mL fractions. The y-axis represents the mAU (milli-absorbance-units) and the x-axis represents the eluent volume in mL. **B.** Coomassie staining for F1-CX$_3$CL1 chemokine. SDS-PAGE was performed under reducing conditions. The fractions were analyzed on SDS-PAGE in comparison to a SeeBlue® Plus2 marker. Peak 1 (fraction C5-C10) were pooled together and used for further purification.

A.

B.
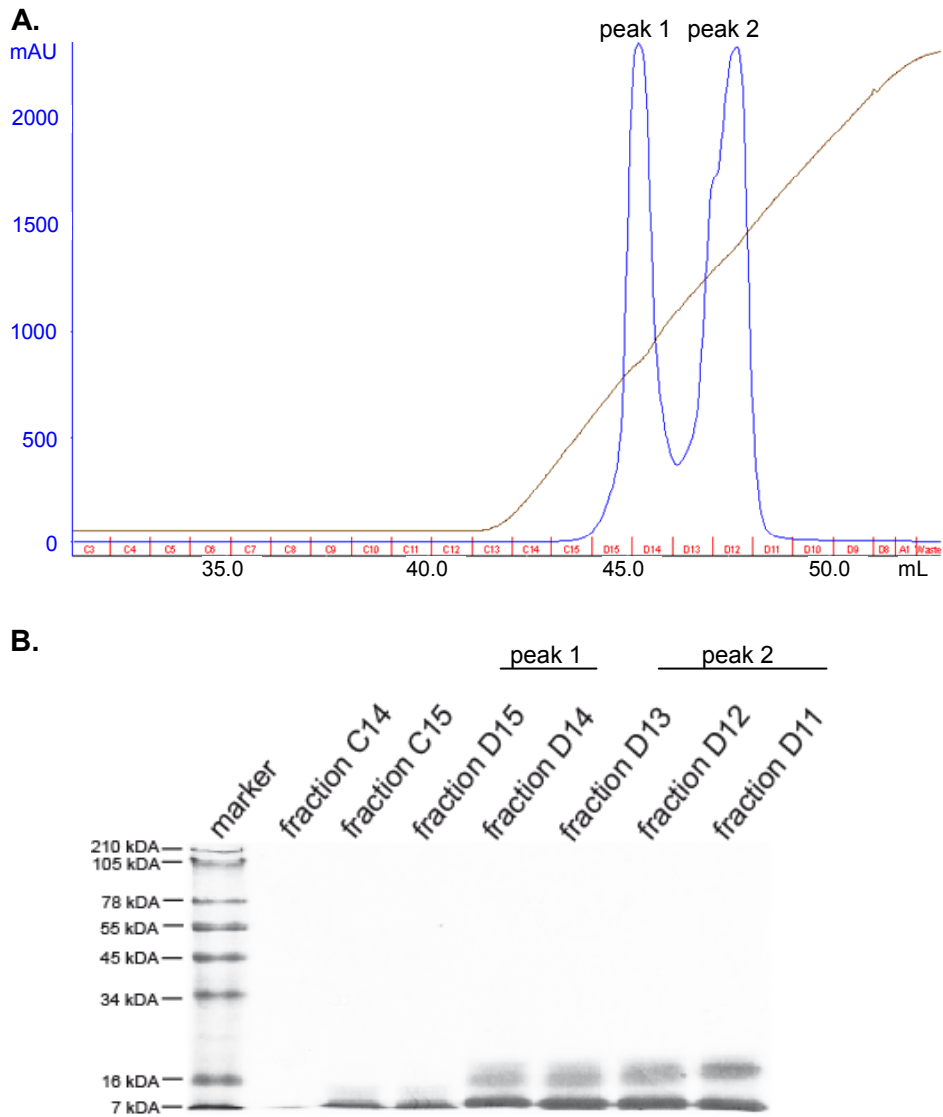
Figure 11: Second isolation step of F1-CX₃CL1. A. Representative FPLC trace using Resource S (ion exchange chromatography) column. The protein was eluted using buffer B (20 mM MES pH 6, 1 M NaCl) and collected in 1 mL fractions. The y-axis represents the mAU (milli-absorbance-units) and the x-axis represents the eluent volume in mL. **B.** Coomassie staining for F1-CX₃CL1 chemokine. SDS-PAGE was performed under reducing conditions. The fractions under the peak were analyzed on SDS-PAGE in comparison to a SeeBlue® Plus2 marker. Peak 1 (fraction D15-D14) and peak 2 (fraction D13-D11) were used for further examination.

A. Applied Biosystems 4700 Proteomics Analyzer 35

B.
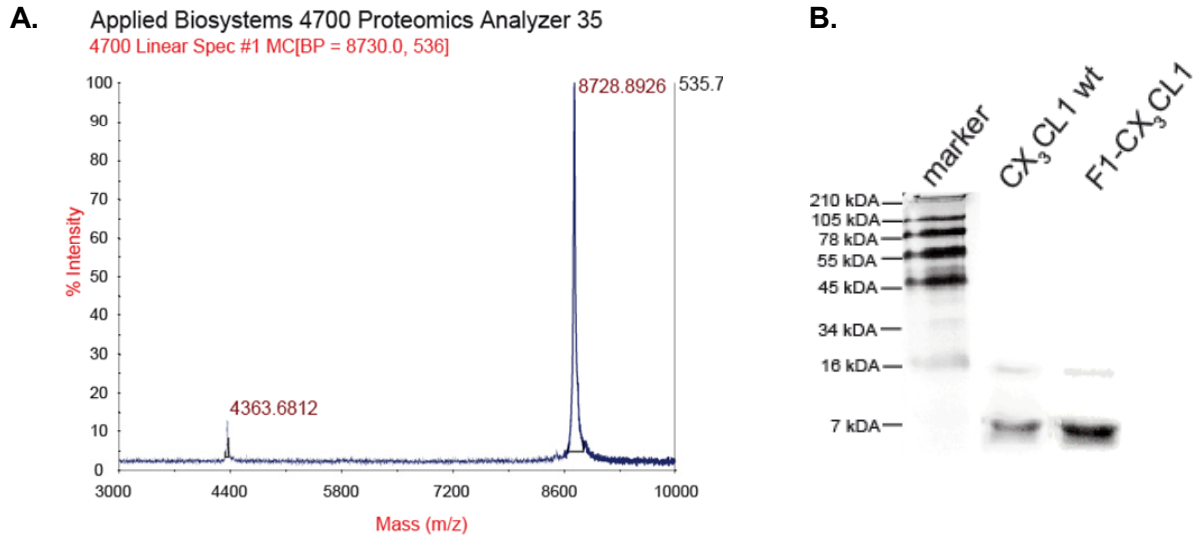
Figure 12: Purity and mass determination of F1-CX₃CL1 chemokine. A. The mass determination was done by means of MALDI-TOF. The mass of F1-CX$_3$CL1 chemokine corresponds to 8.73 kDa. The y-axis represents the signal intensity in % and the x-axis represents the mass to charge ration (m/z). **B.** Western blot analysis of the isolated F1-CX$_3$CL1 chemokine in comparison to the commercially available CX$_3$CL1 *wild type* and a SeeBlue® Plus2 marker.

5.1.2. Met-CCL5 expression and isolation

The Met-CCL5 protein was expressed in *E. coli* as "*inclusion bodies*" (Figure 9). To dissolve the "*inclusion bodies*", 6 M guanidine-HCl was used. Because the Met-CCL5 was denatured with guanidine-HCl, a refolding step was necessary to obtain the proper conformation of the protein. The refolding of the protein was done over night at 4°C using 50 mM Tris pH 8, 0.01 mM oxidized glutathione, 0.1 mM reduced glutathione. After adjusting the pH to < 5, and the conductivity to < 20 mS, the first purification step using the FPLC and SP-Sepharose FF (Fast Flow) column followed. SP Sepharose FF is a strong cation exchanger, which is composed of cross-linked 6% agarose beads and shows high chemical stability. The run was done at a flow rate of 1 mL/min and 1 mL fractions were collected (Figure 13A). The fractions under the chromatogram peak were analyzed on dot blot (Figure 13B) and the protein concentrations for each fraction were measured by Lowry protein assay. The fractions of interest B14-B9 containing the Met-CCL5 were pooled for further purification.
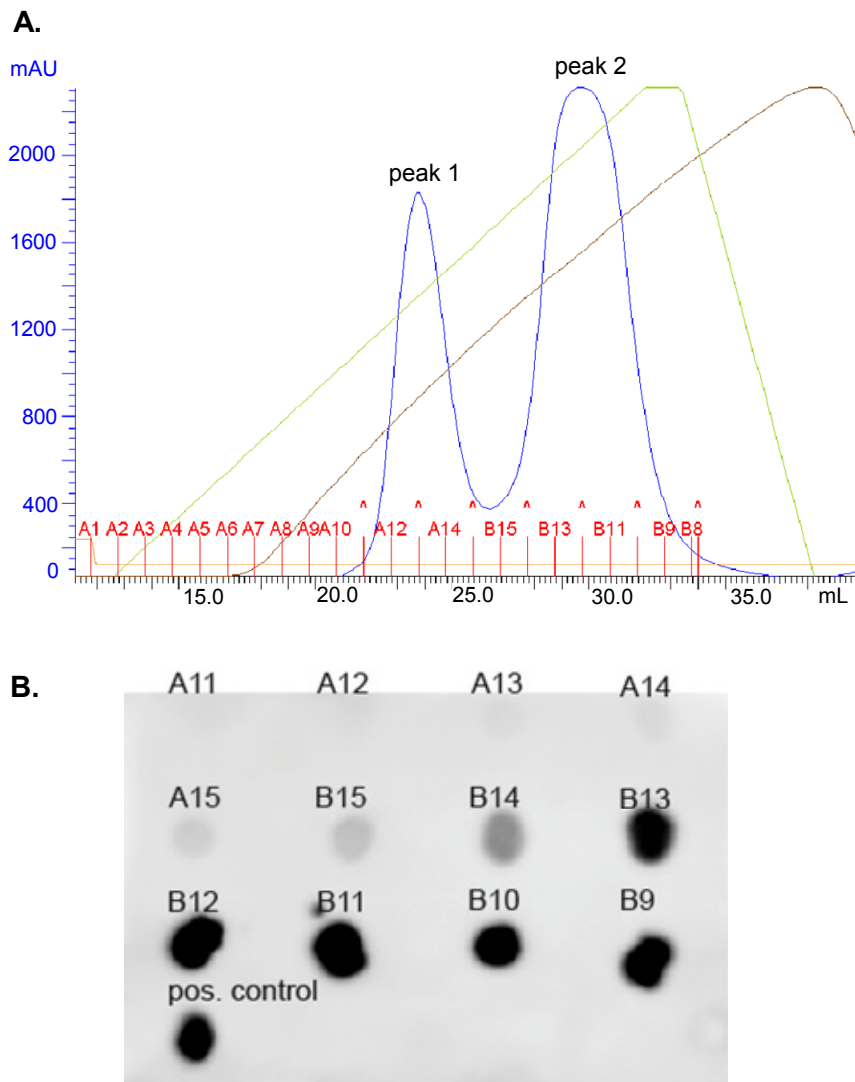
A.

B.

Figure 13: First isolation step of Met-CCL5. A. Representative FPLC trace using SP-Sepharose FF column. The protein was eluted using buffer B (50 mM sodium acetate pH 4.5 and 2 M NaCl) and collected in 1 mL fractions. The y-axis represents the mAU (milli-absorbance-units) and the x-axis represents the eluent volume in mL. **B.** Dot blot for Met-CCL5 chemokine. The fractions under the peak were analyzed. Fractions B14-B9 were pooled together and used for further purification.

In the second step, Met-CCL5 protein was purified by means of reversed phase (RP) HPLC using the Vydac® column C8 250 x 10mm, 5 µm. The stationary phase is a thin film of non-polar liquid phase that is chemically anchored to an inert material (silica particles). The silica particles on the surface are chemically linked to a non-polar layer. C8 column has a packing material composed of silica particles attached to C8 carbon units. The run was done using buffer A (0.1% TFA) and buffer B (0.1% TFA and 90% acetonitrile) applying gradient elution (0 min: A:B 100:0; 25 min: A:B 0:67) with a flow of 2 mL/min (Figure 14A). The fraction under the chromatogram peak 1, were analyzed on SDS-PAGE (Figure 14B) and the protein concentrations for each fraction were measured by Lowry protein assay. Peak 1 was used for further analysis. The Met-CCL5 was provided from Birgit Kramp and Dr. Marcella Langer

from the working group of PD Dr. Rory Koenen (University Hospital of the LMU Munich, Institute for Cardiovascular Prevention (IPEK), Munich, Germany).

The purity of the Met-CCL5 chemokine was > 95% determined by HPLC (Figure 14A), Coomassie staining (Figure 14B) and mass determination by means of MALDI-TOF was confirmed (Figure 15A). The mass of chemokine corresponds to the expected mass of 7.98 kDa. The identity of the isolated Met-CCL5 was confirmed by western blot analysis in comparison to the commercially available CCL5 *wild type* (Figure 15B).
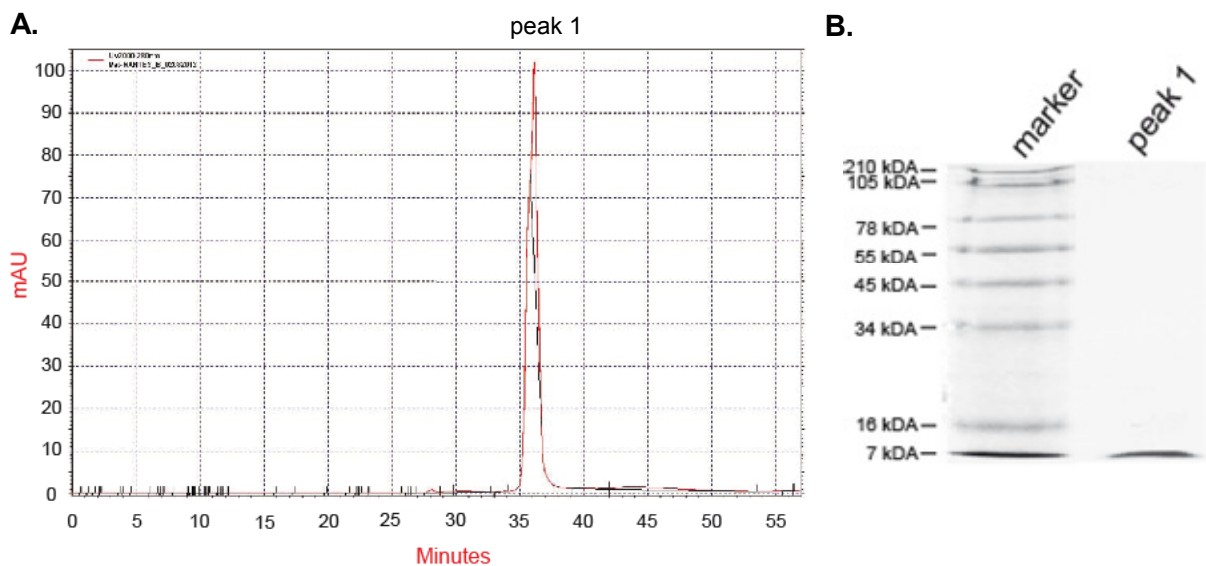
Figure 14: Second isolation step of Met-CCL5. A. Representative HPLC trace using Vydac® C8 column. The protein was eluted using 0.1% TFA and 90% acetonitrile. The y-axis represents the mAU (milli-absorbance-units) and the x-axis represents the eluent volume in mL. **B.** Coomassie staining for Met-CCL5 chemokine. SDS-PAGE was performed under reducing conditions. The fraction under peak 1 was analyzed on SDS-PAGE in comparison to a SeeBlue® Plus2 marker.

A.

B.
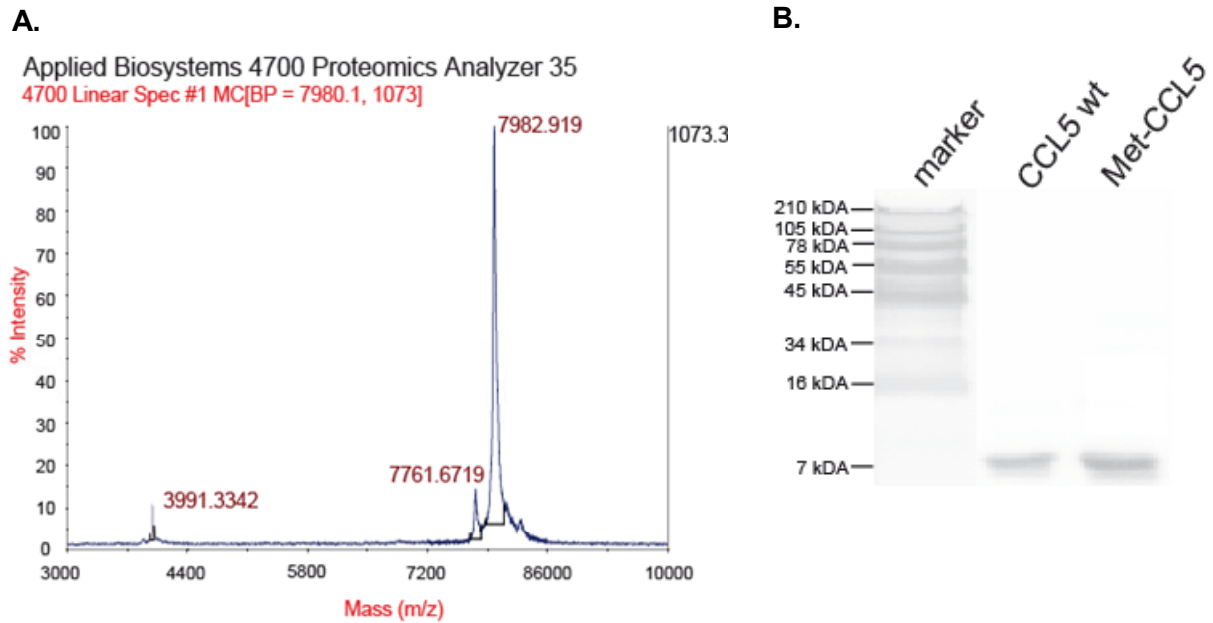
Figure 15: A. Purity and mass determination of Met-CCL5 chemokine. The mass determination was done by means of MALDI-TOF. The mass of Met-CCL5 chemokine corresponds to 7.98 kDA. The y-axis represents the signal intensity in % and the x-axis represents the mass to charge ration (m/z). **B.** Western blot analysis of the isolated Met-CCL5 chemokine in comparison to the commercially available CCL5 *wild type* and a SeeBlue® Plus2 marker.

5.1.3. Protease-resistant CXCL12 expression and isolation

The protease-resistant CXCL12 (S4V) and CXCL12 (S2G4V) proteins were expressed in *E. coli* as "*inclusion bodies*" (Figure 9). The expression and isolation of the protease-resistant CXCL12 (S4V) and CXCL12 (S2G4V) have been published earlier[168]. The pure "*inclusion bodies*" were denatured in 6 M guanidine-HCl. To obtain the proper conformation, the fusion proteins were refolded overnight at 4°C by a 6-fold dilution in a 50 mM sodium phosphate pH 7.5 buffer containing 6 mM cysteine and 8 mM cystine as redox additives. The protease-resistant CXCL12 (S4V) and CXCL12 (S2G4V) proteins contain a Trx Tag on their N-terminus (Figure 8C-D). The fist purification step was done using FPLC and the NiNTA column, which is an immobilized metal affinity chromatography. The Trx Tag is able to bind nickel ions on the NiNTA column. The run was performed at a flow rate of 0.5 mL/min and 1 mL fractions were collected (Figure 16A). The fractions under the chromatogram peak were analyzed on SDS-PAGE (Figure 16B) and the protein concentrations for each fraction were measured using Lowry protein assay. Fractions B12-B7 under peak 3 contains the protease-resistant CXCL12 and were pooled together for further purification. The second purification step was performed by means of FPLC using the heparin sepharose column, which is an affinity chromatography. The heparin sepharose column purifies proteins with an affinity for heparin. The run was performed at a flow rate of 1 mL/min and 1 mL fractions were collected (Figure 17A). The fractions under the chromatogram peak were analyzed on SDS-PAGE (Figure 17B) and the protein concentrations for each fraction were measured

using Lowry protein assay. The fractions C12-D14 under the peak 1 were pooled together and used for the further purification.
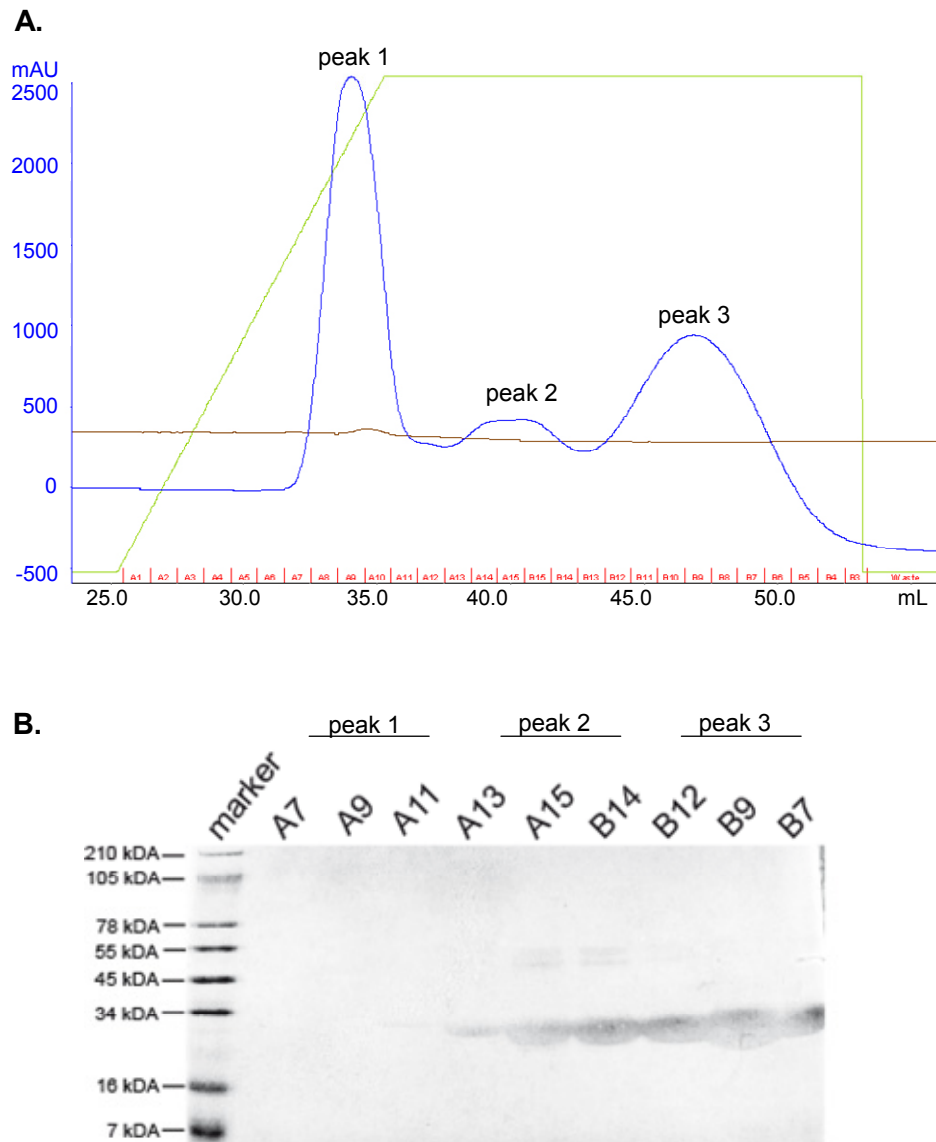

Figure 16: First isolation step of CXCL12 (S4V). A. Representative FPLC trace using NiNTA column. The protein was eluted using buffer B (20 mM phosphate pH 7.5, 1 mM cysteine, 500 mM imidazol) and collected in 1 mL fractions. The y-axis represents the mAU (milli-absorbance-units) and the x-axis represents the eluent volume in mL. **B.** Coomassie staining for CXCL12 (S4V) chemokine. SDS-PAGE was performed under reducing conditions. The fractions under the peak were analyzed on SDS-PAGE in comparison to a SeeBlue® Plus2 marker. Fractions B12-B7 under peak 3 were pooled together and used for further purification.

The enterokinase digestion was required to digest the Trx Tag and then to separate the protease-resistant CXCL12 from the Trx Tag using FPLC and the strong cationic exchanger, Mono S column. The run was performed at a flow rate of 1 ml/min and 1 mL fractions were collected (Figure 18A). The fractions under the chromatogram peaks were evaluated on SDS-PAGE (Figure 18B) and the protein concentrations for each fraction were determined using Lowry protein assay. The fractions of interest B9-B7 containing the protease-resistant CXCL12 were pooled for further evaluation. The purity and mass of CXCL12 (S4V) and

CXCL12 (S2G4V) chemokines was > 95% and corresponds to 8.07 kDa and 8.03 kDa respectively (Figure 20A-B). The identity of the isolated chemokines was confirmed by western blot analysis in comparison to the commercially available CXCL12 *wild type* using specific mAb (Figure 19).
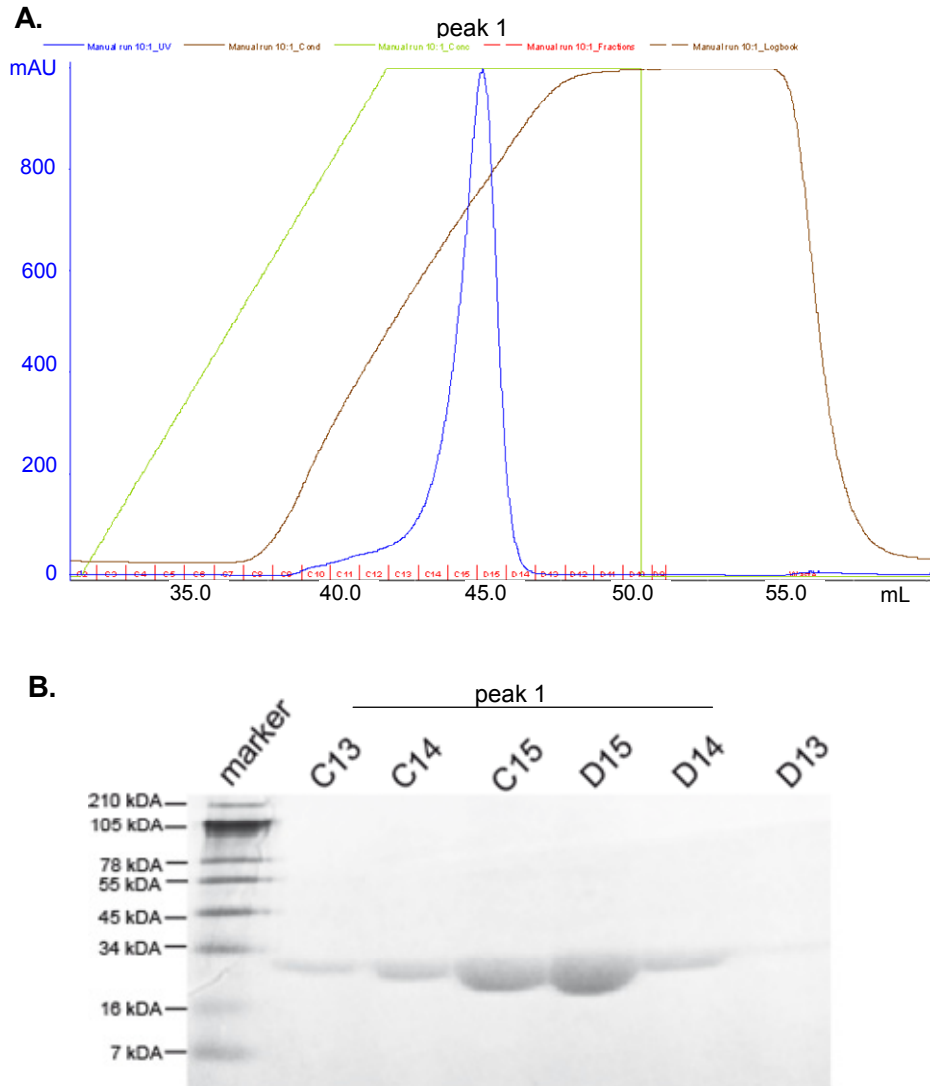

Figure 17: Second isolation step of CXCL12 (S4V). A. Representative FPLC trace using heparin sepharose column. The protein was eluted using buffer B (50 mM Tris pH 8, 1 mM cysteine, 1 M NaCl) and collected in 1 mL fractions. The y-axis represents the mAU (milli-absorbance-units) and the x-axis represents the eluent volume in mL. **B.** Coomassie staining for CXCL12 (S4V) chemokine. SDS-PAGE was performed under reducing conditions. The fractions under the peak were analyzed on SDS-PAGE in comparison to a SeeBlue® Plus2 marker. Fractions C13-D14 were pooled together and used for further purification.
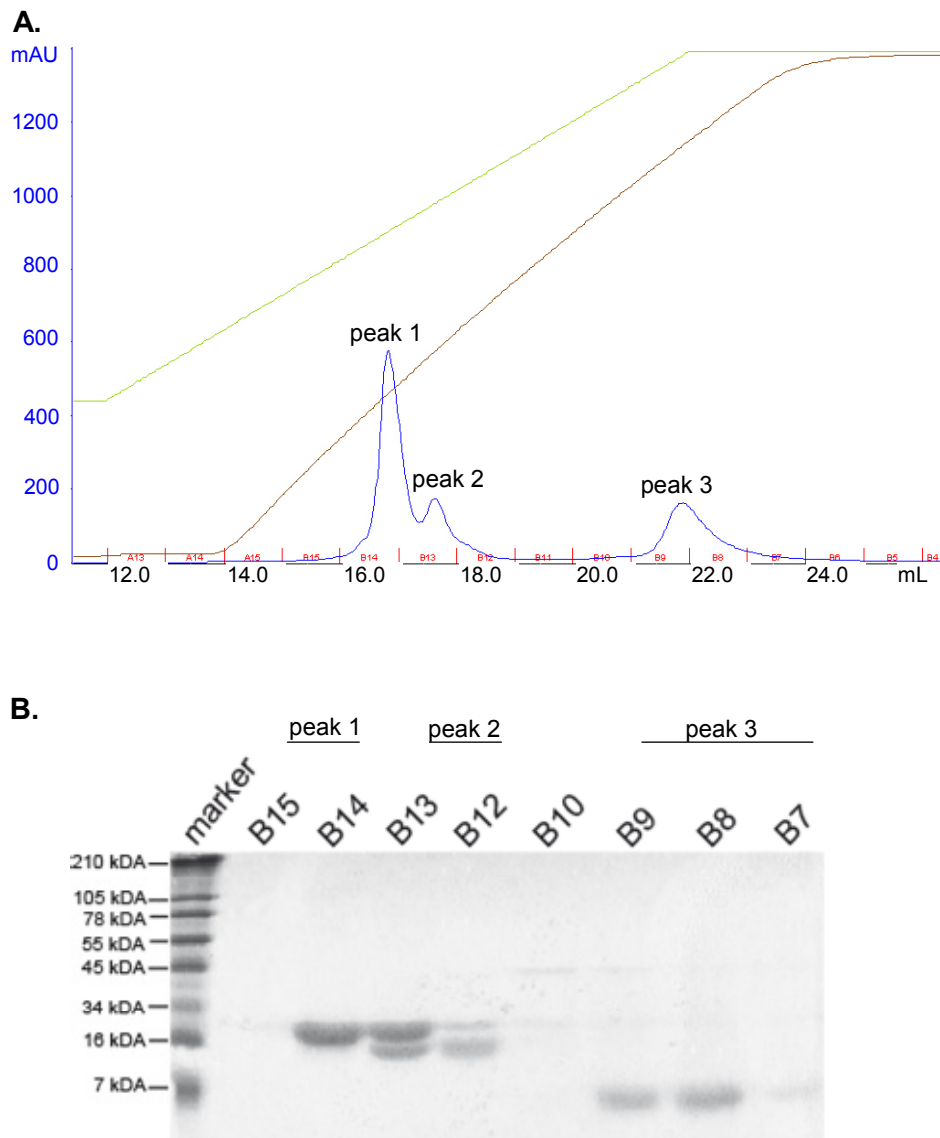
A.

B.

Figure 18: Third isolation step of CXCL12 (S4V). A. Representative FPLC trace using cationic Mono S column. The protein was eluted using buffer B (50 mM MES pH 6, 1 M NaCl) and collected in 1 mL fractions. The y-axis represents the mAU (milli-absorbance-units) and the x-axis represents the eluent volume in mL. **B.** Coomassie staining for CXCL12 (S4V) chemokine. SDS-PAGE was performed under reducing conditions. The fractions under the peaks were analyzed on SDS-PAGE in comparison to a SeeBlue® Plus2 marker. Fractions B9-B7 were pooled together and used for further purification.
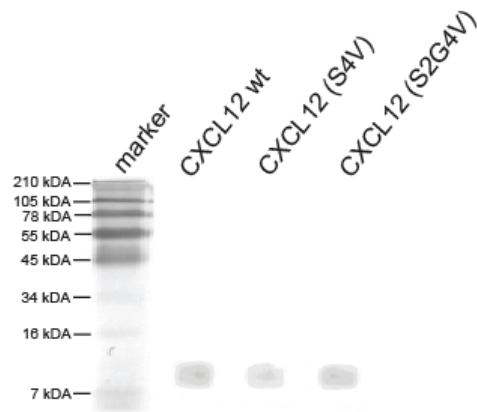
Figure 19: Identity of the isolated CXCL12 (S4V and S2G4V) chemokines. Western blot analysis of the isolated chemokines in comparison to the commercially available CXCL12 *wild type*.
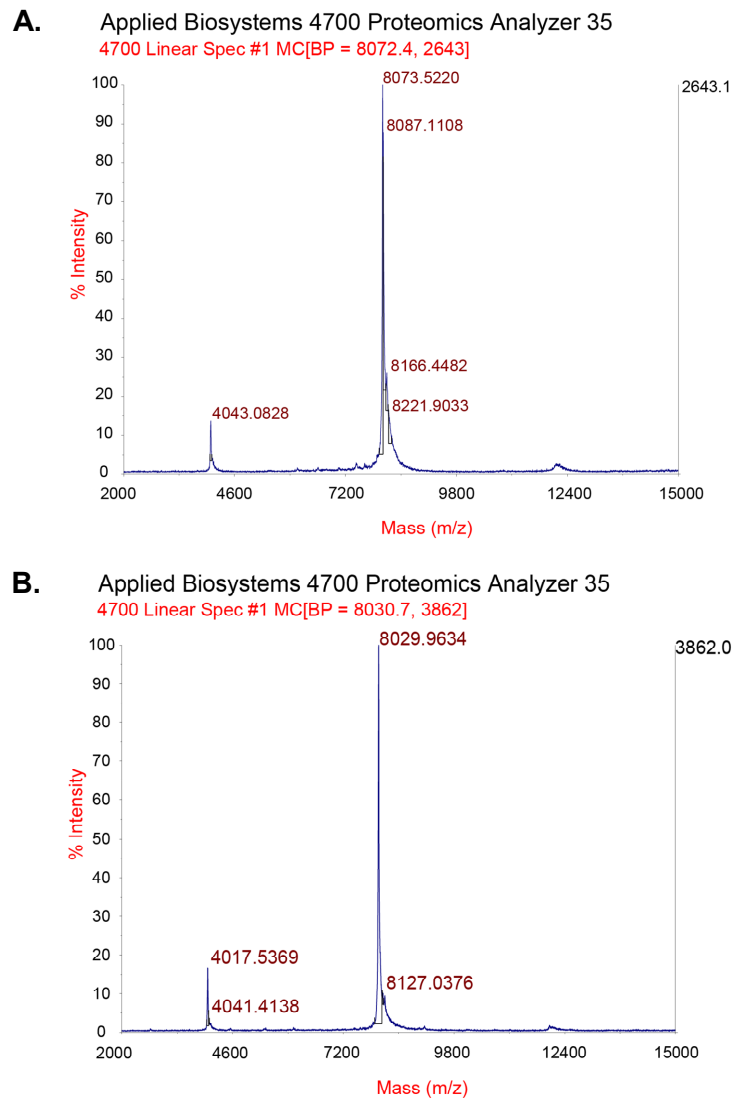

Figure 20: Purity and mass determination of CXCL12 (S4V and S2G4V) chemokines by means of MALDI-TOF. A. The mass of CXCL12 (S4V) chemokine corresponds to 8.07 kDa. **B.** The mass of CXCL12 (S2G4V) chemokine corresponds to 8.03 kDa. The y-axis represents the signal intensity in % and the x-axis represents the mass to charge ration (m/z).

5.2.   Synthesis of biocompatible and degradable hydrogels

Hydrogels are networks of hydrophilic crosslinked polymeric particles with submicrometer size. The characteristics of hydrogels are biocompatibility, high-water content as well as tunable chemical and mechanical properties with the features of nanoparticles such as high-surface area and overall sizes in the range of cellular compartments[121]. Hydrogels feature a high degree of flexibility similar to natural tissue. These properties make them intriguing candidates for entrapment of hydrophilic bioactive molecules such as proteins to provide a hydrophilic environment and protect them from degradation[121]. Two different biocompatible and degradable hydrogels were chosen as a scaffold to entrap the Met-CCL5 in a fast degradable hydrogel (FDH) for a very fast release over 24 h and the protease-resistant CXCL12 (S4V) in a slow degradable hydrogel (SDH) for a slow release over 4 weeks, to control the local release of the chemokines over time in the infracted myocardium of the mice.

A star-shaped polymer sP(EO-*stat*-PO) and linear poly(glycol) (PG) were chosen as precursor for the hydrogels. Both polymers are hydrophilic and biocompatible, and the molecular weight is well below 30 kDa, which is set as a limit that allows renal clearance for linear polyethylene oxide (PEO)[169]. They were successfully functionalized with thiol groups through carbodiimide-mediated Steglich esterification between the free hydroxyl groups of the polymers and the disulfide containing dicarboxyacid[121]. The preparation of disulfide crosslinked particles from SH-sP(EO-*stat*-Po) polymers was performed by oxidation of thiol groups to disulfides and by Michael addition between thiol groups and acrylate (Figure 21). Disulfide formation proceeds through the deprotonated form of thiol groups. Thus, to maintain slightly basic reduction conditions, PBS buffer (pH 7.4) was used as a dispersed phase. The lyophilized chemokines were dissolved in PBS buffer. The oxidized hydrogels were mixed with PBS buffer containing Met-CCL5 for a fast delivery over 24 h in the tissue. The hydrogels obtained by Michael addition were mixed with the PBS buffer containing protease-resistant CXCL12 for a slow delivery over 4 weeks in the tissue. The described hydrogels were provided by Smriti Singh in the group of Prof. Dr. Jürgen Groll (University of Würzburg, Institute for Technology of Functional Materials in the Medicine, Würzburg, Germany).
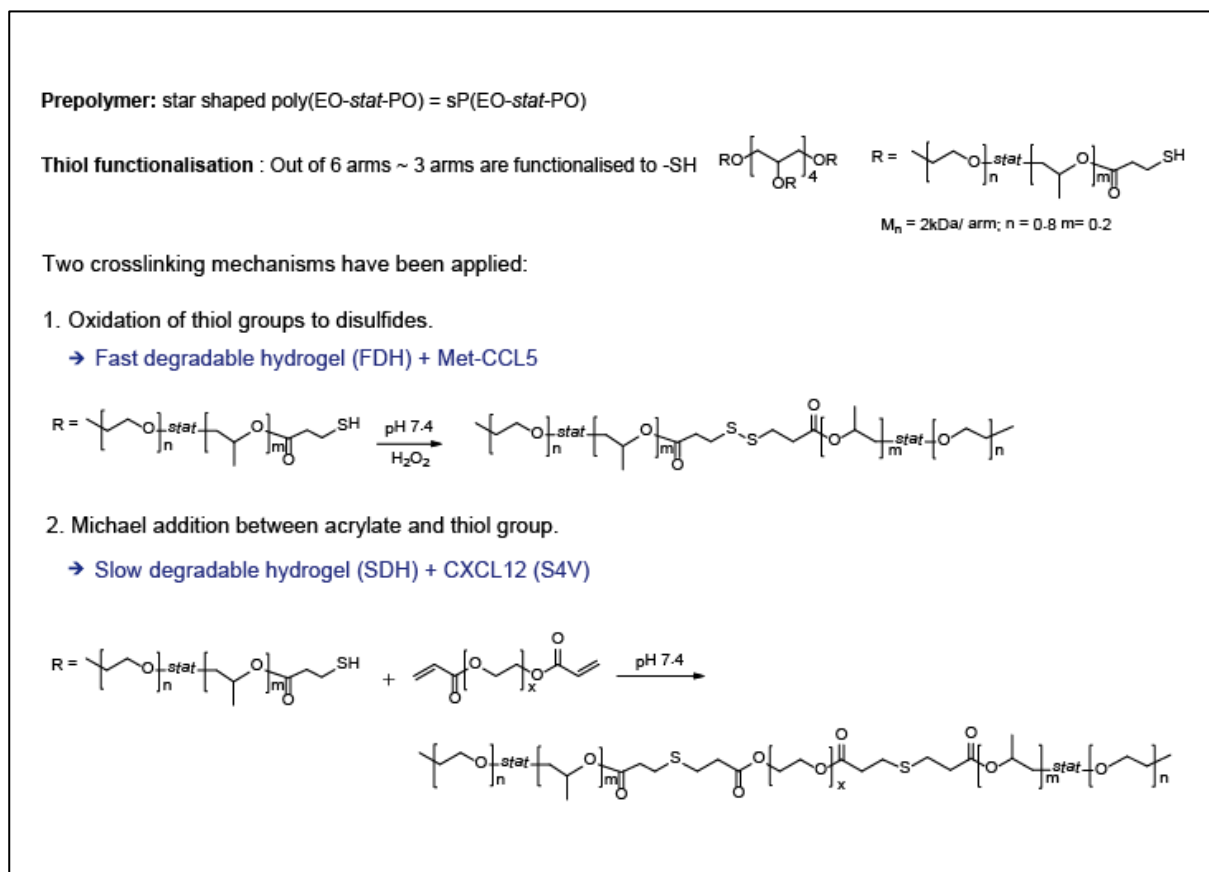
Figure 21: Synthesis of biodegradable hydrogels. The thiolated polymer termed sP(EO-stat-PO) was crosslinked by two mechanisms: The first mechanism is an oxidation (by H_2O_2) of thiol groups to disulfides, which represents the fast degradable hydrogel (FDH) and was mixed with Met-CCL5 for a very fast delivery over 24 h. The second mechanism is a Michael addition between acrylate and thiol group, which represents the slow degradable hydrogel (SDH) and was mixed with protease-resistant CXCL12 (S4V) for a slow delivery over 4 weeks.

## 5.3.	Intramyocardial release of engineered chemokines using biodegradable hydrogels prevents injury extension after myocardial infarction (MI)

Before examination of the local therapy of MI with protease-resistant CXCL12 (S4V) in slow degradable hydrogels (SDH) and Met-CCL5 in fast degradable hydrogels (FDH), their functionality and biocompatibility was shown *in vitro*. Subsequently, the chemokines and hydrogels were injected *in vivo*, locally into the mouse myocardium as a potential therapeutic agent for the therapy after MI.

### 5.3.1.	Met-CCL5 antagonizes CCR1, CCR3 and CCR5 receptors and prevents neutrophil recruitment

A variety of inflammatory diseases are characterized by tissue infiltration of neutrophils through its CCR1, CCR2, CCR3, CCR5, CXCR3 and CXCR4 receptors[170]. CCL5 activates the G-protein coupled receptor GPR75[171] and interacts with CCR3[172, 173], CCR5[173, 174] and CCR1[173, 175]. Met-CCL5 antagonizes CCR5 activation and functions in response to its natural ligand *in vitro*[74]. The chemokines CXCL8 and CCL5 are strong chemoattractants of neutrophils in comparison to Met-CCL5 which antagonizes the neutrophil activation. The activity of recombinant Met-CCL5 was assessed using cell-recruitment assay with the designated target cell types. Isolated neutrophils stimulated with CXCL8 and/or CCL5 showed considerable chemotaxis. Met-CCL5 specifically blocked the action of CCL5, but not of CXCL8. These results indicate that Met-CCL5 antagonizes the CCL5 receptor but not the CXCL8 receptor function (Figure 22A). The adhesion assay of stimulated neutrophils on HUVEC under flow conditions agreed with the above cell recruitment assay. The adhesion of neutrophils stimulated with CXCL8, CCL5 and in combination with CXCL8 and Met-CCL5 on HUVEC under flow conditions showed a high cell adhesion number. Met-CCL5 specifically blocked the action of CCL5, but not of CXCL8 (Figure 22B). The evaluation of cell cycle progression and the estimation of the number of viable cells were essential to exclude side effects before treating mice with the recombinant Met-CCL5. The proliferation was quantified using bromodeoxyuridine (BrdU) which was incorporated into newly synthesized DNA of actively proliferating HUVECs. The proliferation of HUVECs incubated with Met-CCL5 was analyzed in comparison to untreated cells. The data are expressed as the relative signal (RFU) and indicated the same proliferation of Met-CCL5-treated HUVECs in comparison to the negative controls (Figure 23A). For the estimation of cell viability the indicator dye resazurin was used, to measure the metabolic capacity of HUVECs, which is an indicator of cell viability. Viable HUVECs reduce resazurin into resorufin, which is a fluorescent dye. Nonviable HUVECs rapidly lose metabolic capacity, are not able to reduce the indicator dye, and are not able to generate a fluorescent signal. Met-CCL5-treated HUVECs indicated the same number of viable cells incubated over 12 h in comparison to untreated and viable cells

(Figure 23B). The treatment with Met-CCL5 did not impair the proliferation and viability of cultured HUVEC cells (Figure 23).
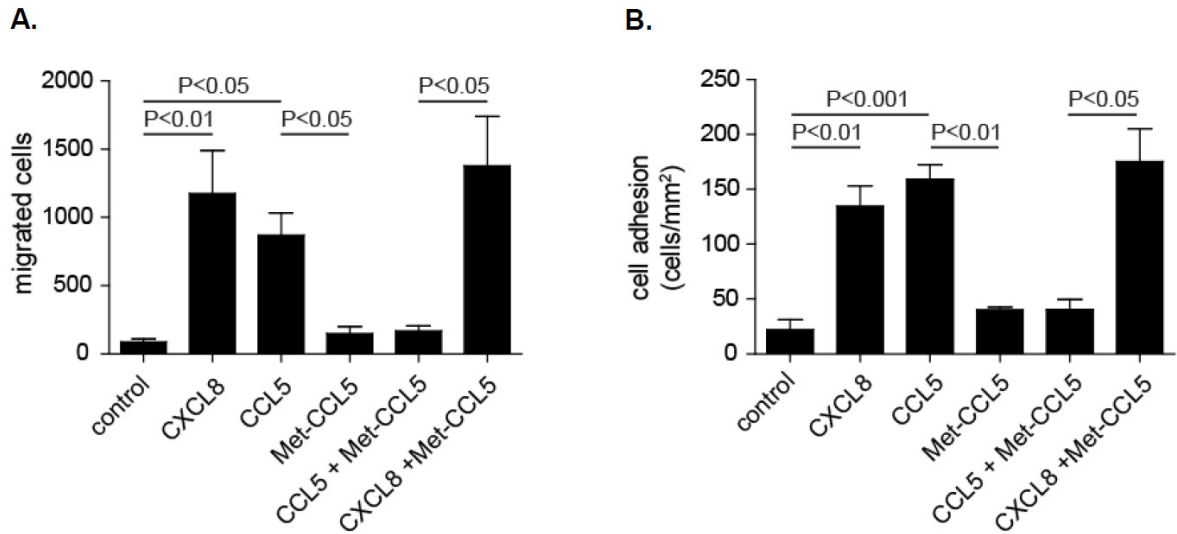
A.

B.

Figure 22: Chemotaxis and adhesion assay with Met-CCL5-stimulated neutrophils. A. Chemotaxis assay of neutrophils towards Met-CCL5, CCL5 *wild type* and commercially available CXCL8 *wild type*. **B.** Adhesion assay under flow on activated HUVEC using Met-CCL5, CCL5 *wild type* and CXCL8-stimulated neutrophils. Depicted P-values are based on parametric evaluation, (n=9).
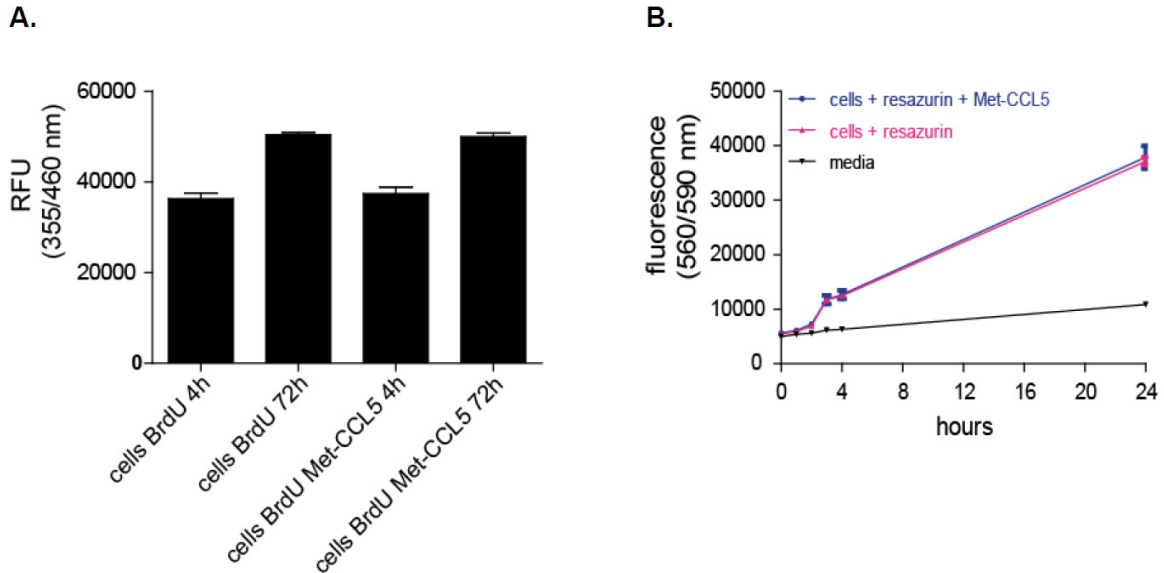
A.

B.

Figure 23: Influence of Met-CCL5 on proliferation and cell viability of HUVECs. A. Proliferation assay and **B.** cell viability assay of BrdU labeled HUVEC (1000 cells/well) incubated with/without Met-CCL5 (A, B) until 24 or 72 h, (n=2).

5.3.2. Protease-resistant CXCL12 retains receptor specificity and activity of native CXCL12

The CXCL12 receptor binding site for CXCR4 and CXCR7 is located on the N-terminal site of the chemokine[166]. The cleavage sites of MMP-2 and DPPIV for CXCL12 are also located on the N-terminal site of the chemokine, which limit the effectiveness of CXCL12[53]. The CXCL12 chemokine was modified on the N-terminal side to obtain a protease-resistant CXCL12 (S4V) and CXCL12 (S2G4V) chemokines (Figure 7) (Table 1). The chemotactic activity and receptor specifity were analysed for both protease-resistant CXCL12 (S4V) and CXCL12 (S2G4V) chemokines. The activity of the recombinant CXCL12 (S4V) was assessed using cell-recruitment assay with the designated target cell types. The recombinant CXCL12 (S4V) induced the migration of angiogenic EOC to a slightly lower extent than CXCL12 *wild type*, whereas the activity of CXCL12 (S2G4V) was comparable with the negative control (Figure 24A). Adhesion assay of CXCL12 (S4V)-stimulated Jurkat cells on HUVEC under flow conditions was comparable with the commercially available CXCL12 *wild type*. CXCL12 (S2G4V) showed significantly less adhesion compared to the CXCL12 (S4V) and CXCL12 *wild type* (Figure 24B). To exclude side effects of recombinant protease-resistant CXCL12 (S4V) before treating the mice, cell cycle proliferation and cell viability assay were performed. The proliferation assay for BrdU incorporation into newly synthesized DNA of actively proliferating cells (HUVECs) showed the same relative signals (RFU or proliferation) incubated with the recombinant protease-resistant CXCL12 (S4V) in comparison to the negative controls (Figure 25A). For the viability assay, HUVECs were treated with the CXCL12 (S4V) in comparison to non-treated cells and the results indicated no difference between the groups. The recombinant CXCL12 (S4V) showed neither effects on the proliferation and cell viability of cells (Figure 25B).
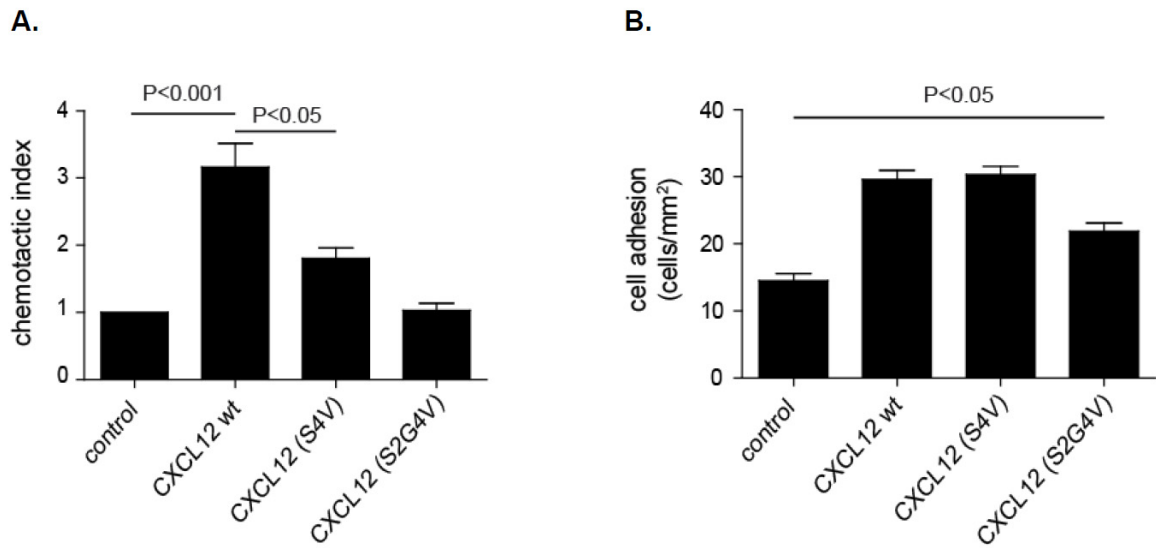
A.

B.

Figure 24: Chemotaxis and adhesion assay with CXCL12 (S4V and S2G4V)-stimulated angiogenic early outgrowth cells (EOCs). A. Chemotactic index of angiogenic EOC towards CXCL12 (S4V and S2G4V) and commercially available CXCL12 *wild type*. B. Adhesion assay using CXCL12 (S4V and S2G4V)-stimulated Jurkat cells on activated HUVEC under flow conditions in comparison to the commercially available CXCL12 *wild type*. Depicted P-values are based on parametric B. or non-parametric A. ANOVA (n=6-9).
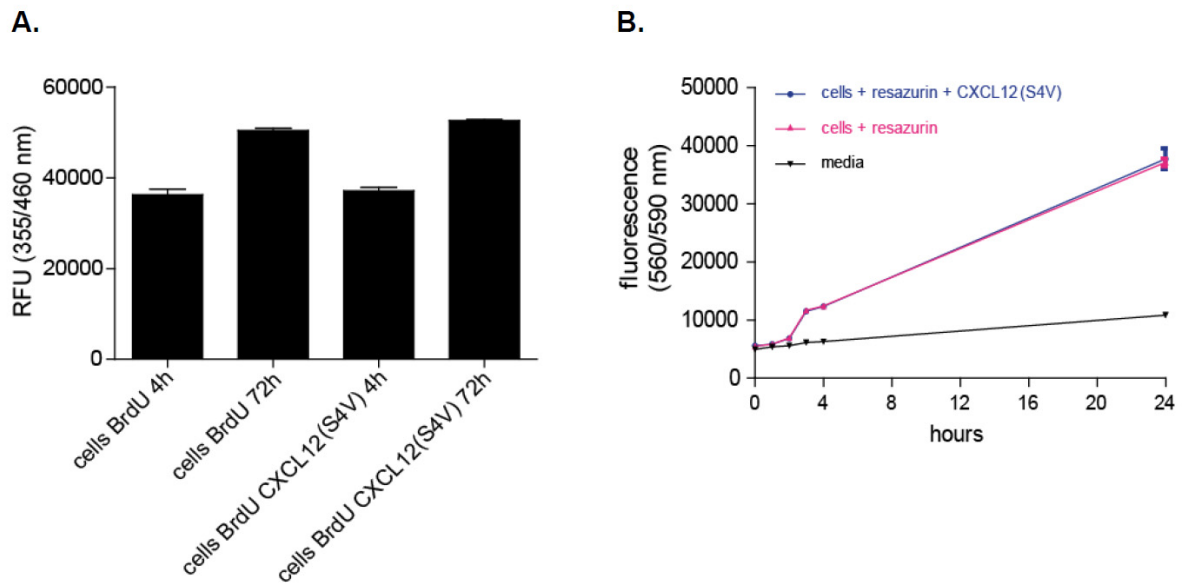
A.

B.

Figure 25: Influence of CXCL12 (S4V) on proliferation and cell viability. A. Proliferation assay and **B**. cell viability assay of BrdU labeled HUVEC (1000 cells/well) incubated with/without CXCL12 (S4V) (A, B) until 24 or 72 h, (n=2).

5.3.3. Controlled release of chemokines using biocompatible and degradable hydrogels

Hydrogels used for the application into the heart must simultaneously promote desirable functions for tissue regeneration, while not eliciting a severe and chronic inflammatory response. Hydrogels forming polymers are generally designed to be nontoxic to the cells of the surrounding tissue of the application site. The hydrogels should theoretically interact favorably with the heart tissue, on condition that they have not been contaminated during processing and that there are no cross-species immunological issues[91]. For testing of the compatibility of the hydrogels before injection into mice heart *in vitro* studies were performed. The proliferation of HUVECs in presence of the thiolated hydrogels compared to untreated cells was analyzed. Thiolated hydrogels-treated HUVECs show no effect on the proliferation (Figure 26A). Also, cell viability assay of hydrogel-treated HUVECs show similar results in comparison to untreated cells (Figure 26B) Currently, the majority of small and large molecule drugs are delivered into patients systemically without the use of scaffolds. Consequently, large doses are usually required for a desired local effect because of degradation of the drug and nonspecific uptake by other tissue. Hydrogel scaffolds are often utilized to stabilize and deliver bioactive molecules[91]. For an accurate delivery of the chemokines into the mouse hearts, the FDH and the SDH were used. In order to control the local release of the chemokines into the mice heart, delivery assay of both hydrogels (SDH and FDH) were performed. The SDH was conceived for formulation with the protease-resistant CXCL12 (S4V) for a gradual release in order to recruit HCs from the circulating blood during a time period of 4 weeks after MI. In order to confirm the release rate, the CXCL12 (S4V)-SDH was incubated for 33 days in PBS to detect the local release over time. After 33 days the SDH was entirely degraded due to the hydrolytic cleavage of ester bonds in the backbone and release of chemokine was no longer detected (Figure 27A). The FDH is used for the formulation with Met-CCL5 for a quick release over 24 hours to inhibit neutrophil infiltration within the first hours after MI. This fast release of Met-CCL5 from FDH was confirmed by incubation in PBS and 5mmol/L glutathione, which led to complete degradation of the gel after 24 h due to disulfide bond cleavage. After 24 h the FDH is totally degraded and no chemokine could be detected (Figure 27B).
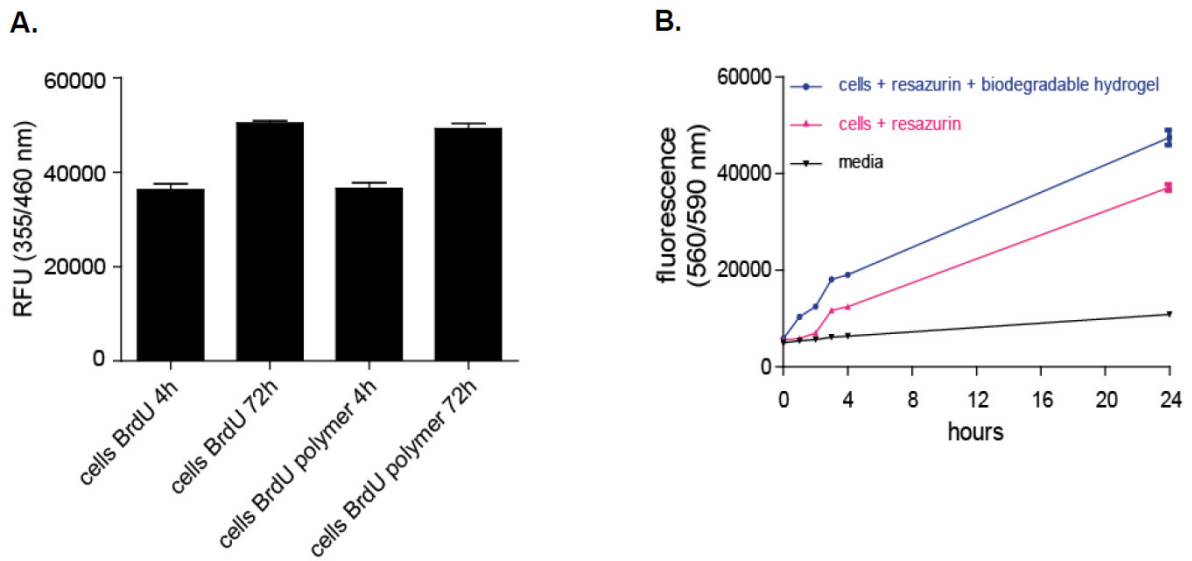
Figure 26: Influence of biopolymer on proliferation and cell viability. A. Proliferation assay and **B**. cell viability assay of BrdU labeled HUVEC (1000 cells/well) incubated with/without degradable polymer (A, B) until 24 or 72 h, (n=2).
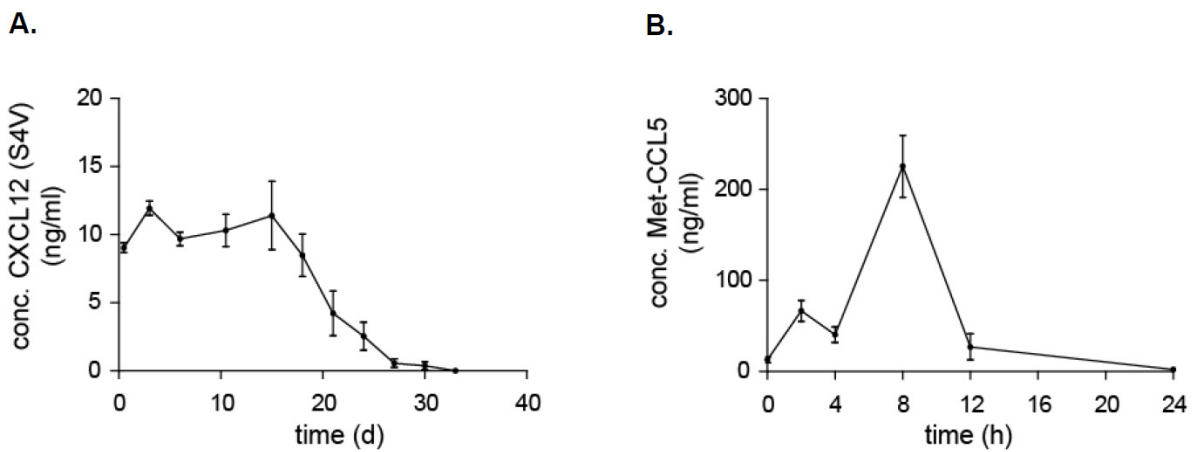

Figure 27: Release assay from hydrogels. A. Release of the protease-resistant CXCL12 (S4V) chemokine from the slow degradable hydrogel (SDH) over 33 d and **B.** of the Met-CCL5 chemokine from the fast degradable hydrogel (FDH) over 24 h.

5.3.4. Improvement of cardiac function *in vivo* after MI in mice by combined treatment with the protease-resistant CXCL12 and Met-CCL5 and biodegradable hydrogels

MI is a common cause of heart failure, and recruitment of SC by CXCL12 could improve cardiac function[176]. *In vivo*, Met-CCL5 is able to reduce inflammation in models of induced inflammatory and autoimmune diseases[74]. Hydrogels ensure the local delivery of the chemokines over time in the body[91]. In order to investigate a possible beneficial role of a blocked short-term neutrophil influx after cardiac ischemia, combined with a longer-term recruitment of hematopoietic cells, the chemokine-loaded hydrogels were applied in an experimental model of MI. First, heart function of the mice was evaluated one day before and four weeks after MI induction using echocardiography. One day after analyzing the heart function the MI induction was performed followed by the local injection of Met-CCL5 and CXCL12 (S4V) formulated in two different hydrogels. The CXCL12 (S4V) was formulated in a SDH (CXCL12 (S4V)-SDH) for a slow delivery of the protease-resistant CXCL12 (S4V) for the recruitment of HC from the circulating blood, and the Met-CCL5 was formulated in the FDH (Met-CCL5-FDH) to prevent neutrophil-infiltration during the first 24 h, after MI. The mice were sacrificed 1 day after induction of MI to investigate the mobilization and recruitment of inflammatory cells, and 4 weeks after MI induction to examine the MI area and the neovascularization (Figure 28). In a study involving 44 mice surviving surgery, the effects of the injected chemokines on MI were examined in 4 groups (Table 2).
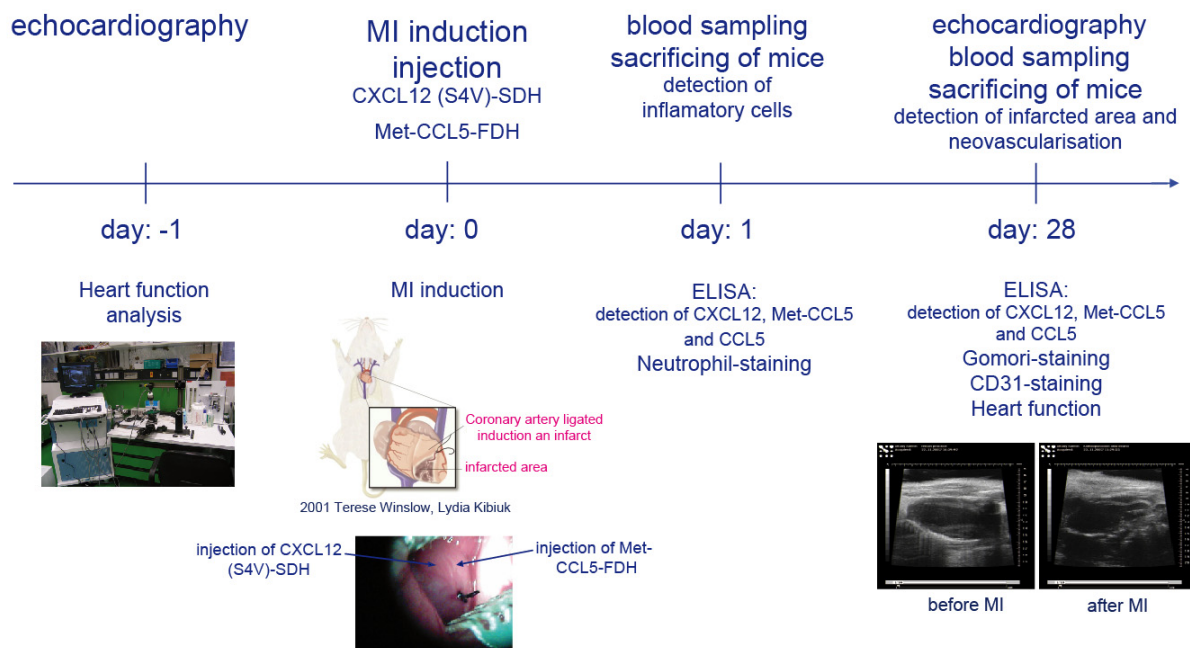

Figure 28: Overview of mouse experiments.

	group 1	group 2	group 3	group 4	group 5
treatment	control	FDH SDH	Met-CCL5-FDH	CXCL12 (S4V)-SDH	Met-CCL5-FDH CXCL12 (S4V)-SDH

Table 2: Overview of the groups with MI therapy.

5.3.4.1.   Functional changes of the hearts after MI were detected by echocardiography

Heart function of the mice was evaluated 1 day before, and 4 weeks after MI using the Vevo 700 software. The evaluation of the functional parameters of the heart revealed a significant improvement of cardiac function in the Met-CCL5-FDH + CXCL12 (S4V)-SDH group that received a combined treatment (Table 3 and Figure 29). The ejection fraction was increased in the group with Met-CCL5-FDH and CXCL12 (S4V)-SDH in comparison to the hydrogel and control group, but the combined treatment with Met-CCL5-FDH + CXCL12 (S4V)-SDH show the highest preservation of the heart function comparing to all other groups (Figure 29A, Table 3). Remarkably, the combined treatment with Met-CCL5-FDH + CXCL12 (S4V)-SDH was also able to improve cardiac output compared with the control group, hydrogel group and single chemokine-treated groups (Figure 29B, Table 3). No changes in heart weight were observed between the treated groups (Table 3).

	Control	FDH SDH	Met-CCL5-FDH	CXCL12-SDH	Met-CCL5-FDH CXCL12-SDH
EF (%)	$35.8 \pm 1.85^{\S\S\S}$	31.6 ± 1.30	$41.3 \pm 2.31^{\S\S}$	$40.5 \pm 1.83^{\S\S\S}$	$50.1 \pm 1.59^{***}$
CO (mL/min)	15.8 ± 0.42	13.8 ± 1.59	19.4 ± 1.92	16.5 ± 1.73	$22.6 \pm 2.43^{**}$
Heart rate (BMP)	442 ± 11.4	426 ± 38.2	501 ± 36.7	502 ± 34.4	414 ± 34.9
Heart weight (mg)	107 ± 6.58	119 ± 7.93	100 ± 8.77	104 ± 6.70	103 ± 4.86

Table 3: Echocardiographic parameters. Ejection fraction (EF); Cardiac output (CO); Fast degradable hydrogel (FDH); Slow degradable hydrogel (SDH). **, ***; P<0.01, 0.001 vs. FDH SDH, respectively; n=6-9; §§, §§§; P<0.01, 0.001 vs Met-CCL5-FDH+CXCL12 (S4V)-SDH, respectively; n=6-9 mice; ANOVA
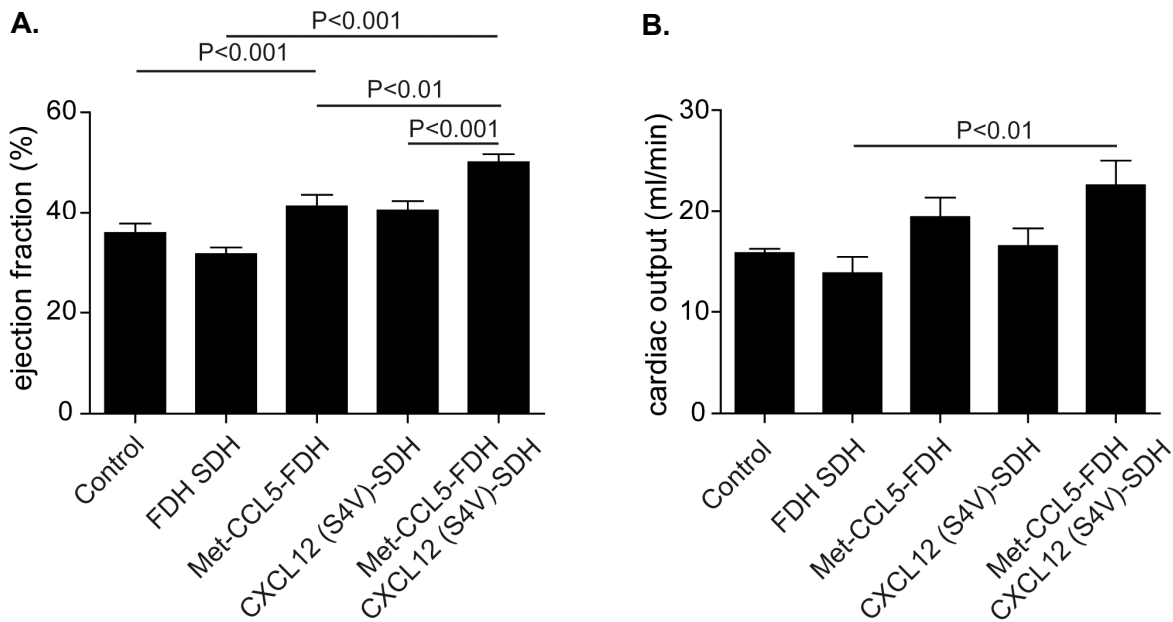
Figure 29: Cardiac function after experimental MI. Ejection fraction (EF) **A.** and cardiac output **B.** of FDH SDH, Met-CCL5-FDH, CXCL12 (S4V)-FDH and Met-CCL5-FDH+CXCL12 (S4V)-FDH -treated mice (n=6-9 per group), 4 weeks after MI. Depicted P-values are based on ANOVA.

5.3.4.2.   Treatment with protease-resistant CXCL12 and Met-CCL5 in biodegradable hydrogels after MI prevent neutrophil cell recruitment

Recovered mouse myocardium was analyzed 1 day after MI and injection of chemokines in biodegradable hydrogels for mobilization and recruitment of inflammatory cells. The immediate infiltration of MI-induced neutrophils in the infarcted area (after 1 day) was reduced in both the Met-CCL5-FDH (272 ± 35.8 mm^{-2}) and the Met-CCL5-FDH+CXCL12 (S4V)-SDH groups (299 ± 33.6 mm^{-2}), but not in the CXCL12 (S4V)-SDH group (876 ± 235.9 mm^{-2}), compared with the control groups that received only hydrogel (810 ± 51.3 mm^{-2}) or PBS (760.7 ± 72.2 mm–2) (Figure 30A-B). Thus, this confirmed the specificity of the administration of the CCR1 and CCR5 antagonist Met-CCL5 for the prevention of neutrophil recruitment.
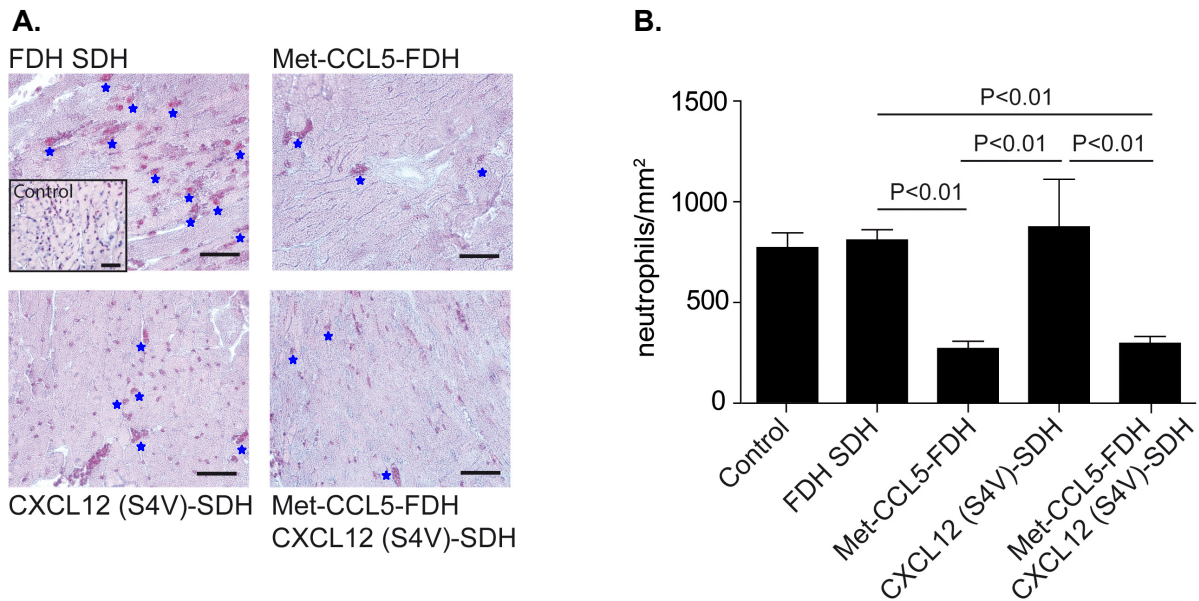
A.

FDH SDH   Met-CCL5-FDH

CXCL12 (S4V)-SDH   Met-CCL5-FDH
                    CXCL12 (S4V)-SDH

B.

Figure 30: Assessment of cardiac tissue damage after experimental MI. Neutrophil infiltration in the myocardium by esterase-staining **A.** and quantification **B.** of control (PBS), FDH SDH, Met-CCL5-FDH, CXCL12 (S4V)-SDH and Met-CCL5-FDH+CXCL12 (S4V)-FDH -treated mice, 1 d after MI. Examples of stained neutrophils are marked with asterisks. Scale bars: 50 µm. Depicted P-values are based on parametric evaluation, n=6-9.

5.3.4.3. *Treatment with the protease-resistant CXCL12 and Met-CCL5 in biodegradable hydrogels after MI reducse infarct size and promotes neoangiogenesis*

Besides the evaluation of neutrophil content, the capability of the reduction of infarct size and neovascularization was examined. After 4 weeks, the infarcted area was notably reduced in the CXCL12 (S4V)-SDH (13.4±2.85 %) and in the combined Met-CCL5-FDH+CXCL12 (S4V)-SDH group (12.8±4.18 %), compared to the groups that received hydrogel only (30.7±5.51 %) and Met-CCL5-FDH (25.7±4.73 %) (Figure 31A-B). Administration of the hydrogel itself did not affect infarct size, since the infarcted area of the control group was similar (30.3±3.72 %) (Figure 31A-B)

Similarly, neovascularization after MI was also improved in both the CXCL12 (S4V) SDH (788±28.8 mm^{-2}) and Met CCL5-FDH+CXCL12 (S4V)-SDH groups (1022±63.1 mm^{-2}), to a higher extent as the Met-CCL5 FDH (466±29.4 mm^{-2}), hydrogel group (328±32.5 mm^{-2}) and control groups (407±62.4 mm^{-2}), as quantified by CD31-staining (Figure 32A-B). This indicates a CXCL12 (S4V)-mediated increase of angiogenesis in infarcted myocardium, supporting our hypothesis. Interestingly, these findings also suggest that recruitment of hematopoietic cells through CXCR4 would serve to reduce infarct size rather than the blockade of initial neutrophil infiltration.
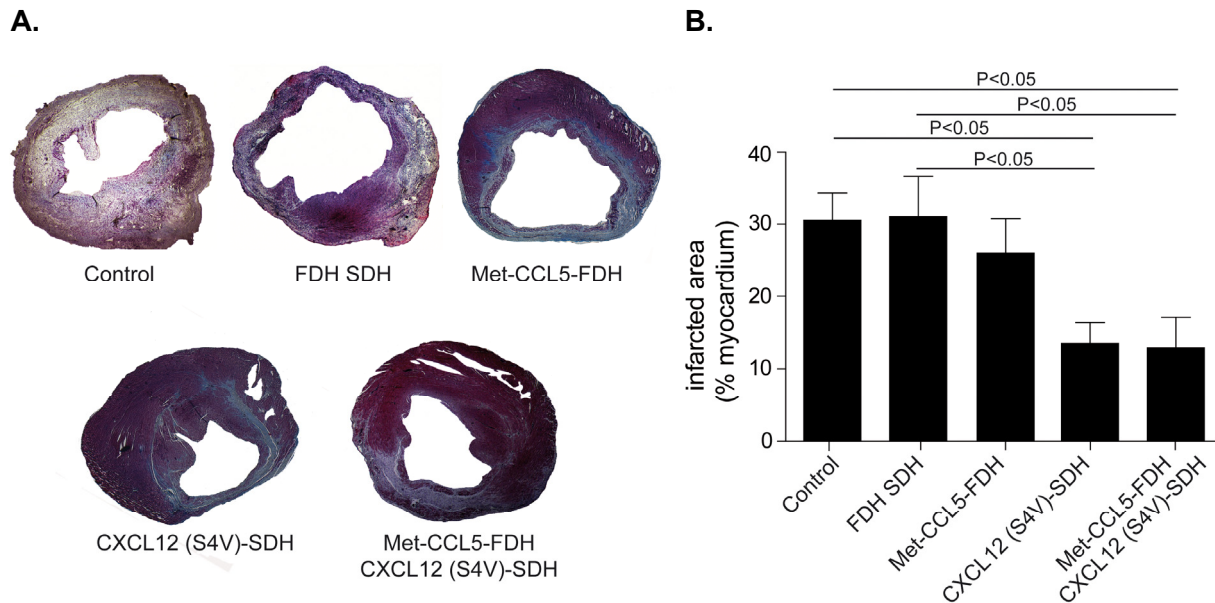
A.

Control   FDH SDH   Met-CCL5-FDH

CXCL12 (S4V)-SDH   Met-CCL5-FDH
                          CXCL12 (S4V)-SDH

B.

Figure 31: Assessment of cardiac tissue damage after experimental MI. Representative Gomori-stained heart sections **A.** and histomorphometric quantifications **B.** of the hearts of FDH SDH, Met-CCL5-FDH, CXCL12 (S4V)-SDH and Met-CCL5-FDH CXCL12 (S4V)-SDH treated mice, 4 weeks after MI. Depicted P-values are based on ANOVA (n = 6-9).

A.

FDH SDH   Met-CCL5-FDH

Control

CXCL12 (S4V)-SDH   Met-CCL5-FDH
                          CXCL12 (S4V)-SDH

B.
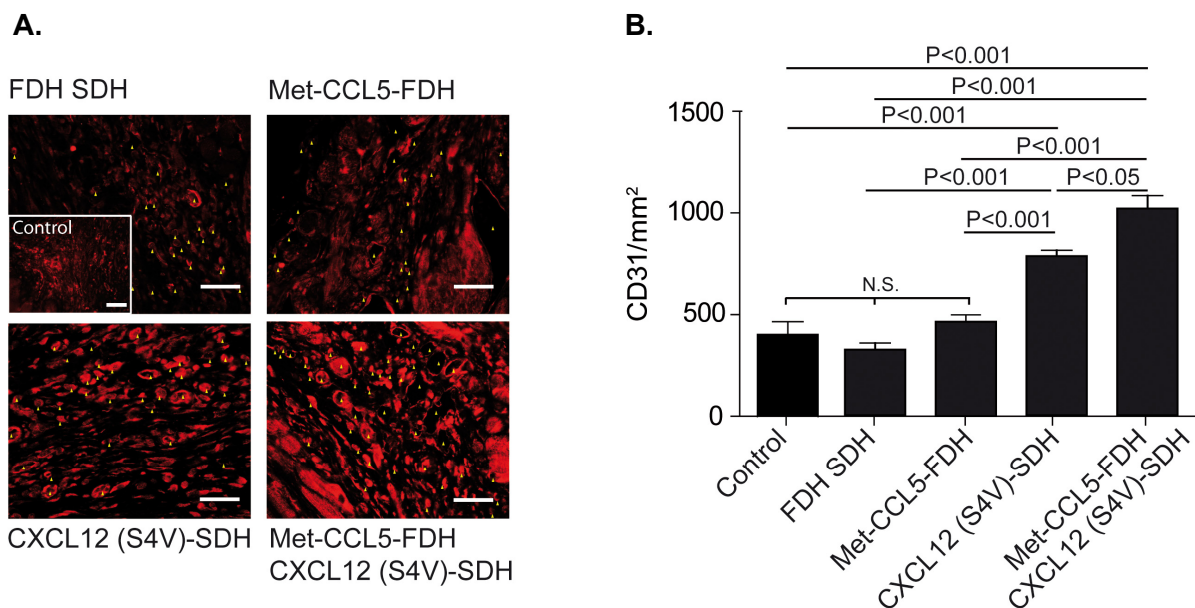
Figure 32: Assessment of cardiac tissue damage after experimental MI. Neovascularization as quantified by representative CD31 staining **A.** and quantification **B.** of FDH SDH, Met-CCL5-FDH, CXCL12 (S4V)-FDH and Met-CCL5-FDH+CXCL12 (S4V)-FDH treated mice, 4 weeks after MI. Examples of capillaries are marked with asterisks. Scale bars: 50 µm. Depicted P-values are based on non-parametric B. ANOVA (n≥6).

5.3.4.4.   Detection of chemokines in mouse sera after MI and treatment with the protease-resistant CXCL12 and Met-CCL5 in biodegradable hydrogels

During treatment, the levels of CXCL12 (S4V) in mouse sera after 1 day and 4 weeks were not increased (Figure 33A-B), due to the very slow release rate from the hydrogel and the local application. Human Met-CCL5 levels were increased after one day of treatment with

Met-CCL5-containing FDH (Figure 33C), due to the quick release of human Met-CCL5 from these hydrogels. As expected, the human Met-CCL5 was no longer detected in the mouse sera after 4 weeks (Figure 33D). The concentrations of mouse CCL5 in sera were slightly increased after administration of any hydrogel variant (Figure 33E-F).
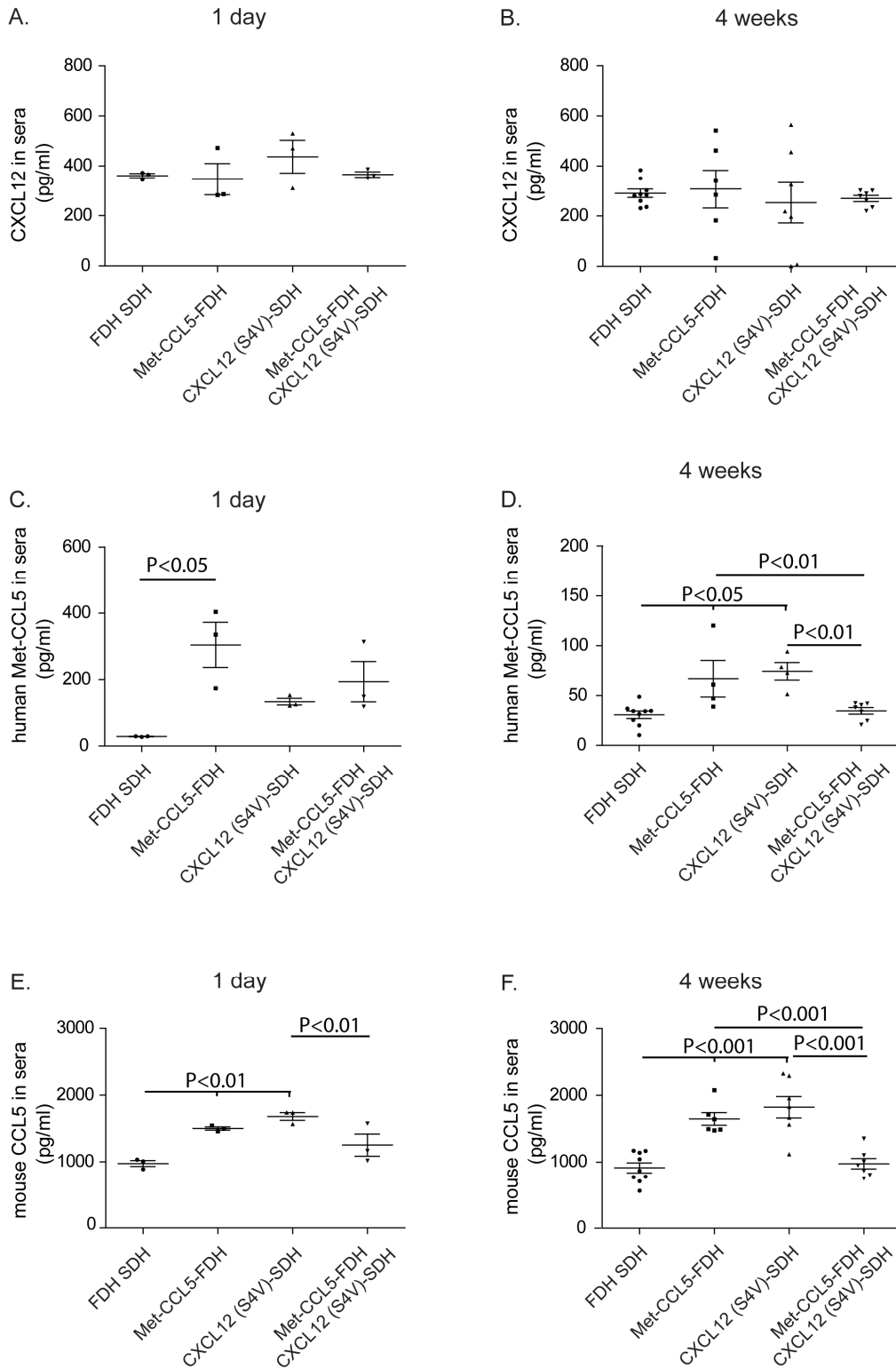

Figure 33: Concentrations of chemokines in mouse sera. Detection of the amount of mouse CXCL12, human Met-CCL5 and mouse Met-CCL5 in mouse sera using ELISA. Depicted P-values are based on ANOVA (n = 6-9).

5.4.   Role of platelet F1-CX$_3$CL1 antagonist in platelet-monocyte complex (PMC) formation

5.4.1.   F1-CX$_3$CR1 prevents PMC formation

Incubation of THP-1 monocytic cells with TRAP-6-activated but not resting human platelets resulted in a significant PMC formation as shown by increased staining of the platelet marker CD61 in the monocyte-gated population (Figure 34). To test whether platelet-CX$_3$CR1 plays a role in PMC formation, the platelets were preincubated with the CX$_3$CR1-antagonist F1-CX$_3$CL1[27], this significantly decreased the PMC formation (Figure 34). The complete disruption of the PMC was achieved by their incubation with EDTA (10 mM for 15 min, 37°C), indicating the reversibility of their formation.
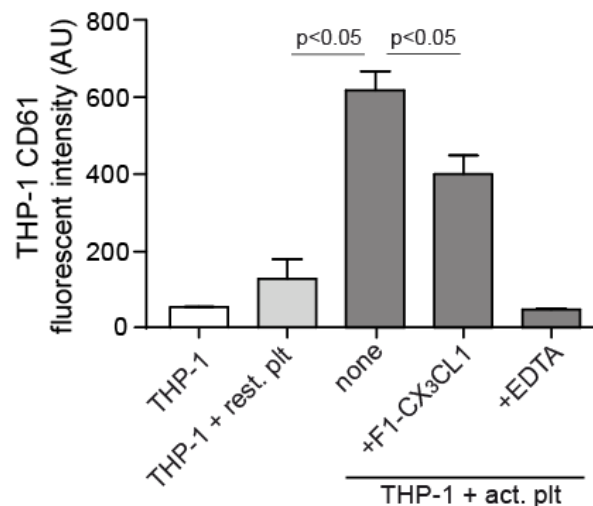

Figure 34: Role of CX$_3$CR1-CX$_3$CL1 axis in PMC formation. PMC are dependent on the CX$_3$CR1-CX$_3$CL1 interaction as their formation can be prevented by incubation of platelets with F1-CX$_3$CL1 antagonist (0.5 µg/mL).

5.4.2.   Platelet-CX$_3$CR1 enhances CX$_3$CL1-mediated adhesion of platelets and of PMC to SMC

Upon arterial denudation, CX$_3$CL1 expression is strongly upregulated on SMC[177] and mediates interactions with CX$_3$CR1-expressing cells[109]. In the following experiment, adhesion of TRAP-6-activated platelets to immobilized rhCX$_3$CL1 was specifically increased by 35.8%±6.13 (Figure 35A) (p< 0.05) as compared with adhesion to plastic and HSA and as shown by preincubation with a CX$_3$CR1 neutralizing antibody. Together, these data indicate that CX$_3$CR1 exposed on activated platelets is able to stably bind CX$_3$CL1. In line, TNFα-stimulated SMC, which have been shown to express CX$_3$CL1 upon activation[178] supported robust adhesion of blood leukocytes to smooth muscle cells, only when platelets were activated by the addition of TRAP-6 (Figure 35B). Pretreatment of the perfused SMC with a neutralizing CX$_3$CL1 antibody blocked leukocyte adhesion, compared to an isotype control (Figure 35B). In addition, incubating the TRAP-6-activated whole blood with F1-CX$_3$CL1

reduced stable leukocyte arrest to the same extent, indicating that the process was strongly mediated by the CX_3CL1-CX_3CR1 axis. All data studying the role of F1-CX_3CL1 antagonist were published by Postea et. al.[117].

A.

B.
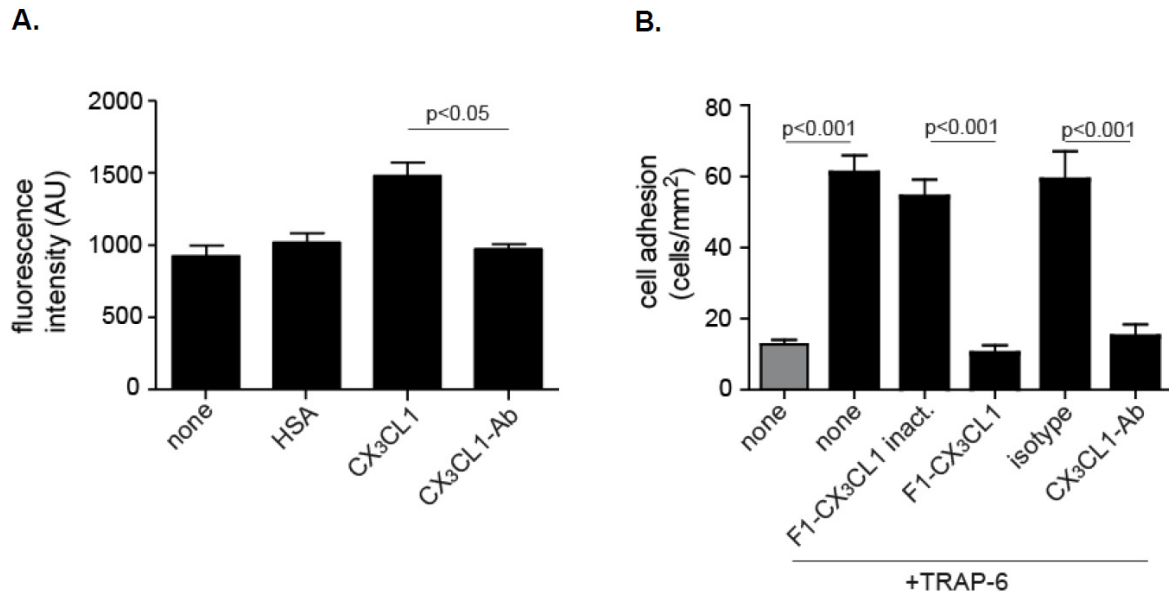
Figure 35: Recruitment of CX_3CR1-expressing platelets on inflamed SMCs. A. Static adhesion of calcein-loaded human platelets to plastic (none), HSA (1%) and rhCX_3CL1 (0.25 µg/well) in the absence or presence of a neutralizing CX_3CL1 antibody (5 µg/mL). Data are representative of 3 different donors. **B.** Perfusion of rhodamine-labeled anticoagulated whole blood untreated (grey bar) or pretreated with TRAP-6 (15 µM, black bars) over aortic SMC activated with TNFα (10 ng/ml, 4h). Stimulated SMC were pre-incubated with anti-CX_3CL1 neutralizing mAb or isotype control (5 µg/mL). Alternatively, the blood was treated with F1-CX_3CL1 or heat-inactivated F1-CX_3CL1 (5 µg/mL) (n>3 independent experiments.

6.   Discussion

6.1.   Expression and isolation strategies

Atherosclerosis ultimately leads to MI which is the major cause of death world wide[179]. Chemokines have a fundamental importance in the development of atherosclerosis and in the possible therapy of MI. Because chemokines have a fundamental importance, new therapeutic strategies are urgently needed to prevent the development of atherosclerosis and to cure the consequences of MI. Angiogenesis is a natural mechanism to restore reperfusion to the ischemic myocardium after MI[180]. This might be achieved by local proliferation of EC and by attraction of EOC through chemotaxis. To analyze the effects of F1-CX$_3$CL1, Met-CCL5 and protease-resistant CXCL12 on atherosclerosis and MI, it was necessary to express, isolate and purify these chemokines. To regulate the expression of the recombinant chemokines and / or antagonists the pET vector system was used, which is accomplished through the T7 promoter-driven system[181-183]. The pET system is a powerful system developed for the cloning and expression of recombinant chemokines or proteins in *E. coli*[181-183]. The proteins were expressed in the cytoplasm of *E. coli* as "*inclusion bodies*". As inclusion bodies are characterized by a relatively high specific density, they can be harvested after cell lysis by centrifugation at moderate rotor speed. To lyse the bacterial cells, it is important to prevent co-sedimentation of cell debris in order to obtain a maximum effect of lysis. An effective method the disruption of bacterial cells can be achieved by repetitive cell lysis, followed by high pressure dispersion, followed by repetitive high pressure dispersion of the "*inclusion body*" isolate[184]. A further notable way for extraction of "*inclusion bodies*" is the usage of chaotropic agents such as urea or guanidine-HCl. Caution needs to be taken though during this step, as the "*inclusion bodies*" may not completely disintegrate during this extraction procedure. Proteins expressed in "*inclusion bodies*" are generally in a misfolded condition and thus biologically inactive. Under normal cellular conditions, a subset of cytoplasmic proteins are able to fold spontaneously[185] while aggregation-prone proteins require the existence of a number of molecular chaperones that interact reversibly with nascent polypeptide chains to prevent aggregation during the folding process[186]. Until now, no universal approach has been established for the efficient folding of aggregation-prone recombinant proteins[187]. Therefore a new optimal strategy has to be developed for each recombinant protein of interest.

6.1.1. F1-CX$_3$CL1 expression and isolation

Mizoue et. al.[188] have reported that N-terminal modifications to CX$_3$CL1 result in proteins with reduced agonistic properties. It was also shown that removal of the first seven residues of hCX$_3$CL1 leads to an inactive analog with poor affinity for CX$_3$CR1[188]. The study published by Inoue et. al.[189] has reported that mCX$_3$CL1 lacking the four N-terminal residues, behaves as an antagonist for mCX$_3$CR1 *in vitro* and *in vivo* but there was no evidence that it binds also to hCX$_3$CR1. In 2009, Dorgham et. al.[27] described a phage-display strategy to select antagonistic CX$_3$CL1 chemokine analogs, for which ligands are able to bind the CX$_3$CR1 receptor without triggering antagonist-induced signaling. The clone-ILDNGVS, also called F1 showed the most potent antagonistic behaviour[27]. For this study, the same CX$_3$CL1 antagonist as Dorgham et. al.[27] has been used. The recombinant F1-CX$_3$CL1 protein was expressed in *E. coli* as insoluble "*inclusion bodies*" using the pET-26b(+) vector system (4.4.1). The recombinant protein possessed a His Tag in its N-terminal part. As discussed before it is necessary to find an optimal solubilizing and refolding agent to obtain an active conformation. An adequate solubilizing agent for F1-CX$_3$CL1 was found to be guanidine-HCl with the addition of DTT that keeps the cysteines in the reduced state and cleaves disulfide bonds formed during preparation. For the first purification step the His Tag, which is located on the N-terminal part of the F1-CX$_3$CL1, was applied for the binding on the His Trap HP to Ni^{2+} ions (Figure 10). To obtain the desired conformation of the protein oxidized and reduced glutathione were the best refolding agents for this process. Reduced glutathione disulfide bonds formed within cytoplasmic proteins to cysteines by serving as an electron donor. During this process, reduced glutathione is converted to its oxidized form glutathione disulfide[190]. The His Tag was removed from his F1-CX$_3$CL1 by digestion with enterokinase and F1-CX$_3$CL1 was purified using cation exchange chromatography (Resource S column). The isoelectric point of the F1-CX$_3$CL1 differs from the His Tag and the undigested one. Due to the increase of the isoelectric point from 8.87 to 9.34 of the F1-CX$_3$CL1 after digestion, the presumed cleaved F1-CX$_3$CL1 chemokine was located under peak 2 (Figure 11) could be confirmed by mass spectrometry (Figure 12A) and western blotting (Figure 12B).

6.1.2. Met-CCL5 expression and isolation

The chemokine CCL5 plays a crucial role as neutrophil and macrophage activator in atherosclerosis and MI[67]. The treatment with anti-CCL5 mAb significantly reduced both infarct size and post-infarction heart failure in a mouse model of chronic cardiac ischemia[67]. The cardioprotective effects were associated with the reduction of leukocyte recruitment in the infarcted hearts. Marino et. al.[142] showed that the injection of an antagonist against CCL5, reduced leukocyte infiltration in a mouse model of myocarditis. Blocking the chemokine CCL5 suggests a possible therapeutic application aiming at reducing

inflammation during the reperfusion period of the heart. Proudfoot et al[153]. have published about a CCL5 receptor antagonist Met-CCL5 that contains an additional methionine at the N-terminus of the protein that reduces leukocyte infiltration[191]. For this study the same Met-CCL5 as described by Proudfoot et. al.[153] has been used. The recombinant Met-CCL5 was also expressed in "*inclusion bodies*" of the *E. coli* bacterial strain using the pET-26b(+) vector (4.4.2). As discussed before, the best solubilizing agent for Met-CCL5 was guanidine-HCl and DTT. For the first purification step of the Met-CCL5 a strong cation exchanger (SP Sepharose FF) was utilized, which is suitable for a small-scale of protein purification (Figure **13**A). A proper technique for the second purification step of Met-CCL5 was reverse phase chromatography using Vydac® C8 column (Figure 14). A relatively short retention time was necessary for the purification of Met-CCL5, by this reason the C8 column was the best in comparison to C18 which shows a higher retention and C4 which shows less retention towards non-polar compounds. The identity of the purified Met-CCL5 chemokine was confirmed by mass spectrometry (Figure 15A) and western blotting (Figure 15B).

6.1.3. CXCL12 (S4V and S2G4V) expression and isolation

The protease-resistant CXCL12 (S4V), which was already published by Segers et al[53]. to be resistant to MMP-2 and DPPIV/CD26 cleavage, was expressed and purified. First, the native CXCL12 chemokine was modified on the N-terminal site at position 4 from serine to valine and an additional serine in front of the sequence obtaining the same modifications as previously published[53]. To verify, if an additional modification would lead to the inactivation of this chemokine, a proline at position 2 was modified to glycine generating the following CXCL12 (S2G4V) chemokine. The recombinant CXCL12 (S4V and S2G4V) proteins were expressed in *E. coli* as insoluble "*inclusion bodies*" employing the Trx Tag, and using the pET-32a(+) vector system (4.4.3). When the Trx Tag is expressed from pET-32a(+) vector in *E. coli*, it can accumulate approximately to 40% of the total cellular protein while remaining fully soluble[192]. The very good soluble expression suggests that Trx Tag is translated very efficiently, especially when the Trx Tag is positioned at the aminoterminus of the fusion where protein translation initiates[193]. The very compact folding of the Trx Tag which is >90% of its primary sequence is involved in strong elements of secondary structure. This explain his high thermal stability ($T_m = 85°C$), the robust folding characteristics and its success as a fusion partner protein[194]. It was proposed that Trx Tag may serve a covalent joined chaperon protein by keeping folding intermediates of linked heterologous proteins in solution long enough for them to adopt their correct final conformation[194]. Guanidine-HCl was used as optimal solubilizing agent for the CXCL12 (S4V and S2G4V)-Trx in inclusion bodies. The CXCL12 (S4V and S2G4V) chemokines contain disulfide bonds and the addition of reduced and oxidized forms of low molecular weight thiol reagents like cysteine provides the

appropriate redox potential and allow formation and reshuffling of disulfides[195]. To obtain the desired conformation of the protein, cystine redox agent were found to be the best refolding agent for this process in comparison to glutathione that was also investigated during optimizing this method. For the first purification step, the Trx which is located on the N-terminal end of the CXCL12 (S4V and S2G4V) chemokines were applied for the binding on the Ni-NTA column (Figure 16). For further purification, affinity chromatograpy using Heparin Sepharose, which allows the separation of biomolecules with affinity to heparin (Figure 17) was performed for CXCL12 (S4V and S2G4V). Heparin is a natural ligand for CXCL12. During the purification the correct folded CXCL12 (S4V and S2G4V) binds stronger to heparin while the wrongly folded CXCL12 (S4V and S2G4V) binds not as strongly to the column. After the Heparin Sepharose purification, a very pure protein with the correct folding was obtained. Subsequently, the Trx Tag was removed from CXCL12 (S4V and S2G4V) by means of enterokinase digestion. Cleaved Trx Tag were finally separated by means of cation exchange chromatography using the Mono S. The isoelectric point of the CXCL12 (S4V and S2G4V) differs from the Trx Tag and the undigested chemokine. Because of an increase of the isoelectric point from 7.68 to 9.90 of the CXCL12 (S4V and S2G4V) after digestion, the assumption was that the desired CXCL12 (S4V and S2G4V) chemokines are located under peak 2 (Figure 18). The mass and identity of CXCL12 (S4V and S2G4V) was confirmed by means of mass spectrometry and western blotting the (Figure 19, Figure 20).

6.2. Intramyocardial release of engineered chemokines using biodegradable hydrogels prevents injury extension after MI

In this study, a novel strategy of combining the Met-CCL5 and protease-resistant CXCL12 treatment was proposed, for the simultaneous activation of two important mechanisms for preservation of heart function: inhibition of neutrophil infiltration and enhanced neovascularization by increasing recruitment of HCs. Met-CCL5 antagonizes CCR1 and CCR5 activation and function in response to its natural ligand CCL5, and is able to reduce inflammation in models of induced inflammatory and autoimmune diseases, but also after MI[71]. Recombinant Met-CCL5 chemokine was formulated in a synthetic, biodegradable hydrogel for a fast release and was shown to reduce inflammation and the migration of neutrophils during the first hours after MI. On the other hand, it is well known that CXCL12 plays a very important role in driving chemotaxis of SC and progenitor cells to the infarcted myocardium and promoting neovascularization and tissue regeneration[53]. Due to the fast degradation, CXCL12 quickly disappears after very short action. Therefore in this study, the mutant CXCL12 was used, which is resistant to MMP-2 and DPPIV/CD26 cleavage formulated in a synthetic, biodegradable hydrogel for a controlled long term release. Combined treatment with CXCL12 (S4V) in a slowly degrading gel improved the heart function, decreased infarction area and increased capillary density 4 weeks after MI compared with control group (Figure 36).

Currently, the majority of small and large molecular drugs are delivered into patients systemically (e.g. oral or intravenous release) without the use of a scaffold. Consequently, large doses are usually required for a desired local effect because of non-specific uptake by other tissue, which can lead to serious side effects. Thus, biodegradable hydrogels are utilized here to stabilize and deliver bioactive molecules in the desired tissue for a better dose monitoring and an exact release[122] allowing a local and specific release of Met-CCL5 and protease-resistant CXCL12 into the heart tissue over 24 h or 4 weeks, respectively. Natural CXCL12 was broadly used in models of MI. However, the injection of CXCL12 after MI has shown limited results[40]. One reason for the inefficiency of natural CXCL12 might be the rapid cleavage by MMP-2[53]. Until now, the physiological role of this cleavage is unknown, yet CXCL12 inactivation by MMPs stops mobilization of HCs from the BM[53]. Up-regulation of MMP-2 after MI is well known and plays an important role in the extracellular matrix turnover and remodeling. Therefore, to sustain the CXCL12 function *in vivo* it is essential to block its degradation. The protease-resistant CXCL12 chemokine is resistant to MMP-2 and DPPIV cleavage[53], with preserved ability to recruit SC *in vitro* and *in vivo*, confirmed on migration of angiogenic EOC, on cell adhesion of CXCL12 (S4V)-stimulated Jurkat cells on HUVEC under flow conditions and in experimental model of MI. For the herein described mouse *in vivo* study, the protease-resistant CXCL12 variant was implemented to investigate the

improvement of cardiac function after MI. When incorporated into a slowly degradable hydrogel, CXCL12 is released gradually over weeks, assuring a local high amount of chemokine and a continuous stimulation of SC recruitment. Accordingly, neo-angiogenesis after MI was increased after treatment with CXCL12 (S4V)-containing hydrogels, demonstrating the efficiency of the treatment (Figure 36).
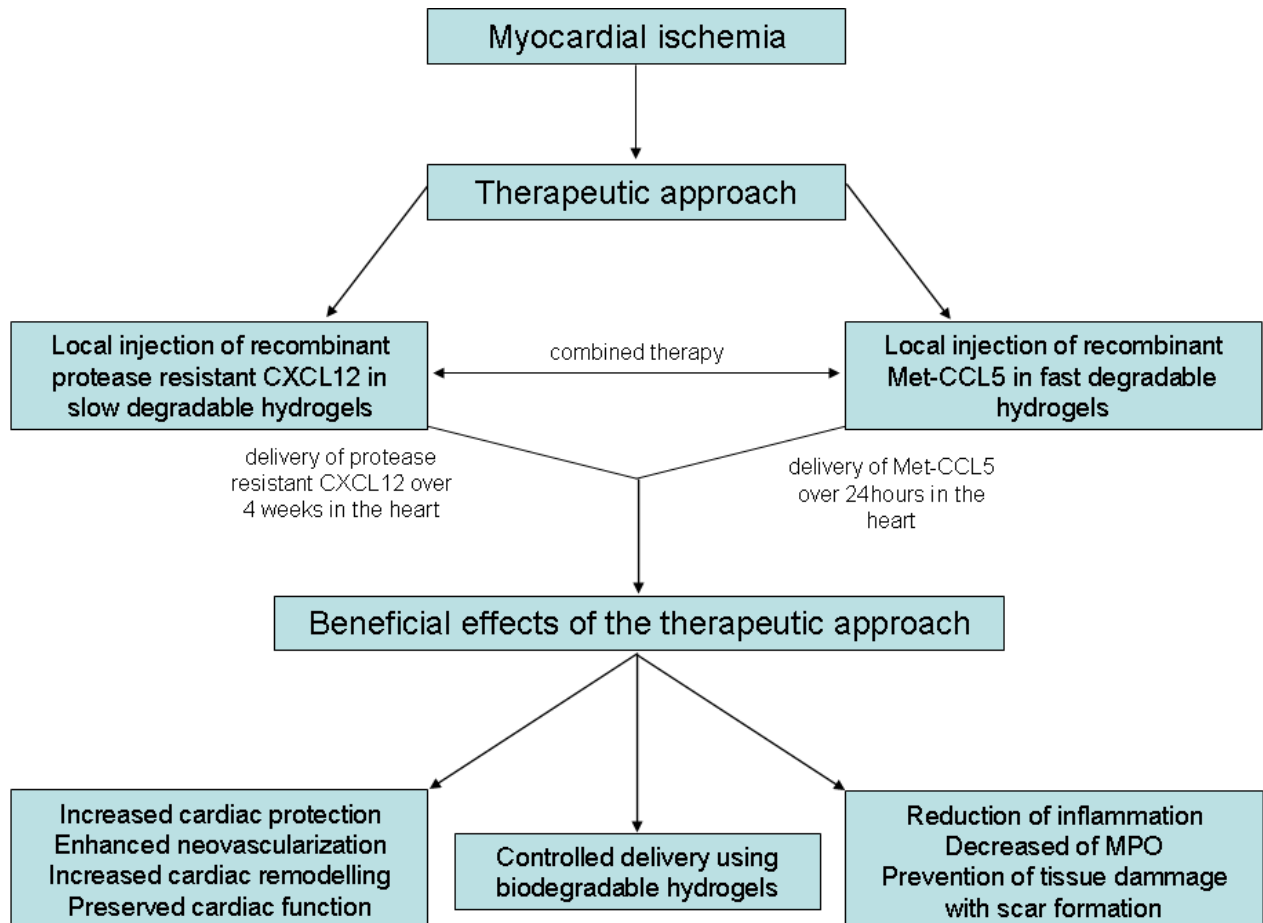
Figure 36: Schematic representation of the therapeutic approach using protease-resistant CXCL12 in SDHs and Met-CCL5 in FDHs in experimental models of MI. Modified from Ghadge et. al.[21].

On the other hand, to reduce inflammation induced by MI, recombinant Met-CCL5 was used to inhibit neutrophil infiltration. It is well established that CXCL8 and CCL5 are strong agonists for neutrophil recruitment. Met-CCL5 is able to antagonize the actions of CCL5 not only *in vitro*, but also *in vivo*[71]. Since the infiltration of neutrophils occurs only for a short time period[190], the Met-CCL5 was combined with a very quickly biodegradable hydrogel, which assures the release of this antagonist only for several hours. This is essential to avoid the blocking of later functions of CCL5, e.g. over CCR5, such as recruitment of reparatory monocytes or T regulatory cells[196], which is necessary for a proper healing and scar formation (Figure 36).

The combined treatment with both recombinant chemokines formulated in a time-dependent degradable hydrogel, show significantly preserved heart function and improved remodeling of the ventricle. The cardioprotective effects of the Met-CCL5 and protease-resistant CXCL12 are mediated through reduced infiltration of neutrophils in the infarcted myocardium and increased recruitment of HCs, respectively. Indeed, it was found a decreased neutrophil infiltration after treatment with Met-CCL5-FDH, and after combined treatment with Met-CCL5-FDH and protease-resistant CXCL12 (S4V)-SDH. These results are comparable with those found in CCR1-deficient mice, or after anti-CCL5 mAb treatment, which showed that the initial inhibition of CCL5 exerts cardioprotective effects during early MI through its anti-inflammatory properties[71], reducing both infarct size and post-infarction heart failure in mouse model of chronic cardiac ischemia[67] (Figure 36).

Moreover, increased angiogenesis was noticed after CXCL12 (S4V)-SDH alone and combined CXCL12 (S4V)-SDH and Met-CCL5-FDH treatment, suggesting that the preserved ability of protease-resistant CXCL12 mediated HC recruitment through its CXCR4 receptor. As expected, Met-CCL5 alone was not able to promote angiogenesis. However, although a decrease in infarction size was observed in all treated groups, it appears that only combined treatment with CXCL12 (S4V) and Met-CCL5 is able to additionally improve the heart function and to assure the optimal healing and remodeling of the ventricle after MI.

In summary, my thesis provides evidence that the combined therapy of the protease-resistant CXCL12-SDH and Met-CCL5-FDH preserves cardiac function, promotes angiogenesis and facilitates wound healing by recruitment of hematopoietic stem cells from the circulating blood and attenuating neutrophil-induced myocardial inflammation. This novel strategy might constitute an additional option to optimize cardiac repair and remodeling after myocardial injury and might complement cell-based therapies.

6.3.   Role of platelet F1-CX$_3$CL1 antagonist to PMC formation

In the present part of this study, the contribution of platelet-derived F1-CX$_3$CR1 on monocyte recruitment to endothelium was investigated. The presence of functional platelet-derived CX$_3$CR1 was demonstrated before, but only in the context of adhesion to ECs[197-199]. As it is known from literature, CX$_3$CL1 is able to induce chemotaxis, adhesion and cell signaling through CX$_3$CR1[200]. It is well-established that platelets do not act as single players in the inflammatory process. For example, interaction of monocytes with platelets increases the adhesive properties of monocytes towards inflamed or atherosclerotic endothelium[200, 201] and platelets interact with adherent leukocytes *via* the adhesion receptor GP1B and the leukocyte integrin $\alpha_M\beta_2$ (CD11b/CD18)[202]. An important finding in this study is that activated but not resting human platelets led to a significant platelet-THP-1 complex formation as measured by increased staining of the platelet marker CD61 in the monocyte-gated population. Platelet-CX$_3$CR1 thus appears to play a notable role in PMC assembly, as pre-incubation of platelets with the CX$_3$CR1-antagonist F1-CX$_3$CL1 significantly decreased PMC formation (Figure 34).

In *in vitro* static adhesion assay, a pronounced role of platelet-derived CX$_3$CR1 in the adhesion to immobilized CX$_3$CL1 was observed, which is consistent with a recent study showing CX$_3$CR1-dependent binding of platelets to CX$_3$CL1-coated microbeads[199]. Furthermore, under shear flow in whole blood, a robust adhesion of leukocytes on activated SMC, which express CX$_3$CL1 after stimulation[178, 203], was recorded only after activation of the blood platelets with TRAP-6, hinting towards an involvement of platelet-leukocyte interactions in this process. By blocking CX$_3$CL1 or CX$_3$CR1 it was shown that the leukocyte adhesion strongly depended on the CX3CL1–CX3CR1 axis.

In conclusion, this part of the study clearly shows that human platelets carry the functional chemokine receptor CX$_3$CR1 which can be enhanced on the surface upon activation by inflammatory stimuli, similarly as seen for platelet activation by classical agonists.

7.   Summary

Chemotactic cytokines and their receptors play an important role in CVDs. The progress of atherosclerosis may cause MI. MI induces an inflammatory immune response, which causes a progressive expansion of the infarcted area and dilation of the ventricles with replacement of the adjacent myocardium by connective tissue, the so-called "remodeling" of the heart muscle. The regeneration of the blood vessel network system by recruitment of HCs for recovering the supply of the infarcted area with oxygen, nutrients, and the prevention of apoptosis of myocytes can be beneficial for heart function. In order to gain further knowledge in the development of atherosclerosis the role of platelet-CX_3CR1 receptor and his CX_3CL1 ligand was studied during the formation of PMC.

The first part of this study includes the recombinant expression of the Met-CCL5, protease-resistant CXCL12 (S4V) and F1-CX_3CL1 in *E. coli*. The chemokines were expressed with different techniques as inclusion bodies in the cytoplasm and were purified by sequential steps with chromatographic methods using FPLC. The second part of this study includes the design of a novel therapeutic strategy with Met-CCL5, a chemokine receptor antagonist to suppress initial neutrophil infiltration, and a protease-resistant CXCL12 (S4V) variant, which is inert to MMP-2 and exopeptidase cleavage, but retains its chemotactic bioactivity for recruitment of circulating HCs, promoting neovascularization after MI. To control the proper timing and local release of Met-CCL5 and CXCL12 (S4V), two different biodegradable hydrogels were implemented, a FDH for delivering Met-CCL5 over 24 h and a SDH for a gradual release of CXCL12 (S4V) over 4 weeks. In a mouse model, intramyocardial injection of these agents reduced infarct size, blocked neutrophil recruitment into the affected tissue, stimulated capillary formation, and improved cardiac function after MI. Last part of this study showed whether platelet-CX_3CR1 plays a role in PMC formation. The platelets were preincubated with the CX_3CR1-antagonist F1-CX_3CL1 and the PMC formation was evaluated.

This study describes the expression of different chemokines which play an important role in CVDs. Furthermore, time-controlled release of Met-CCL5-FDH and CXCL12 (S4V)-SDH could demonstrate blocking of neutrophil recruitment to the inflamed myocardium and recruiting HC from circulating blood, thereby improving cardiac function after MI. As result, this study describes a novel and a promising therapeutic strategy to sustain the endogenous reparatory mechanisms, and may represent a potentially clinical relevant alternative to cell-based therapies. Additionally, the formation of PMC and the detection of platelet-bound CX_3CL1 on SMCs suggest a significant involvement of the CX_3CR1–CX_3CL1 axis in platelet accumulation and monocyte recruitment at sites of arterial injury in atherosclerosis. The F1-

CX_3CL1 antagonist inhibits the formation of the interaction of the CX_3CR1–CX_3CL1 axis and the formation of PMC is reduced.

8. Zusammenfassung

Chemotaktische Cytokine und ihre Rezeptoren spielen eine wichtige Rolle bei der Entwicklung von kardiovaskulären Erkrankungen und ihren Folgen. Das Fortschreiten von Atherosklerose kann zum Herzinfarkt führen. Der Myokardinfarkt induziert eine entzündliche Immunantwort, die zu einer progressiven Expansion des Infarktbereichs und Dilatation der Herzkammern mit Erneuerung des benachbarten Myokardbindegewebes führt, welche das sogenannte "Remodelling" des Herzmuskels verursacht. Für die Verbesserung der Herzfunktion, ist die Regeneration des Blutgefäß-Netzwerk-Systems durch Rekrutierung von hämatopoetischen Stammzellen notwendig, welche die Versorgung des infarktierten Bereiches mit Sauerstoff und Nährstoffen begünstigt, und die Apoptose von Myozyten verhindert. Um neue Erkenntnisse auf dem Gebiet der Atheroskleroseentwicklung zu gewinnen wurde die Rolle von Blutplättchen-CX_3CR1 Rezeptor und dessen CX_3CL1 Liganden untersucht. Dabei wurde die Rolle der CX_3CR1- CX_3CL1 Achse bei der Bildung von Blutplättchen-Monozyten-Komplexen (PMC) mit Hilfe des F1-CX_3CL1 Antagonisten überprüft.

Der erste Teil dieser Arbeit umfasst die rekombinante Expression von Met-CCL5, protease-resistentem CXCL12 (S4V) und F1-CX_3CL1 in *E. coli*. Die Chemokine wurden mit unterschiedlichen Methoden als Einschlusskörper im Zytoplasma exprimiert und durch sequentielle Schritte mit chromatographischen Methoden unter Verwendung von FPLC aufgereinigt. Der darauffolgende Teil dieser Arbeit umfasst die Entwicklung einer neuartigen therapeutischen Strategie mit Met-CCL5, einem Chemokin-Rezeptor-Antagonist zur Unterdrückung der ersten Neutrophilinfiltration, und einer proteaseresistenten CXCL12 (S4V) Variante, die von Matrixmetalloproteinase-2 und Exopeptidase nicht gespalten werden kann, aber seine chemotaktische Bioaktivität für die Rekrutierung von zirkulierenden hämatopoetischen Stammzellen behält, welche die Neovaskularisierung nach Myokardinfarkt fördert. Um die genaue lokale Freisetzung von Met-CCL5 und CXCL12 (S4V) zu gewährleisten, wurden zwei verschiedene biologisch abbaubare Hydrogele implementiert, ein schnell abbaubares Hydrogel (FDH) zur Abgabe von Met-CCL5 über 24 h und ein langsam abbaubares Hydrogel (SDH) für eine langsame Freisetzung von CXCL12 (S4V) über 4 Wochen. Im Mausmodell konnte gezeigt werden, dass die intramyokardiale Injektion dieser Komponenten zu einer Verringerung der Infarktgröße, zu einer Blockierung der Neutrophil-Rekrutierung in das betroffene Gewebe, zu einer Stimulation von Kapillargefäßbildung und zu einer insgesamt verbesserten Herzfunktion nach Myokardinfarkt geführt haben. Der letzte Teil dieser Arbeit beinhaltet die Untersuchung des thrombozytären-CX_3CR1 Rezeptors und CX_3CL1 Liganden bei der Bildung von PMC. Dabei wurden Plättchen mit dem F1-CX_3CR1-Antagonisten vorinkubiert und die PMC-Bildung bewertet.

Diese Arbeit beschreibt die Expression verschiedener Chemokine die eine wichtige Rolle bei der Entwicklung von kardiovaskulären Erkrankungen und ihren Folgen darstellen. Des Weiteren konnte gezeigt werden, dass eine zeitlich kontrollierte Freisetzung von Met-CCL5-FDH und CXCL12 (S4V)-SDH, die Rekrutierung von Neutrophilen im entzündeten Myokardium hemmt, als auch die Rekrutierung von hämatopoetischen Stammzellen aus dem zirkulierenden Blut fördert, welche die Herzfunktion nach Myokardinfarkt verbessern. Als ein Ergebnis dieser Arbeit konnte eine neue und vielversprechende therapeutische Strategie zur Aufrechterhaltung des endogenen reparatorischen Mechanismus aufgezeigt werden, welche eine potentiell klinisch relevante Alternative zur Zelltherapie darstellen kann.

Weiterhin wurde die Rolle von thrombozytär-gebundenem CX_3CL1 auf glatte Muskelzellen (SMC) bei der Bildung von PMC untersucht. Hierbei konnte gezeigt werden, dass die CX_3CR1-CX_3CL1 Achse bei der Akkumulation von Blutplättchen und der Rekrutierung von Monozyten während der Gefäßverletzung und bei der Bildung von Atherosklerose eine wichtige Rolle spielt, indem der F1-CX_3CL1 Antagonist die Wechselwirkung der CX_3CR1-CX_3CL1 Achse hemmt und die Bildung von PMC reduziert.

9.   Literature

1.   Weber C. Frontiers of vascular biology: Mechanisms of inflammation and immunoregulation during arterial remodelling. *Thrombosis and haemostasis*. 2009;102:188-190

2.   http://www.who.int/mediacentre/factsheets/fs317/en/index.html WCDC*WHO*Aa.

3.   Weber C, Noels H. Atherosclerosis: Current pathogenesis and therapeutic options. *Nature medicine*. 2011;17:1410-1422

4.   Lobstein J. Traité d'anatomie pathologique. *Levrault, Paris*. 1833;2

5.   Mayerl C, Lukasser M, Sedivy R, Niederegger H, Seiler R, Wick G. Atherosclerosis research from past to present--on the track of two pathologists with opposing views, carl von rokitansky and rudolf virchow. *Virchows Archiv : an international journal of pathology*. 2006;449:96-103

6.   Weber C, Zernecke A, Libby P. The multifaceted contributions of leukocyte subsets to atherosclerosis: Lessons from mouse models. *Nature reviews. Immunology*. 2008;8:802-815

7.   Virchow R. Phlogose and thrombose im gefasssystem. *Abhandlungen zur Wissenschaftlichen Medizin. Frankfurt, Meininger Sohn nad Co.* 1856:458

8.   Duguid JB. Pathogenesis of atherosclerosis. *Lancet*. 1949;2:925-927

9.   French JE. Atherosclerosis in relation to the structure and function of the arterial intima, with special reference to th endothelium. *International review of experimental pathology*. 1966;5:253-353

10.   Mustard JF, Packham MA. The role of blood and platelets in atherosclerosis and the complications of atherosclerosis. *Thrombosis et diathesis haemorrhagica*. 1975;33:444-456

11.   Wissler RW. Development of the atherosclerotic plaque. *Braunwald E editors. The Myocardium: Failure and Infarction, New York: HP Publishing Co*. 1974:155-166

12.   Thomas WA, Jones R, Scott RF, Morrison E, Goodale MF, Imai H. Production of early atherosclerotic lesions in rats characterized by proliferation of "modified smooth muscle cells". *Experimental and molecular pathology*. 1963;52:SUPPL1:40-61

13.   Ross R, Glomset J, Harker L. Response to injury and atherogenesis. *The American journal of pathology*. 1977;86:675-684

14.   Steinberg D. Arterial metabolism of lipoproteins in relation to atherogenesis. *Annals of the New York Academy of Sciences*. 1990;598:125-135

15.   Ross R. The pathogenesis of atherosclerosis: A perspective for the 1990s. *Nature*. 1993;362:801-809

16.   Skalen K, Gustafsson M, Rydberg EK, Hulten LM, Wiklund O, Innerarity TL, Boren J. Subendothelial retention of atherogenic lipoproteins in early atherosclerosis. *Nature*. 2002;417:750-754

17.   Hansson GK. Inflammation, atherosclerosis, and coronary artery disease. *The New England journal of medicine*. 2005;352:1685-1695

18.   Massberg S, Brand K, Gruner S, Page S, Muller E, Muller I, Bergmeier W, Richter T, Lorenz M, Konrad I, Nieswandt B, Gawaz M. A critical role of platelet adhesion in the initiation of atherosclerotic lesion formation. *The Journal of experimental medicine*. 2002;196:887-896

19.   Ross R. Atherosclerosis is an inflammatory disease. *American heart journal*. 1999;138:S419-420

20.   Liehn EA, Postea O, Curaj A, Marx N. Repair after myocardial infarction, between fantasy and reality: The role of chemokines. *J Am Coll Cardiol*. 2011;58:2357-2362

21.   Ghadge SK, Muhlstedt S, Ozcelik C, Bader M. Sdf-1alpha as a therapeutic stem cell homing factor in myocardial infarction. *Pharmacology & therapeutics*. 2011;129:97-108

22.   Fox KF, Cowie MR, Wood DA, Coats AJ, Gibbs JS, Underwood SR, Turner RM, Poole-Wilson PA, Davies SW, Sutton GC. Coronary artery disease as the cause of incident heart failure in the population. *European heart journal*. 2001;22:228-236

23. Steffens S, Montecucco F, Mach F. The inflammatory response as a target to reduce myocardial ischaemia and reperfusion injury. *Thrombosis and haemostasis*. 2009;102:240-247

24. Delgado RM, 3rd, Willerson JT. Pathophysiology of heart failure: A look at the future. *Texas Heart Institute journal / from the Texas Heart Institute of St. Luke's Episcopal Hospital, Texas Children's Hospital*. 1999;26:28-33

25. Keeley EC, Boura JA, Grines CL. Primary angioplasty versus intravenous thrombolytic therapy for acute myocardial infarction: A quantitative review of 23 randomised trials. *Lancet*. 2003;361:13-20

26. Kanki S, Segers VF, Wu W, Kakkar R, Gannon J, Sys SU, Sandrasagra A, Lee RT. Stromal cell-derived factor-1 retention and cardioprotection for ischemic myocardium. *Circulation. Heart failure*. 2011;4:509-518

27. Dorgham K, Ghadiri A, Hermand P, Rodero M, Poupel L, Iga M, Hartley O, Gorochov G, Combadiere C, Deterre P. An engineered cx3cr1 antagonist endowed with anti-inflammatory activity. *Journal of leukocyte biology*. 2009;86:903-911

28. Yellon DM, Hausenloy DJ. Myocardial reperfusion injury. *The New England journal of medicine*. 2007;357:1121-1135

29. Frangogiannis NG, Smith CW, Entman ML. The inflammatory response in myocardial infarction. *Cardiovasc Res*. 2002;53:31-47

30. Liehn EA, Merx MW, Postea O, Becher S, Djalali-Talab Y, Shagdarsuren E, Kelm M, Zernecke A, Weber C. Ccr1 deficiency reduces inflammatory remodelling and preserves left ventricular function after myocardial infarction. *Journal of cellular and molecular medicine*. 2008;12:496-506

31. Griselli M, Herbert J, Hutchinson WL, Taylor KM, Sohail M, Krausz T, Pepys MB. C-reactive protein and complement are important mediators of tissue damage in acute myocardial infarction. *The Journal of experimental medicine*. 1999;190:1733-1740

32. Frangogiannis NG. Chemokines in ischemia and reperfusion. *Thrombosis and haemostasis*. 2007;97:738-747

33. Soehnlein O, Zernecke A, Eriksson EE, Rothfuchs AG, Pham CT, Herwald H, Bidzhekov K, Rottenberg ME, Weber C, Lindbom L. Neutrophil secretion products pave the way for inflammatory monocytes. *Blood*. 2008;112:1461-1471

34. Tekin D, Dursun AD, Xi L. Hypoxia inducible factor 1 (hif-1) and cardioprotection. *Acta pharmacologica Sinica*. 2010;31:1085-1094

35. Ceradini DJ, Kulkarni AR, Callaghan MJ, Tepper OM, Bastidas N, Kleinman ME, Capla JM, Galiano RD, Levine JP, Gurtner GC. Progenitor cell trafficking is regulated by hypoxic gradients through hif-1 induction of sdf-1. *Nature medicine*. 2004;10:858-864

36. Auffray C, Fogg D, Garfa M, Elain G, Join-Lambert O, Kayal S, Sarnacki S, Cumano A, Lauvau G, Geissmann F. Monitoring of blood vessels and tissues by a population of monocytes with patrolling behavior. *Science*. 2007;317:666-670

37. Tacke F, Alvarez D, Kaplan TJ, Jakubzick C, Spanbroek R, Llodra J, Garin A, Liu J, Mack M, van Rooijen N, Lira SA, Habenicht AJ, Randolph GJ. Monocyte subsets differentially employ ccr2, ccr5, and cx3cr1 to accumulate within atherosclerotic plaques. *The Journal of clinical investigation*. 2007;117:185-194

38. Abbott JD, Huang Y, Liu D, Hickey R, Krause DS, Giordano FJ. Stromal cell-derived factor-1alpha plays a critical role in stem cell recruitment to the heart after myocardial infarction but is not sufficient to induce homing in the absence of injury. *Circulation*. 2004;110:3300-3305

39. Dobaczewski M, Gonzalez-Quesada C, Frangogiannis NG. The extracellular matrix as a modulator of the inflammatory and reparative response following myocardial infarction. *Journal of molecular and cellular cardiology*. 2010;48:504-511

40. Schuh A, Liehn EA, Sasse A, Hristov M, Sobota R, Kelm M, Merx MW, Weber C. Transplantation of endothelial progenitor cells improves neovascularization and left ventricular function after myocardial infarction in a rat model. *Basic research in cardiology*. 2008;103:69-77

41.   Rot A, von Andrian UH. Chemokines in innate and adaptive host defense: Basic chemokinese grammar for immune cells. *Annual review of immunology*. 2004;22:891-928

42.   Graves DT, Jiang Y. Chemokines, a family of chemotactic cytokines. *Critical reviews in oral biology and medicine : an official publication of the American Association of Oral Biologists*. 1995;6:109-118

43.   D'Amico G, Frascaroli G, Bianchi G, Transidico P, Doni A, Vecchi A, Sozzani S, Allavena P, Mantovani A. Uncoupling of inflammatory chemokine receptors by il-10: Generation of functional decoys. *Nature immunology*. 2000;1:387-391

44.   Xanthou G, Duchesnes CE, Williams TJ, Pease JE. Ccr3 functional responses are regulated by both cxcr3 and its ligands cxcl9, cxcl10 and cxcl11. *European journal of immunology*. 2003;33:2241-2250

45.   Kenakin T, Onaran O. The ligand paradox between affinity and efficacy: Can you be there and not make a difference? *Trends in pharmacological sciences*. 2002;23:275-280

46.   Kenakin T. Ligand-selective receptor conformations revisited: The promise and the problem. *Trends in pharmacological sciences*. 2003;24:346-354

47.   Charo IF, Ransohoff RM. The many roles of chemokines and chemokine receptors in inflammation. *The New England journal of medicine*. 2006;354:610-621

48.   Rostene W, Kitabgi P, Parsadaniantz SM. Chemokines: A new class of neuromodulator? *Nature reviews. Neuroscience*. 2007;8:895-903

49.   Ganju RK, Brubaker SA, Meyer J, Dutt P, Yang Y, Qin S, Newman W, Groopman JE. The alpha-chemokine, stromal cell-derived factor-1alpha, binds to the transmembrane g-protein-coupled cxcr-4 receptor and activates multiple signal transduction pathways. *The Journal of biological chemistry*. 1998;273:23169-23175

50.   Luster AD. Chemokines--chemotactic cytokines that mediate inflammation. *The New England journal of medicine*. 1998;338:436-445

51.   Rollins BJ. Chemokines. *Blood*. 1997;90:909-928

52.   Gevrey JC, Isaac BM, Cox D. Syk is required for monocyte/macrophage chemotaxis to cx3cl1 (fractalkine). *J Immunol*. 2005;175:3737-3745

53.   Segers VF, Tokunou T, Higgins LJ, MacGillivray C, Gannon J, Lee RT. Local delivery of protease-resistant stromal cell derived factor-1 for stem cell recruitment after myocardial infarction. *Circulation*. 2007;116:1683-1692

54.   Sanchez-Martin L, Sanchez-Mateos P, Cabanas C. Cxcr7 impact on cxcl12 biology and disease. *Trends in molecular medicine*. 2013;19:12-22

55.   Rankin SM. Chemokines and adult bone marrow stem cells. *Immunology letters*. 2012;145:47-54

56.   Laguri C, Arenzana-Seisdedos F, Lortat-Jacob H. Relationships between glycosaminoglycan and receptor binding sites in chemokines-the cxcl12 example. *Carbohydrate research*. 2008;343:2018-2023

57.   Mantovani A, Bonecchi R, Locati M. Tuning inflammation and immunity by chemokine sequestration: Decoys and more. *Nature reviews. Immunology*. 2006;6:907-918

58.   Laguri C, Sadir R, Rueda P, Baleux F, Gans P, Arenzana-Seisdedos F, Lortat-Jacob H. The novel cxcl12gamma isoform encodes an unstructured cationic domain which regulates bioactivity and interaction with both glycosaminoglycans and cxcr4. *PloS one*. 2007;2:e1110

59.   Bernfield M, Gotte M, Park PW, Reizes O, Fitzgerald ML, Lincecum J, Zako M. Functions of cell surface heparan sulfate proteoglycans. *Annual review of biochemistry*. 1999;68:729-777

60.   Johnson Z, Proudfoot AE, Handel TM. Interaction of chemokines and glycosaminoglycans: A new twist in the regulation of chemokine function with opportunities for therapeutic intervention. *Cytokine & growth factor reviews*. 2005;16:625-636

61.   Lortat-Jacob H, Grosdidier A, Imberty A. Structural diversity of heparan sulfate binding domains in chemokines. *Proceedings of the National Academy of Sciences of the United States of America*. 2002;99:1229-1234

62. Proudfoot AE, Handel TM, Johnson Z, Lau EK, LiWang P, Clark-Lewis I, Borlat F, Wells TN, Kosco-Vilbois MH. Glycosaminoglycan binding and oligomerization are essential for the in vivo activity of certain chemokines. *Proceedings of the National Academy of Sciences of the United States of America*. 2003;100:1885-1890

63. Kunkel SL, Strieter RM, Lindley IJ, Westwick J. Chemokines: New ligands, receptors and activities. *Immunology today*. 1995;16:559-561

64. Baltus T, von Hundelshausen P, Mause SF, Buhre W, Rossaint R, Weber C. Differential and additive effects of platelet-derived chemokines on monocyte arrest on inflamed endothelium under flow conditions. *Journal of leukocyte biology*. 2005;78:435-441

65. Suffee N, Richard B, Hlawaty H, Oudar O, Charnaux N, Sutton A. Angiogenic properties of the chemokine rantes/ccl5. *Biochemical Society transactions*. 2011;39:1649-1653

66. Baltus T, Weber KS, Johnson Z, Proudfoot AE, Weber C. Oligomerization of rantes is required for ccr1-mediated arrest but not ccr5-mediated transmigration of leukocytes on inflamed endothelium. *Blood*. 2003;102:1985-1988

67. Montecucco F, Braunersreuther V, Lenglet S, Delattre BM, Pelli G, Buatois V, Guilhot F, Galan K, Vuilleumier N, Ferlin W, Fischer N, Vallee JP, Kosco-Vilbois M, Mach F. Cc chemokine ccl5 plays a central role impacting infarct size and post-infarction heart failure in mice. *European heart journal*. 2012;33:1964-1974

68. Krensky AM, Ahn YT. Mechanisms of disease: Regulation of rantes (ccl5) in renal disease. *Nature clinical practice. Nephrology*. 2007;3:164-170

69. Barcelos LS, Coelho AM, Russo RC, Guabiraba R, Souza AL, Bruno-Lima G, Jr., Proudfoot AE, Andrade SP, Teixeira MM. Role of the chemokines ccl3/mip-1 alpha and ccl5/rantes in sponge-induced inflammatory angiogenesis in mice. *Microvascular research*. 2009;78:148-154

70. Ambati BK, Anand A, Joussen AM, Kuziel WA, Adamis AP, Ambati J. Sustained inhibition of corneal neovascularization by genetic ablation of ccr5. *Investigative ophthalmology & visual science*. 2003;44:590-593

71. Braunersreuther V, Pellieux C, Pelli G, Burger F, Steffens S, Montessuit C, Weber C, Proudfoot A, Mach F, Arnaud C. Chemokine ccl5/rantes inhibition reduces myocardial reperfusion injury in atherosclerotic mice. *Journal of molecular and cellular cardiology*. 2010;48:789-798

72. Rookmaaker MB, Verhaar MC, de Boer HC, Goldschmeding R, Joles JA, Koomans HA, Grone HJ, Rabelink TJ. Met-rantes reduces endothelial progenitor cell homing to activated (glomerular) endothelium in vitro and in vivo. *American journal of physiology. Renal physiology*. 2007;293:F624-630

73. Koenen RR, von Hundelshausen P, Nesmelova IV, Zernecke A, Liehn EA, Sarabi A, Kramp BK, Piccinini AM, Paludan SR, Kowalska MA, Kungl AJ, Hackeng TM, Mayo KH, Weber C. Disrupting functional interactions between platelet chemokines inhibits atherosclerosis in hyperlipidemic mice. *Nature medicine*. 2009;15:97-103

74. Kiss DL, Longden J, Fechner GA, Avery VM. The functional antagonist met-rantes: A modified agonist that induces differential ccr5 trafficking. *Cell Mol Biol Lett*. 2009;14:537-547

75. Nagasawa T, Hirota S, Tachibana K, Takakura N, Nishikawa S, Kitamura Y, Yoshida N, Kikutani H, Kishimoto T. Defects of b-cell lymphopoiesis and bone-marrow myelopoiesis in mice lacking the cxc chemokine pbsf/sdf-1. *Nature*. 1996;382:635-638

76. Nagasawa T, Nakajima T, Tachibana K, Iizasa H, Bleul CC, Yoshie O, Matsushima K, Yoshida N, Springer TA, Kishimoto T. Molecular cloning and characterization of a murine pre-b-cell growth-stimulating factor/stromal cell-derived factor 1 receptor, a murine homolog of the human immunodeficiency virus 1 entry coreceptor fusin. *Proceedings of the National Academy of Sciences of the United States of America*. 1996;93:14726-14729

77. Ratajczak MZ, Zuba-Surma E, Kucia M, Reca R, Wojakowski W, Ratajczak J. The pleiotropic effects of the sdf-1-cxcr4 axis in organogenesis, regeneration and

tumorigenesis. *Leukemia : official journal of the Leukemia Society of America, Leukemia Research Fund, U.K.* 2006;20:1915-1924

78.   Schober A, Karshovska E, Zernecke A, Weber C. Sdf-1alpha-mediated tissue repair by stem cells: A promising tool in cardiovascular medicine? *Trends in cardiovascular medicine*. 2006;16:103-108

79.   Zou YR, Kottmann AH, Kuroda M, Taniuchi I, Littman DR. Function of the chemokine receptor cxcr4 in haematopoiesis and in cerebellar development. *Nature*. 1998;393:595-599

80.   Ara T, Tokoyoda K, Okamoto R, Koni PA, Nagasawa T. The role of cxcl12 in the organ-specific process of artery formation. *Blood*. 2005;105:3155-3161

81.   Bleul CC, Farzan M, Choe H, Parolin C, Clark-Lewis I, Sodroski J, Springer TA. The lymphocyte chemoattractant sdf-1 is a ligand for lestr/fusin and blocks hiv-1 entry. *Nature*. 1996;382:829-833

82.   Oberlin E, Amara A, Bachelerie F, Bessia C, Virelizier JL, Arenzana-Seisdedos F, Schwartz O, Heard JM, Clark-Lewis I, Legler DF, Loetscher M, Baggiolini M, Moser B. The cxc chemokine sdf-1 is the ligand for lestr/fusin and prevents infection by t-cell-line-adapted hiv-1. *Nature*. 1996;382:833-835

83.   Orsini MJ, Parent JL, Mundell SJ, Marchese A, Benovic JL. Trafficking of the hiv coreceptor cxcr4. Role of arrestins and identification of residues in the c-terminal tail that mediate receptor internalization. *The Journal of biological chemistry*. 1999;274:31076-31086

84.   Heesen M, Berman MA, Charest A, Housman D, Gerard C, Dorf ME. Cloning and chromosomal mapping of an orphan chemokine receptor: Mouse rdc1. *Immunogenetics*. 1998;47:364-370

85.   Balabanian K, Lagane B, Infantino S, Chow KY, Harriague J, Moepps B, Arenzana-Seisdedos F, Thelen M, Bachelerie F. The chemokine sdf-1/cxcl12 binds to and signals through the orphan receptor rdc1 in t lymphocytes. *The Journal of biological chemistry*. 2005;280:35760-35766

86.   Gao H, Priebe W, Glod J, Banerjee D. Activation of signal transducers and activators of transcription 3 and focal adhesion kinase by stromal cell-derived factor 1 is required for migration of human mesenchymal stem cells in response to tumor cell-conditioned medium. *Stem Cells*. 2009;27:857-865

87.   Gleichmann M, Gillen C, Czardybon M, Bosse F, Greiner-Petter R, Auer J, Muller HW. Cloning and characterization of sdf-1gamma, a novel sdf-1 chemokine transcript with developmentally regulated expression in the nervous system. *The European journal of neuroscience*. 2000;12:1857-1866

88.   Yu L, Cecil J, Peng SB, Schrementi J, Kovacevic S, Paul D, Su EW, Wang J. Identification and expression of novel isoforms of human stromal cell-derived factor 1. *Gene*. 2006;374:174-179

89.   Pillarisetti K, Gupta SK. Cloning and relative expression analysis of rat stromal cell derived factor-1 (sdf-1)1: Sdf-1 alpha mrna is selectively induced in rat model of myocardial infarction. *Inflammation*. 2001;25:293-300

90.   Schober A. Chemokines in vascular dysfunction and remodeling. *Arteriosclerosis, thrombosis, and vascular biology*. 2008;28:1950-1959

91.   Drury JL, Mooney DJ. Hydrogels for tissue engineering: Scaffold design variables and applications. *Biomaterials*. 2003;24:4337-4351

92.   Van Damme J, Struyf S, Opdenakker G. Chemokine-protease interactions in cancer. *Seminars in cancer biology*. 2004;14:201-208

93.   McQuibban GA, Butler GS, Gong JH, Bendall L, Power C, Clark-Lewis I, Overall CM. Matrix metalloproteinase activity inactivates the cxc chemokine stromal cell-derived factor-1. *The Journal of biological chemistry*. 2001;276:43503-43508

94.   Zhang K, McQuibban GA, Silva C, Butler GS, Johnston JB, Holden J, Clark-Lewis I, Overall CM, Power C. Hiv-induced metalloproteinase processing of the chemokine stromal cell derived factor-1 causes neurodegeneration. *Nature neuroscience*. 2003;6:1064-1071

95. De La Luz Sierra M, Yang F, Narazaki M, Salvucci O, Davis D, Yarchoan R, Zhang HH, Fales H, Tosato G. Differential processing of stromal-derived factor-1alpha and stromal-derived factor-1beta explains functional diversity. *Blood*. 2004;103:2452-2459

96. Mentlein R. Dipeptidyl-peptidase iv (cd26)--role in the inactivation of regulatory peptides. *Regulatory peptides*. 1999;85:9-24

97. Umehara H, Bloom ET, Okazaki T, Nagano Y, Yoshie O, Imai T. Fractalkine in vascular biology: From basic research to clinical disease. *Arteriosclerosis, thrombosis, and vascular biology*. 2004;24:34-40

98. Bazan JF, Bacon KB, Hardiman G, Wang W, Soo K, Rossi D, Greaves DR, Zlotnik A, Schall TJ. A new class of membrane-bound chemokine with a cx3c motif. *Nature*. 1997;385:640-644

99. Garton KJ, Gough PJ, Blobel CP, Murphy G, Greaves DR, Dempsey PJ, Raines EW. Tumor necrosis factor-alpha-converting enzyme (adam17) mediates the cleavage and shedding of fractalkine (cx3cl1). *The Journal of biological chemistry*. 2001;276:37993-38001

100. Tsou CL, Haskell CA, Charo IF. Tumor necrosis factor-alpha-converting enzyme mediates the inducible cleavage of fractalkine. *The Journal of biological chemistry*. 2001;276:44622-44626

101. Pan Y, Lloyd C, Zhou H, Dolich S, Deeds J, Gonzalo JA, Vath J, Gosselin M, Ma J, Dussault B, Woolf E, Alperin G, Culpepper J, Gutierrez-Ramos JC, Gearing D. Neurotactin, a membrane-anchored chemokine upregulated in brain inflammation. *Nature*. 1997;387:611-617

102. Imai T, Hieshima K, Haskell C, Baba M, Nagira M, Nishimura M, Kakizaki M, Takagi S, Nomiyama H, Schall TJ, Yoshie O. Identification and molecular characterization of fractalkine receptor cx3cr1, which mediates both leukocyte migration and adhesion. *Cell*. 1997;91:521-530

103. Goda S, Imai T, Yoshie O, Yoneda O, Inoue H, Nagano Y, Okazaki T, Imai H, Bloom ET, Domae N, Umehara H. Cx3c-chemokine, fractalkine-enhanced adhesion of thp-1 cells to endothelial cells through integrin-dependent and -independent mechanisms. *J Immunol*. 2000;164:4313-4320

104. Fong AM, Robinson LA, Steeber DA, Tedder TF, Yoshie O, Imai T, Patel DD. Fractalkine and cx3cr1 mediate a novel mechanism of leukocyte capture, firm adhesion, and activation under physiologic flow. *The Journal of experimental medicine*. 1998;188:1413-1419

105. Haskell CA, Cleary MD, Charo IF. Molecular uncoupling of fractalkine-mediated cell adhesion and signal transduction. Rapid flow arrest of cx3cr1-expressing cells is independent of g-protein activation. *The Journal of biological chemistry*. 1999;274:10053-10058

106. Saederup N, Chan L, Lira SA, Charo IF. Fractalkine deficiency markedly reduces macrophage accumulation and atherosclerotic lesion formation in ccr2-/- mice: Evidence for independent chemokine functions in atherogenesis. *Circulation*. 2008;117:1642-1648

107. Zeiffer U, Schober A, Lietz M, Liehn EA, Erl W, Emans N, Yan ZQ, Weber C. Neointimal smooth muscle cells display a proinflammatory phenotype resulting in increased leukocyte recruitment mediated by p-selectin and chemokines. *Circulation research*. 2004;94:776-784

108. Chandrasekar B, Mummidi S, Perla RP, Bysani S, Dulin NO, Liu F, Melby PC. Fractalkine (cx3cl1) stimulated by nuclear factor kappab (nf-kappab)-dependent inflammatory signals induces aortic smooth muscle cell proliferation through an autocrine pathway. *The Biochemical journal*. 2003;373:547-558

109. Liu P, Patil S, Rojas M, Fong AM, Smyth SS, Patel DD. Cx3cr1 deficiency confers protection from intimal hyperplasia after arterial injury. *Arteriosclerosis, thrombosis, and vascular biology*. 2006;26:2056-2062

110. Schober A, Weber C. Mechanisms of monocyte recruitment in vascular repair after injury. *Antioxidants & redox signaling*. 2005;7:1249-1257

111. Greaves DR, Hakkinen T, Lucas AD, Liddiard K, Jones E, Quinn CM, Senaratne J, Green FR, Tyson K, Boyle J, Shanahan C, Weissberg PL, Gordon S, Yla-Hertualla S. Linked chromosome 16q13 chemokines, macrophage-derived chemokine, fractalkine, and thymus- and activation-regulated chemokine, are expressed in human atherosclerotic lesions. *Arteriosclerosis, thrombosis, and vascular biology*. 2001;21:923-929

112. Wong BW, Wong D, McManus BM. Characterization of fractalkine (cx3cl1) and cx3cr1 in human coronary arteries with native atherosclerosis, diabetes mellitus, and transplant vascular disease. *Cardiovascular pathology : the official journal of the Society for Cardiovascular Pathology*. 2002;11:332-338

113. Lesnik P, Haskell CA, Charo IF. Decreased atherosclerosis in cx3cr1-/- mice reveals a role for fractalkine in atherogenesis. *The Journal of clinical investigation*. 2003;111:333-340

114. Combadiere C, Potteaux S, Gao JL, Esposito B, Casanova S, Lee EJ, Debre P, Tedgui A, Murphy PM, Mallat Z. Decreased atherosclerotic lesion formation in cx3cr1/apolipoprotein e double knockout mice. *Circulation*. 2003;107:1009-1016

115. Teupser D, Pavlides S, Tan M, Gutierrez-Ramos JC, Kolbeck R, Breslow JL. Major reduction of atherosclerosis in fractalkine (cx3cl1)-deficient mice is at the brachiocephalic artery, not the aortic root. *Proceedings of the National Academy of Sciences of the United States of America*. 2004;101:17795-17800

116. Noels H, Weber C. Fractalkine as an important target of aspirin in the prevention of atherogenesis : Editorial to: "Aspirin inhibits fractalkine expression in atherosclerotic plaques and reduces atherosclerosis in apoe gene knockout mice" by h. Liu et al. *Cardiovascular drugs and therapy / sponsored by the International Society of Cardiovascular Pharmacotherapy*. 2010;24:1-3

117. Postea O, Vasina EM, Cauwenberghs S, Projahn D, Liehn EA, Lievens D, Theelen W, Kramp BK, Butoi ED, Soehnlein O, Heemskerk JW, Ludwig A, Weber C, Koenen RR. Contribution of platelet cx(3)cr1 to platelet-monocyte complex formation and vascular recruitment during hyperlipidemia. *Arteriosclerosis, thrombosis, and vascular biology*. 2012;32:1186-1193

118. Hamidi M, Azadi A, Rafiei P. Hydrogel nanoparticles in drug delivery. *Advanced drug delivery reviews*. 2008;60:1638-1649

119. Moghimi SM, Hunter AC, Murray JC. Long-circulating and target-specific nanoparticles: Theory to practice. *Pharmacological reviews*. 2001;53:283-318

120. Wichterle OL, D. Hydrophilic gels for biological use,. *Nature*. 1960;185:2

121. GROLL J. SS, ALBRECHT K., MOELLER M. Biocompatible and degradable nanogels via oxidation reactions of synthetic thiomers in inverse miniemulsion. *Journal of Polymer Science: Part A: Polymer Chemistry*. 2009;47:5543-5549

122. Yu L, Ding J. Injectable hydrogels as unique biomedical materials. *Chemical Society reviews*. 2008;37:1473-1481

123. Hoffman AS. Hydrogels for biomedical applications. *Advanced drug delivery reviews*. 2002;54:3-12

124. Campoccia D, Doherty P, Radice M, Brun P, Abatangelo G, Williams DF. Semisynthetic resorbable materials from hyaluronan esterification. *Biomaterials*. 1998;19:2101-2127

125. Prestwich GD, Marecak DM, Marecek JF, Vercruysse KP, Ziebell MR. Controlled chemical modification of hyaluronic acid: Synthesis, applications, and biodegradation of hydrazide derivatives. *Journal of controlled release : official journal of the Controlled Release Society*. 1998;53:93-103

126. Lin CC, Metters AT. Hydrogels in controlled release formulations: Network design and mathematical modeling. *Advanced drug delivery reviews*. 2006;58:1379-1408

127. Jeong B, Kim SW, Bae YH. Thermosensitive sol-gel reversible hydrogels. *Advanced drug delivery reviews*. 2002;54:37-51

128. Zentner GM, Rathi R, Shih C, McRea JC, Seo MH, Oh H, Rhee BG, Mestecky J, Moldoveanu Z, Morgan M, Weitman S. Biodegradable block copolymers for delivery

of proteins and water-insoluble drugs. *Journal of controlled release : official journal of the Controlled Release Society*. 2001;72:203-215

129.   Steg PG, James SK, Atar D, Badano LP, Blomstrom-Lundqvist C, Borger MA, Di Mario C, Dickstein K, Ducrocq G, Fernandez-Aviles F, Gershlick AH, Giannuzzi P, Halvorsen S, Huber K, Juni P, Kastrati A, Knuuti J, Lenzen MJ, Mahaffey KW, Valgimigli M, van 't Hof A, Widimsky P, Zahger D. Esc guidelines for the management of acute myocardial infarction in patients presenting with st-segment elevation. *European heart journal*. 2012;33:2569-2619

130.   Hirsh J, Fuster V. Guide to anticoagulant therapy. Part 1: Heparin. American heart association. *Circulation*. 1994;89:1449-1468

131.   Ferguson JJ, Vaisman D. Therapeutic potential of gp iib/iiia receptor antagonists in acute myocardial infarction. *Expert opinion on investigational drugs*. 2001;10:1965-1976

132.   Pritchett AM, Redfield MM. Beta-blockers: New standard therapy for heart failure. *Mayo Clinic proceedings. Mayo Clinic*. 2002;77:839-845; quiz 845-836

133.   Latini R, Maggioni AP, Flather M, Sleight P, Tognoni G. Ace inhibitor use in patients with myocardial infarction. Summary of evidence from clinical trials. *Circulation*. 1995;92:3132-3137

134.   Baigent C, Keech A, Kearney PM, Blackwell L, Buck G, Pollicino C, Kirby A, Sourjina T, Peto R, Collins R, Simes R. Efficacy and safety of cholesterol-lowering treatment: Prospective meta-analysis of data from 90,056 participants in 14 randomised trials of statins. *Lancet*. 2005;366:1267-1278

135.   Schwartz GG, Olsson AG, Ezekowitz MD, Ganz P, Oliver MF, Waters D, Zeiher A, Chaitman BR. Atorvastatin for acute coronary syndromes. *JAMA : the journal of the American Medical Association*. 2001;286:533-535

136.   Cannon CP, Braunwald E, McCabe CH, Rader DJ, Rouleau JL, Belder R, Joyal SV, Hill KA, Pfeffer MA, Skene AM. Intensive versus moderate lipid lowering with statins after acute coronary syndromes. *The New England journal of medicine*. 2004;350:1495-1504

137.   Jackson KA, Majka SM, Wang H, Pocius J, Hartley CJ, Majesky MW, Entman ML, Michael LH, Hirschi KK, Goodell MA. Regeneration of ischemic cardiac muscle and vascular endothelium by adult stem cells. *The Journal of clinical investigation*. 2001;107:1395-1402

138.   Kawamoto A, Gwon HC, Iwaguro H, Yamaguchi JI, Uchida S, Masuda H, Silver M, Ma H, Kearney M, Isner JM, Asahara T. Therapeutic potential of ex vivo expanded endothelial progenitor cells for myocardial ischemia. *Circulation*. 2001;103:634-637

139.   Hristov M, Weber C. The therapeutic potential of progenitor cells in ischemic heart disease--past, present and future. *Basic research in cardiology*. 2006;101:1-7

140.   Schuh A, Liehn EA, Sasse A, Schneider R, Neuss S, Weber C, Kelm M, Merx MW. Improved left ventricular function after transplantation of microspheres and fibroblasts in a rat model of myocardial infarction. *Basic research in cardiology*. 2009;104:403-411

141.   Proudfoot AE, Power CA, Rommel C, Wells TN. Strategies for chemokine antagonists as therapeutics. *Seminars in immunology*. 2003;15:57-65

142.   Marino AP, da Silva A, dos Santos P, Pinto LM, Gazzinelli RT, Teixeira MM, Lannes-Vieira J. Regulated on activation, normal t cell expressed and secreted (rantes) antagonist (met-rantes) controls the early phase of trypanosoma cruzi-elicited myocarditis. *Circulation*. 2004;110:1443-1449

143.   Tarzami ST. Chemokines and inflammation in heart disease: Adaptive or maladaptive? *International journal of clinical and experimental medicine*. 2011;4:74-80

144.   Dimmeler S. Regulation of bone marrow-derived vascular progenitor cell mobilization and maintenance. *Arteriosclerosis, thrombosis, and vascular biology*. 2010;30:1088-1093

145.   Hughes S. Cardiac stem cells. *The Journal of pathology*. 2002;197:468-478

146. Jo DY, Rafii S, Hamada T, Moore MA. Chemotaxis of primitive hematopoietic cells in response to stromal cell-derived factor-1. *The Journal of clinical investigation*. 2000;105:101-111

147. Moore MA, Hattori K, Heissig B, Shieh JH, Dias S, Crystal RG, Rafii S. Mobilization of endothelial and hematopoietic stem and progenitor cells by adenovector-mediated elevation of serum levels of sdf-1, vegf, and angiopoietin-1. *Annals of the New York Academy of Sciences*. 2001;938:36-45; discussion 45-37

148. Hiasa K, Ishibashi M, Ohtani K, Inoue S, Zhao Q, Kitamoto S, Sata M, Ichiki T, Takeshita A, Egashira K. Gene transfer of stromal cell-derived factor-1alpha enhances ischemic vasculogenesis and angiogenesis via vascular endothelial growth factor/endothelial nitric oxide synthase-related pathway: Next-generation chemokine therapy for therapeutic neovascularization. *Circulation*. 2004;109:2454-2461

149. Saiki RK, Gelfand DH, Stoffel S, Scharf SJ, Higuchi R, Horn GT, Mullis KB, Erlich HA. Primer-directed enzymatic amplification of DNA with a thermostable DNA polymerase. *Science*. 1988;239:487-491

150. Sambrook JR. Molecular cloning : A laboratory manual. *Cold Spring Harbor Laboratory Press, Cold Spring Harbor*. . 2001

151. Altschul SF, Madden TL, Schaffer AA, Zhang J, Zhang Z, Miller W, Lipman DJ. Gapped blast and psi-blast: A new generation of protein database search programs. *Nucleic acids research*. 1997;25:3389-3402

152. Lowry OH, Rosebrough NJ, Farr AL, Randall RJ. Protein measurement with the folin phenol reagent. *The Journal of biological chemistry*. 1951;193:265-275

153. Proudfoot AE, Power CA, Hoogewerf AJ, Montjovent MO, Borlat F, Offord RE, Wells TN. Extension of recombinant human rantes by the retention of the initiating methionine produces a potent antagonist. *The Journal of biological chemistry*. 1996;271:2599-2603

154. Hristov M, Leyendecker T, Schuhmann C, von Hundelshausen P, Heussen N, Kehmeier E, Krotz F, Sohn HY, Klauss V, Weber C. Circulating monocyte subsets and cardiovascular risk factors in coronary artery disease. *Thrombosis and haemostasis*. 2010;104:412-414

155. Boyum A. Separation of leukocytes from blood and bone marrow. Introduction. *Scandinavian journal of clinical and laboratory investigation. Supplementum*. 1968;97:7

156. Ferrante A, Thong YH. Optimal conditions for simultaneous purification of mononuclear and polymorphonuclear leucocytes from human blood by the hypaque-ficoll method. *Journal of immunological methods*. 1980;36:109-117

157. Liehn EA, Piccinini AM, Koenen RR, Soehnlein O, Adage T, Fatu R, Curaj A, Popescu A, Zernecke A, Kungl AJ, Weber C. A new monocyte chemotactic protein-1/chemokine cc motif ligand-2 competitor limiting neointima formation and myocardial ischemia/reperfusion injury in mice. *Journal of the American College of Cardiology*. 2010;56:1847-1857

158. Liehn EA, Tuchscheerer N, Kanzler I, Drechsler M, Fraemohs L, Schuh A, Koenen RR, Zander S, Soehnlein O, Hristov M, Grigorescu G, Urs AO, Leabu M, Bucur I, Merx MW, Zernecke A, Ehling J, Gremse F, Lammers T, Kiessling F, Bernhagen J, Schober A, Weber C. Double-edged role of the cxcl12/cxcr4 axis in experimental myocardial infarction. *Journal of the American College of Cardiology*. 2011;58:2415-2423

159. Kijowski J, Baj-Krzyworzeka M, Majka M, Reca R, Marquez LA, Christofidou-Solomidou M, Janowska-Wieczorek A, Ratajczak MZ. The sdf-1-cxcr4 axis stimulates vegf secretion and activates integrins but does not affect proliferation and survival in lymphohematopoietic cells. *Stem Cells*. 2001;19:453-466

160. Salcedo R, Wasserman K, Young HA, Grimm MC, Howard OM, Anver MR, Kleinman HK, Murphy WJ, Oppenheim JJ. Vascular endothelial growth factor and basic fibroblast growth factor induce expression of cxcr4 on human endothelial cells: In vivo neovascularization induced by stromal-derived factor-1alpha. *The American journal of pathology*. 1999;154:1125-1135

161. Weber C, Schober A, Zernecke A. Chemokines: Key regulators of mononuclear cell recruitment in atherosclerotic vascular disease. *Arteriosclerosis, thrombosis, and vascular biology*. 2004;24:1997-2008

162. Kortesidis A, Zannettino A, Isenmann S, Shi S, Lapidot T, Gronthos S. Stromal-derived factor-1 promotes the growth, survival, and development of human bone marrow stromal stem cells. *Blood*. 2005;105:3793-3801

163. Vlahakis SR, Villasis-Keever A, Gomez T, Vanegas M, Vlahakis N, Paya CV. G protein-coupled chemokine receptors induce both survival and apoptotic signaling pathways. *J Immunol*. 2002;169:5546-5554

164. Zhang D, Fan GC, Zhou X, Zhao T, Pasha Z, Xu M, Zhu Y, Ashraf M, Wang Y. Over-expression of cxcr4 on mesenchymal stem cells augments myoangiogenesis in the infarcted myocardium. *Journal of molecular and cellular cardiology*. 2008;44:281-292

165. Schober A, Knarren S, Lietz M, Lin EA, Weber C. Crucial role of stromal cell-derived factor-1alpha in neointima formation after vascular injury in apolipoprotein e-deficient mice. *Circulation*. 2003;108:2491-2497

166. Ryu EK, Kim TG, Kwon TH, Jung ID, Ryu D, Park YM, Kim J, Ahn KH, Ban C. Crystal structure of recombinant human stromal cell-derived factor-1alpha. *Proteins*. 2007;67:1193-1197

167. Segers VF, Revin V, Wu W, Qiu H, Yan Z, Lee RT, Sandrasagra A. Protease-resistant stromal cell-derived factor-1 for the treatment of experimental peripheral artery disease. *Circulation*. 2011;123:1306-1315

168. Gliga D. Die generierung von einer protease-resistenten cxcl12 variante für die lokale beförderung der neovaskularisierung in vivo. *Master-Thesis*. 2009

169. Yamaoka TT, Y; Ikada, Y. Distribution ans tissue uptake of poly(ethylene glycol) with different molecular weights after intravenous administration to mice. *American Chemical Society and American Pharmaceutical Association*. 1993;83:5

170. Hartl D, Krauss-Etschmann S, Koller B, Hordijk PL, Kuijpers TW, Hoffmann F, Hector A, Eber E, Marcos V, Bittmann I, Eickelberg O, Griese M, Roos D. Infiltrated neutrophils acquire novel chemokine receptor expression and chemokine responsiveness in chronic inflammatory lung diseases. *J Immunol*. 2008;181:8053-8067

171. Ignatov A, Robert J, Gregory-Evans C, Schaller HC. Rantes stimulates ca2+ mobilization and inositol trisphosphate (ip3) formation in cells transfected with g protein-coupled receptor 75. *British journal of pharmacology*. 2006;149:490-497

172. Daugherty BL, Siciliano SJ, DeMartino JA, Malkowitz L, Sirotina A, Springer MS. Cloning, expression, and characterization of the human eosinophil eotaxin receptor. *The Journal of experimental medicine*. 1996;183:2349-2354

173. Struyf S, Menten P, Lenaerts JP, Put W, D'Haese A, De Clercq E, Schols D, Proost P, Van Damme J. Diverging binding capacities of natural ld78beta isoforms of macrophage inflammatory protein-1alpha to the cc chemokine receptors 1, 3 and 5 affect their anti-hiv-1 activity and chemotactic potencies for neutrophils and eosinophils. *European journal of immunology*. 2001;31:2170-2178

174. Slimani H, Charnaux N, Mbemba E, Saffar L, Vassy R, Vita C, Gattegno L. Interaction of rantes with syndecan-1 and syndecan-4 expressed by human primary macrophages. *Biochimica et biophysica acta*. 2003;1617:80-88

175. Proudfoot AE, Fritchley S, Borlat F, Shaw JP, Vilbois F, Zwahlen C, Trkola A, Marchant D, Clapham PR, Wells TN. The bbxb motif of rantes is the principal site for heparin binding and controls receptor selectivity. *The Journal of biological chemistry*. 2001;276:10620-10626

176. Askari AT, Unzek S, Popovic ZB, Goldman CK, Forudi F, Kiedrowski M, Rovner A, Ellis SG, Thomas JD, DiCorleto PE, Topol EJ, Penn MS. Effect of stromal-cell-derived factor 1 on stem-cell homing and tissue regeneration in ischaemic cardiomyopathy. *Lancet*. 2003;362:697-703

177. Barlic J, Zhang Y, Murphy PM. Atherogenic lipids induce adhesion of human coronary artery smooth muscle cells to macrophages by up-regulating chemokine cx3cl1 on

smooth muscle cells in a tnfalpha-nfkappab-dependent manner. *The Journal of biological chemistry*. 2007;282:19167-19176

178. Ludwig A, Berkhout T, Moores K, Groot P, Chapman G. Fractalkine is expressed by smooth muscle cells in response to ifn-gamma and tnf-alpha and is modulated by metalloproteinase activity. *J Immunol*. 2002;168:604-612

179. Braunersreuther V, Mach F, Steffens S. The specific role of chemokines in atherosclerosis. *Thrombosis and haemostasis*. 2007;97:714-721

180. Oostendorp M, Douma K, Wagenaar A, Slenter JM, Hackeng TM, van Zandvoort MA, Post MJ, Backes WH. Molecular magnetic resonance imaging of myocardial angiogenesis after acute myocardial infarction. *Circulation*. 2010;121:775-783

181. Studier FW, Moffatt BA. Use of bacteriophage t7 rna polymerase to direct selective high-level expression of cloned genes. *Journal of molecular biology*. 1986;189:113-130

182. Rosenberg AH, Lade BN, Chui DS, Lin SW, Dunn JJ, Studier FW. Vectors for selective expression of cloned dnas by t7 rna polymerase. *Gene*. 1987;56:125-135

183. Studier FW, Rosenberg AH, Dunn JJ, Dubendorff JW. Use of t7 rna polymerase to direct expression of cloned genes. *Methods in enzymology*. 1990;185:60-89

184. Diaz-Collier JA, Palmier MO, Kretzmer KK, Bishop BF, Combs RG, Obukowicz MG, Frazier RB, Bild GS, Joy WD, Hill SR, et al. Refold and characterization of recombinant tissue factor pathway inhibitor expressed in escherichia coli. *Thrombosis and haemostasis*. 1994;71:339-346

185. Anfinsen CB. Principles that govern the folding of protein chains. *Science*. 1973;181:223-230

186. Sakahira H, Breuer P, Hayer-Hartl MK, Hartl FU. Molecular chaperones as modulators of polyglutamine protein aggregation and toxicity. *Proceedings of the National Academy of Sciences of the United States of America*. 2002;99 Suppl 4:16412-16418

187. Sorensen HP, Mortensen KK. Advanced genetic strategies for recombinant protein expression in escherichia coli. *Journal of biotechnology*. 2005;115:113-128

188. Mizoue LS, Sullivan SK, King DS, Kledal TN, Schwartz TW, Bacon KB, Handel TM. Molecular determinants of receptor binding and signaling by the cx3c chemokine fractalkine. *The Journal of biological chemistry*. 2001;276:33906-33914

189. Inoue A, Hasegawa H, Kohno M, Ito MR, Terada M, Imai T, Yoshie O, Nose M, Fujita S. Antagonist of fractalkine (cx3cl1) delays the initiation and ameliorates the progression of lupus nephritis in mrl/lpr mice. *Arthritis and rheumatism*. 2005;52:1522-1533

190. Pompella A, Visvikis A, Paolicchi A, De Tata V, Casini AF. The changing faces of glutathione, a cellular protagonist. *Biochemical pharmacology*. 2003;66:1499-1503

191. Veillard NR, Kwak B, Pelli G, Mulhaupt F, James RW, Proudfoot AE, Mach F. Antagonism of rantes receptors reduces atherosclerotic plaque formation in mice. *Circulation research*. 2004;94:253-261

192. Lunn CA, Kathju S, Wallace BJ, Kushner SR, Pigiet V. Amplification and purification of plasmid-encoded thioredoxin from escherichia coli k12. *The Journal of biological chemistry*. 1984;259:10469-10474

193. Katti SK, LeMaster DM, Eklund H. Crystal structure of thioredoxin from escherichia coli at 1.68 a resolution. *Journal of molecular biology*. 1990;212:167-184

194. LaVallie ER, DiBlasio-Smith EA, Collins-Racie LA, Lu Z, McCoy JM. Thioredoxin and related proteins as multifunctional fusion tags for soluble expression in e. Coli. *Methods Mol Biol*. 2003;205:119-140

195. Lilie H, Schwarz E, Rudolph R. Advances in refolding of proteins produced in e. Coli. *Current opinion in biotechnology*. 1998;9:497-501

196. Dobaczewski M, Xia Y, Bujak M, Gonzalez-Quesada C, Frangogiannis NG. Ccr5 signaling suppresses inflammation and reduces adverse remodeling of the infarcted heart, mediating recruitment of regulatory t cells. *The American journal of pathology*. 2010;176:2177-2187

197. Schafer A, Schulz C, Eigenthaler M, Fraccarollo D, Kobsar A, Gawaz M, Ertl G, Walter U, Bauersachs J. Novel role of the membrane-bound chemokine fractalkine in platelet activation and adhesion. *Blood*. 2004;103:407-412

198. Schulz C, Schafer A, Stolla M, Kerstan S, Lorenz M, von Bruhl ML, Schiemann M, Bauersachs J, Gloe T, Busch DH, Gawaz M, Massberg S. Chemokine fractalkine mediates leukocyte recruitment to inflammatory endothelial cells in flowing whole blood: A critical role for p-selectin expressed on activated platelets. *Circulation*. 2007;116:764-773

199. Meyer dos Santos S, Klinkhardt U, Scholich K, Nelson K, Monsefi N, Deckmyn H, Kuczka K, Zorn A, Harder S. The cx3c chemokine fractalkine mediates platelet adhesion via the von willebrand receptor glycoprotein ib. *Blood*. 2011;117:4999-5008

200. Ludwig A, Weber C. Transmembrane chemokines: Versatile 'special agents' in vascular inflammation. *Thrombosis and haemostasis*. 2007;97:694-703

201. Ludwig A, Dietel M, Lage H. Identification of differentially expressed genes in classical and atypical multidrug-resistant gastric carcinoma cells. *Anticancer research*. 2002;22:3213-3221

202. Wang Y, Sakuma M, Chen Z, Ustinov V, Shi C, Croce K, Zago AC, Lopez J, Andre P, Plow E, Simon DI. Leukocyte engagement of platelet glycoprotein ibalpha via the integrin mac-1 is critical for the biological response to vascular injury. *Circulation*. 2005;112:2993-3000

203. Dragomir E, Manduteanu I, Calin M, Gan AM, Stan D, Koenen RR, Weber C, Simionescu M. High glucose conditions induce upregulation of fractalkine and monocyte chemotactic protein-1 in human smooth muscle cells. *Thrombosis and haemostasis*. 2008;100:1155-1165

10.   Acknowledgements

Herrn Univ.-Prof. Dr. med. Christian Weber danke ich für die Möglichkeit an seinem Institut zu promovieren, für seine hervorragende wissenschaftliche Unterstützung während meiner Doktorarbeit und für die Übernahme des Zweitgutachens.

Bei Herrn Univ.-Prof. Dr. rer. nat. Jürgen Bernhagen möchte ich mich sehr herzlich bedanken für die Übernahme des Erstgutachtens meiner Doktorarbeit und für die exzellenten fachlichen Unterstützung während meiner gesamten Zeit bei IMCAR.

Herrn Univ.-Prof. Dr. rer. nat. Lothar Elling möchte ich für die Übernahme des Drittprüfers meiner Doktorarbeit danken.

Besonders bedanken möchte ich mich bei meinem Betreuer PD. Dr. rer. nat. Rory Koenen für die Themenstellung und Betreuung meiner Doktorarbeit, den konstruktiven wissenschaftlichen Austausch und für die Möglichkeit auch eigene Ideen verwirklichen zu können.

Ganz besonders herzlich möchte ich mich bei PD. Dr. nat. med. Dr. med Elisa Anamaria Liehn bedanken, für die freiwillige Betreuung meiner Daktorarbeit, für die exzellente wissenschaftliche Unterstützung, insbesondere für die Hilfe beim Infarktmodell und für die Inspiration neue Ideen zu entwickeln und umzusetzen.

Bei Univ.-Prof. Dr. rer. nat. Jürgen Groll und seiner Mitarbeiterin Smriti Singh möchte ich mich für die sehr gute, jahrelange Kooperation und für die Herstellung und Bereitstellung der Hydrogele, bedanken.

Bei meinen Kolleginnen Birgit Kramp und Marcella Langer möchte ich mich für die Herstellung und Bereitstellung des Met-CCL5 bedanken.

Ein ganz besonderes Dankeschön geht an meine Freundin und Kollegin Sakine Simsekyilmaz, die mir bei der Organisation und Umsetzung der Tierexperimente sehr geholfen hat und für die sehr schöne Zeit in Aachen.

Ich danke allen meinen Arbeitskollegen aus dem IMCAR und IPEK für ihre fachliche Unterstützung und für die schöne Zeit in Aachen und München. Danke außerdem auch für die gute und harmonische Arbeitsathmosphäre im Labor. Danke an Adelina, Ali, Ake, Barbara, Dirk, Ela, Elena, Gitte, Heidi, Holger, Isabella, Jean-Eric, Jolanta, Kathrin, Kiril, Leon, Martin, Melanie, Michael, Norbert, Remco, Roya, Pathricia, Philip, Sabine, Sakine, Santosh, Steffi, Tobi und Xavier.

Weiterhin möchte ich mich bei Frau Mayer für Ihre administrative Hilfe und für die Korrektur der Doktorarbeit bedanken.

Ich möchte meinen Eltern Monica und Viorel Gliga, meiner Oma Gheorgita Guta, meiner Schwester Anca Gliga und Magnus Berntsen ein herzliches Dankeschön aussprechen, die mir mit Rat und Tat zur Seite gestanden haben und mir über die gesamte Zeit sehr geholfen haben.

Meinem Mann Holger Projahn möchte ich für seine unendlich große Liebe und moralische Unterstützung danken, obwohl ich nicht immer sehr einfach war. Er hat mir in jeder Lebenslage Kraft gegeben, was zum Gelingen dieser Arbeit stark beigetragen hat. (*Te iubesc foarte mult!*)

11.   Curriculum Vitae

Persönliche Daten:

Name:	Delia Projahn
Geburtsname:	Gliga
Geburtsdatum:	18.12.1978
Geburtsort:	Hermannstadt/Rumänien
Nationalität:	Deutsch
Familienstand:	verheiratet, keine Kinder

Bildungsweg:

September 1997 – September 2000	Berufsausbildung an der Medizinisch-Technischen-Akademie in Esslingen Abschluss: Medizinisch-Technische-Radiologie-Assistentin (MTA-R)
August 2000 – Juli 2001	Fachhochschulreife an der Fachoberschule für Sozial- und Gesundheitswesen in Köln Abschluss: Fachabitur
Juli 2001 – August 2004	Studium der Biologie an der Fachhochschule Bonn-Rhein-Sieg
Oktober 2004 – Januar 2007	Studium der Molekularen Biologie an der Fachhochschule Gelsenkirchen Abschluss: Bachelor of Science
Oktober 2007 – September 2009	Studium der Medizinischen Biologie an der Universität Duisburg-Essen Abschluss: Master of Science
September 2009 – April 20013	Doktorandin am Institut für Molekulare Herz- Kreislaufforschung (IMCAR), Aachen und Institut für Prophylaxe und Epidemiologie der Kreislaufkrankheiten (IPEK), München unter der Leitung von Univ.-Prof. Dr. med. Christian Weber

12.   Publications

Postea O, Vasina EM, Cauwenberghs S, **Projahn D**, Liehn EA, Lievens D, Theelen W, Kramp BK, Butoi ED, Soehnlein O, Heemskerk JW, Ludwig A, Weber C, Koenen RR. Contribution of platelet cx(3)cr1 to platelet-monocyte complex formation and vascular recruitment during hyperlipidemia. *Arteriosclerosis, thrombosis, and vascular biology.* 2012; 32:1186-1193.

Projahn D, Koenen RR. Platelets: key players in vascular inflammation. *J Leukoc Biol.* 2012 92(6):1167-75.

Projahn D, Simsekyilmaz S, Singh S, Kanzler I, Kramp BK., Langer M, Burlacu A, Bernhagen J, Klee D, Zernecke A, Hackeng TM, Groll J, Weber C, Liehn EA, Koenen RR. Controlled release of engineered chemokines from biodegradable hydrogels prevents injury extension after myocardial infarction. *BRC.* 2013, submitted.

Soehnlein O, Drechsler M, Döring Y, Lievens D, Hartwig H, Kemmerich K, Ortega-Gómez A, Mandl M, Vijayan S, **Projahn D**, Garlichs CD, Koenen RR, Hristov M, Lutgens E, Zernecke A, Weber C. Distinct functions of chemokine receptor axes in the atherogenic mobilization and recruitment of classical monocytes. EMBO Mol Med. 2013 Mar;5(3):471-81.

Conferences:

Oral Presentation:

German Society of Cardiology-76th Annual Meeting 2010, April 8th–10th 2010, Mannheim, Germany.

Gliga D. Die Generierung von bioabbaubaren protease-resistenten CXCL12-derivatisierten Microbeads für die Therapie des Myokardinfarkts.

Annual Symposium of the DFG Graduate School "EuCar" 2010 (GRK 1508/1), October 22nd-23rd 2010 Aachen, Germany

Projahn D, Generation of biodegradeable protease-resistant chemokines-derivatized polymers for the therapy of myocardial infarction

29th Winter School on Proteinases and Their Inhibitors, February 29th – March 4th 2012, Tiers, Italy.

Projahn D, Generation of biodegradeable protease-resistant chemokines-derivatized polymers for the therapy of myocardial infarction.

Poster presentation:

6th International Aachen Symposium on Cytokine Signaling, April 23rd–24th 2010, Aachen, Germany.

Gliga D, Liehn EA, Singh S, Kramp B, Klee D, Groll J Zernecke A, Weber C, Koenen RR. Generation of biodegradable protease-resistant CXCL12- and Met-RANTES-derivatized gels for the therapy of myocardial infarction.

Annual Meeting of the Society for Microcirculation and Vascular Biology (GfMVB), Juli 14th-16th 2010 Berlin, Germany

Gliga D, Liehn EA, Zerneke, A, Klee D, Kramp B, Weber C, Koenen RR. Generation of biodegradable protease-resistant CXCL12-derivatized microbeads for the therapy of myocardial infarction.

9th World Congress for Microcirculation, September 26th-28th 2010 Paris, France.

Projahn D, Liehn EA, Singh S, Kramp B, Klee D, Groll J Zernecke A, Weber C, Koenen RR. Generation of biodegradable protease-resistant CXCL12- and Met-RANTES-derivatized gels for the therapy of myocardial infarction.

Cardiac Stem Cell and Tissue Engineering Conference 2011, May 18th–20th 2011 San Servolo, Italy.

Projahn D, Liehn EA, Singh S, Kramp B, Klee D, Groll J, Zernecke A, Weber C, Koenen RR. Generation of biodegradable protease-resistant CXCL12- and Met-RANTES-derivatized gels for the therapy of myocardial infarction.

Joint meeting of the European Society for Microcirculation and the German Society of Microcirculation and Vascular Biology, October 13th-16th 2011 Munich, Germany.

Projahn D, Singh S, Kramp B, Simsekyilmaz S, Kanzler I, Klee D, Groll J, Zernecke A, Weber C, Liehn EA, Koenen RR. Generation of biodegradable protease-resistant CXCL12- and Met-RANTES-derivatized gels for the therapy of myocardial infarction.

Cardiovascular Network Retreat, March 15th - 17th 2012, Ebsdorfergrund- Rauischholz-hausen, Germany.

Projahn D, Singh S, Kramp B, Simsekyilmaz S, Kanzler I, Klee D, Groll J, Zernecke A, Weber C, Liehn EA, Koenen RR. Combined treatment with engineered chemokines for prevention of heart ischemia-reperfusion injury

Profesional trainings:

CARIM PhD-Training Course 2010,"Thrombosis and Haemostasis" October 11th-15th 2010, Papendal, Arnhem

CARIM PhD Weekend, May 7th-8th 2010, Rolduc/ Kerkrade, The Netherlands

"Presentation and Communication" Workshop Praxis Ellen Gürtler, March 16th-17th
2010, University Hospital Aachen, Germany